DISSERTATION

WEATHERING AND SOIL PROPERTIES ON CATENARY SEQUENCES IN FOREST AND ALPINE ECOSYSTEMS OF THE CENTRAL ROCKY MOUNTAINS

Submitted by

Robert Mark Bergstrom

Department of Soil and Crop Sciences

In partial fulfillment of the requirements

For the Degree of Doctor of Philosophy

Colorado State University

Fort Collins, Colorado

Fall 2017

Doctoral Committee:

Advisor: Eugene F. Kelly

Charles C. Rhoades
Thomas Borch
Suellen Melzer
Patrick H. Martin

ABSTRACT

WEATHERING AND SOIL PROPERTIES ON CATENARY SEQUENCES IN FOREST AND ALPINE ECOSYSTEMS OF THE CENTRAL ROCKY MOUNTAINS.

The evolution of soil landscapes can be evaluated by studying soil properties along catenary sequences—soil sequences that are hydrologically and topographically connected along hillslopes from higher elevation to lower elevation. Using the catena model, I investigated the manifestation of soil forming factors in conditioning weathering and soil development in the Mountain Ecosystems of the Fraser Experimental Forest (FEF), Colorado. The research outlined and presented in this dissertation is preceded by a short narrative on soil forming properties, hillslope models, and assessing weathering in soils. The work presented in this dissertation is a result of a multidisciplinary framework for pedological research, derived from the integration of and consideration of pedology, geomorphology, and hydrology. The future of pedological research will involve the assimilation of multidisciplinary approaches and thinking. This dissertation elucidates on (1) the distribution of soil properties along soil catenas and their implication for hydrologic and biogeochemical linkages across landscapes, (2) the evaluation of chemical alteration thru modeling soil strain along soil catenas, (3) the quantification and distribution of soil elemental fluxes along soil catenas, and (4) the determination of the contributions of weathering and atmospheric inputs to landscapes at FEF.

My field sites were located in FEF, a model site of the alpine and forested environments of the central Rocky Mountains. The FEF is an ideal setting to study the interaction of soil forming factors in complex mountain terrain. A combination of traditional and more modern

methods to explore the linkages between soil properties along mountain catenas were employed in order to gain insight into soil landscape evolution in complex mountain terrain. I established eight catenas along relatively steep mountain hillslopes while constraining the lithologic differences along the soil landscapes. Vegetative changes along these catenas could not be ignored; rather, the differences provided insight into the influence of vegetative cover on soil properties. Soils were sampled along the catenas, beginning in the mountaintop landscapes (crests or summit) and ending in the mountainbase landscapes, where wetlands along riparian corridors dominate. Soil morphology and soil chemistry along the catenas provided understanding into the evolution of soil landscapes at FEF and their connectedness to the hydrologic flowpaths along these hillslopes. Results suggested that these soil landscapes are in various states of evolution, marked by the relative development of illuvial and elluvial horizons, and that the landscapes are dominated by subsurface lateral flow. The data also suggested that atmospheric deposition may be an important contributor to pedogenesis in these landscapes and that there are expected hot-spots of nutrient accumulations in the mountainbase landscapes, where upland soils have transported and deposited dissolved ions and fine soil particles into wetland soils along riparian corridors. The next question became: does the distribution of elements along soil landscapes reflect what was expected from the aforementioned analyses and is the fate of elements controlled by the landscape positions? What is the balance between the atmospheric contributions to weathering and internal cycling of cations?

Subsequently, the analysis for soils along the catenas was extended to model soil strain within the soil landscapes, quantify mass fluxes and distribution of elements within the soil landscapes, and quantify the atmospheric contributions to weathering in these systems. Results indicated that dilation in upper soil horizons reflect the textural patterns in the same horizons across all landscapes—supporting the notion that the soils along theses catenas have been strongly influenced by additions via atmospheric deposition, and this influence is detectable across entire hillslopes. Also, modeled soil strain indicated that great pedogenic additions have occurred in the mountainbase landscapes—supporting the notion that dissolved ions and fine soil material have been transported and deposited downslope via subsurface lateral flow. Calculated elemental flux values indicated that soil nutrients originating the upland landscape positions are transferred to lower landscapes through the mountainflanks, and are deposited in the mountainbase landscapes, where the soils were found to be enriched in the following major elements—Ca, Na, K, Al, Fe, and Mg. In turn, the impact of atmospheric contributions to soil landscapes along a catena was revealed. The data suggested that surface soil horizons are more strongly influenced by atmospheric contributions than subsurface horizons. Likewise, subsurface horizons are increasingly more influenced by the weathering of parent material moving from higher soil landscapes to lower soil landscapes. Lastly, results suggest that the isotopic signature within mountaintop soil landscapes is coupled to vegetative cover and snowfall and snowmelt hydrology dynamics. The soil catena model endures as a framework for providing insight into the relationships of soil forming factors across gradients of variation.

ACKNOWLEDGEMENTS

I express my most sincere gratitude to faculty, staff, friends, and family who supported me in this endeavor. A special thanks to my cohorts and fellow graduate students who made the graduate experience enjoyable. I am very grateful to my advisor Dr. Gene Kelly, as he has been a superior mentor and friend through this process. Gene was always honest with where I was in the process and what I needed to improve upon. He let me also find my own way, and I appreciate him for that support. I anticipate that he will be a great friend and colleague for years to come. Thank you to the rest of my committee for their ideas, suggestions, and expertise; I would not have pushed as hard without them.

I was able to take advantage of multiple opportunities while at CSU to work on projects unrelated to my Ph.D. research with the NPS, NRCS, and USFS. I am grateful of those experiences, as I would not be in the same situation I am today without those interdisciplinary experiences.

My family and close friends deserve much credit for my academic achievements and I would not have pushed on as easily without their support. I wish my mom were around to witness this final step in the journey, and I am thankful that my dad can see this come to fruition. I treasure the memory of a question that my oldest son, Logan, posed when he was a couple years younger “Daddy, why you want be a dirt doctor??”, and in due time I’m sure that my little Andrew and Ella will question my rationality for this choice of specialty as well! I thank my wife, Rebecca, most of all—as she has been my biggest supporter along the way and finishing up, especially. She is my rock. No more will she have to hear that I need to work an evening or weekend in the basement or at the office “writing and editing the dissertation”.

TABLE OF CONTENTS

CHAPTER 1

INTRODUCTION AND DISSERTATION OBJECTIVES

1.1 Conceptual Framework

The fundamental elements (models and theories) of this dissertation research are discussed below. This introduction includes information regarding 1) Soil Forming Factors, 2) Hillslope Models, and 3) Soil Weathering Models.

1.1.1 Soil Forming Factors

Soil forming processes that determine soil properties within ecosystems are regulated by the following conditioning variables: climate, organisms, parent material, relief, time, and humans (Jenny 1941; 1980). These variables are commonly referred to as the soil forming factors and commonly construct the backbone of pedogenic research. Jenny's original approach considered these variables as independent of one another, and independent of the soil as it developed. However, the biological, physical and chemical components within ecosystems are highly interconnected, and the feedbacks among components create complex soil patterns across environments. Soil properties, such as acidity or color, are a function of the soil forming factors and this relationship may be mathematically expressed by the equation: $s = f(cl, o, r, p, t, h, \ldots)$, where any soil property (s) is a function (f) of the driving variables listed previously.

Climate (cl) (temperature and effective precipitation) influences soil formation both directly and indirectly. In the mid-19th Century, Vasily Dokuchaev made observations linking rainfall and morphological changes in Russian soils (Humphreys and Wilkerson 2007). Effective precipitation can be thought of as the water that penetrates into the regolith; this largely depends on topography and permeability of a landscape. Climate has a profound effect on soil properties such as carbonate distribution, pH, organic matter, and clay formation. The variation in global precipitation is partially responsible for differences in many pedogenic processes and soil properties. For example, soil can be heavily leached of nutrients and highly weathered under high annual rainfall regimes (Vitousek 2002). In contrast, areas with very low rainfall (e.g. dry climates) may experience low weathering and minimal soil formation due to lack of biological activity and resulting acid inputs (Ewing et al. 2006).

Organisms (o) (vegetation, microbes, and animals) have a profound effect on soil formation due to their combined influences on the accumulation and conditioning of soil organic matter (SOM). Vegetation can influence soil formation through the activities of roots, chemistry of leaf litter, and the quantity biomass deposited into a system. Microbes play a critical role in decomposition of SOM and may alter the chemistry of soils. Soil animals, such as ants, earthworms, and moles, provide mixing of larger materials and incorporate plant matter into the deeper layers of the soil while creating macropores for the movement of water (Blouin et al. 2013).

Relief (r) or Topography has both direct and indirect influences on soils. Key aspects of relief include slope geometry, slope steepness, aspect and elevation. Water movement is influenced by these aspects of relief as it modifies both local and regional water inputs and affects the degree of pedogenesis. Typically along hillslopes, precipitation is routed from uplands to low lying water basins within a landform. It is also well known that aspect affects soil development; soil properties on south vs. north facing slopes within the same climatic regime commonly differ due to its influence on local soil moisture and temperature. Similarly, elevation affects soil development as it influences the local bioclimatic (and corresponding plants communities) conditions that act concurrently as soil forming factors. Soil properties are controlled by topography within hillslopes that are subjected to long term erosion and deposition of material downslope.

Parent material (p) is defined as rock, dust, alluvium, or another soil that provide the input of primary minerals at the onset of weathering and soil formation (Schaetzl and Anderson 2005). The physical and chemical composition influences pedogenesis mainly by controlling the susceptibility to chemical and physical weathering processes. For example, soils derived from contrasting parent materials, e.g. felsic (granitic) parent material and mafic (basaltic) parent material, will form at very different rates and exhibit chemical properties that reflect these differences in chemical composition. In general, parent materials that are more vulnerable to weathering (e.g. basalt) will weather more quickly and provide a larger contribution of elements, such as Ca, Fe, and Mg to the soils within the landscape.

Time (t) is the period through which soil formation processes occur (Jenny 1941). The state factor *time* (*t*) is defined as the elapsed period since the system began or was exposed to its present assemblage of state factors. For some systems, this is the starting point immediately after an event such as fluvial or volcanic deposition. In other cases, $t = 0$ may be the point at the end of a major environmental disturbance or change. Many soils older than the Holocene (approximately 12,000 yrs) have experienced one or more major climate changes, and possess properties that may be the complex effect of several stages of soil development, and are called polygenetic or relict soils.

Hans Jenny (1941) originally considered humans (h) under the biotic factor because, like other biota, humans contain a genetic component or genotype. However, unlike the other organisms that are not endowed with the ability to reason, humans possess a cultural component that varies from society to society and which operates independently of genotype, arguably making them worthy of a separate factorial treatment. Currently, humans influence ecological processes on a global scale, sometimes on par with the role of climate, geological forces and astronomical variations. The *anthropogenic factor* (*h*) can affect soil formation by a plethora of different interventions (Amundson 1991), such as deforestation and aforestation, grazing, agriculture, urbanization, construction of turnpikes and landfills, induced fires and floods, mining, pollution, bombing, burial of pipelines or cables.

1.1.2 Hillslope Models

The catena concept in soil science originates from the Latin word "catena", which means chain. Conceptually it refers to a sequence of soils in different positions in the landscape (Milne 1935a). He noted "the regular repetition of a certain sequence of soil profiles in association with topography" in East Africa. Milne wrote that "a distinctive word is needed in referring to this phenomenon" hence, he proposed the word catena. He proposed that soils in different positions in the catena exchange materials through transport processes and thus could be compared to the transfer processes between horizons in a soil profile. He and his students have shown that the downward transport of solids or solutions may lead to a direct or an indirect linkage between catena elements (Sommer and Schlichting 1997). In Schlichting's view, the formation of a soil can only be understood if its relation to the other soils in the catena is taken into consideration. The soil catena consists of a sequence of soil types that differ according to their position within the landscape that differ in their soil morphology, as well as in their physical and chemical properties.

One could envision a very general soil catena across a landscape beginning in the uplands and terminating in the lowlands where transfers occur across the catena, moving materials such as mineral and organic matter from higher to lower elevations. Traditionally, soil catenas are thought of as a toposequence, where the soil forming factors described by Jenny are held relatively constant—except for relief (topography). The literature is replete with studies that have investigated soil properties along soil catenas to gain insight into the dynamics of soil landscapes. The catena model has been applied to studies of soil connectivity (Young 1976), soil topographic relationships (Huggett 1975), and biogeochemical properties across soil landscapes (Schimel et al. 1985; Litaor 1992).

1.1.3 Weathering Models in Soils

Relatively recently, soils have drawn widespread interest because they are universally recognized as a critical component in the biogeochemistry of terrestrial ecosystems. Soil formation (pedogenesis) results from the contributions of chemical, physical, and biological weathering that occur at the Earth's surface; the state factors of soil formation give rise to variability in the expression and influence of weathering processes. Physical weathering is mechanical in nature and primarily results in an increase in the surface area of the media being weathered. Biological weathering produces CO_2 and organic acids, which in turn increases weathering rates. Chemical weathering results in chemical transformations of primary minerals and in terrestrial ecosystems becomes a significant sink for atmospheric CO_2. Water is the key agent for chemical weathering in soils. Water enters soil landscapes through direct precipitation, surface pathways, and subsurface pathways, and exits the system through evapotranspiration, runoff, and groundwater discharge. Similarly, hydrologic processes in soil landscapes and the degree to which these processes regulate the residence time of water in soils are critical to the fate and mobility of chemical elements that influence water quality. For example, the residence time and pathways of water through soils influence biogeochemical reaction rates and the supply and removal of C and nutrients. Over the long term chemical weathering exhibits a control over Earth's climate (Kump 2000; Gislason 2009). Soils also provide and/or regulate an array of ecosystems services. The services that soils provide differ, to an extent, according to the soil type found in a particular ecosystem. Likewise, ecosystem productivity is regulated as soils evolve and chemical weathering rates change. Consequently, the ability to quantify and predict the distribution of elements and rates of weathering in a terrestrial landscapes is important in constructing the biogeochemical cycling of key elements. Attempts to integrate soil properties into global and regional simulation models emphasize the temporal and spatial complexities associated with these systems (Schimel et al. 1994).

Two major sources of base cations (soil nutrients) exist in an ecosystem-- bedrock derived elements and elements attributed to atmospheric deposition. Weathering makes nutrients available in terrestrial ecosystems (Ricklefs 2010) and for quite some time studies have noted that local bedrock weathering is a major source of nutrients for vegetation in a variety of ecosystems (Likens 1967). Weathering processes are linked directly to the atmosphere and as soils evolve over time they maintain a biogeochemical balance with the atmosphere. For example, in humid ecosystems, atmospheric CO_2 is taken up by plants and eventually ends up dissolved in soil waters as HCO_3^-, which is a major agent in the weathering of silicate minerals (Chadwick et al. 1994). When precipitation exceeds evapotranspiration and soil water retention, cations (e.g.Ca^{2+}) not taken up by plants or retained on exchange sites combine with HCO_3^- and flow into ground water, streams or oceans (Stallard 1988; Berner et al. 1983). Under these climatic conditions the system experiences a net loss of nutrients derived from parent material as weathering proceeds over time.

Evaluating soil properties such as soil color, structure, and texture remains an enduring method for assessing the degree of weathering in soils—albeit semi-quantitative, at best. The development and application of the constituent mass balance model allowed pedologists to put soil weathering into quantitative terms (Brimhall et al. 1985; Chadwick 1990), whereby elements are used as pedochemical tracers and their behavior is interpreted in relationship to soil properties.

The constituent mass balance model is used to determine elemental gains and losses during pedogenesis and is calculated according to the method described by Chadwick et al. (1990) and revised by Egli and Fitze (2000). Constituent mass balance involves the calculation of three parameters: **strain (ε)**, a measure (%) of the volume change of a soil horizon, relative to an immobile element, usually Ti or Zr; **mass transport function (τ)**, a relative measure (%) of elemental movement between soil horizons; **mass flux**, a measure (mass per unit area, e.g. g cm^{-2}) of the quantity of elemental gain or loss of a mobile element, such as additions of Ca to the soil profile. Pedologists often refer to elemental **enrichment**, a measure of mobile element accumulation or depletion in the soil profile relative to the immobile element.

The constituent mass balance approach has been used in assessing soil development over time through the estimation of soil strain and mass flux (Brimhall et al. 1992); the initial applications of this model were applied to the evaluation of weathering across soil chronosequences. In more recent times, the constituent mass balance approach has been coupled with additional analytical techniques (XRD, soil water chemistry, isotope geochemistry, etc.) to quantify soil weathering in a variety of ecosystems (Bern et al. 2011; Porder et al. 2006; Anderson et al. 2002).

1.2 Research Objectives

This dissertation research aims to broaden our understanding of soil property variability and pedogenic processes in Mountain Ecosystems of the Western U.S. by addressing the following questions:

(1) Can the systematic variation in soil morphological, physical, and biogeochemical properties along catenas be linked to long term hydrologic processes that regulate soil formation within Mountain Ecosystems of the Western U.S.?

(2) How do soil forming factors, specifically parent material and topography, condition the distribution of elements within soils of Mountain Ecosystems of the Western U.S.?

(3) What proportion of nutrients in these ecosystems is derived from weathering versus external inputs (e.g. atmospheric) or internally (from adjacent landscape elements)?

Eight soil catenas within the Fraser Experimental Forest (FEF), Grand County, Colorado were sampled, which allowed for the evaluation of the pedogenic contributions of various soil forming factors along complex soil landscapes. Of particular interest was the evaluation of the internal cycling of nutrients within these soil landscapes. Although weatherable minerals may be depleted, can the ecosystem recycle cations efficiently enough to negate atmospheric inputs? Systems that depend on an efficient internal cycling of nutrients versus atmospheric deposition will respond very differently to disturbances.

By applying both novel (stable isotope geochemistry, constituent mass balance models) and traditional (soil morphology, soil chemistry, mineralogical analyses) analytical techniques to a set of ecosystems that have evolved under similar geological and climatic conditions, I realized the full potential of an interdisciplinary approach to quantifying weathering and atmospheric inputs to the soil geochemical reserve.

This research is significant in that the project 1) provides integration of geochemical, pedological and ecological principles to quantify the importance of weathering inputs in sustaining ecosystems along topographic gradients; 2) critically tests our understanding of mineral weathering potential in a variety of environments; 3) fosters the development of robust, quantitative, interdisciplinary methods that bring pedology more squarely into biogeochemical research.

1.3 Dissertation Format

My dissertation consists of five chapters: an inclusive introduction (Chapter 1), two data chapters, (Chapters 2 and 3) and a general conclusions section (Chapter 4). Chapters 2 and 3 were written as separate manuscripts to be submitted for publication in the peer-reviewed scientific journals listed below after their respective scope is focused, and after the addition of ancillary data analysis. Consequently, some redundancy exists among these two manuscript chapters. Chapter 2, "Topographic influences on soil development in high elevation catenas of the Rocky Mountains, Colorado, U.S.," will be reformatted and submitted to either the journal Catena or Geoderma. Chapter 3, "The generation and redistribution of soil cations in high elevation catenary sequences in the Fraser Experimental Forest, Colorado, U.S.," will be reformatted and submitted to the journal Geoderma. These chapters will be submitted for publication the last half of 2017. There is no stand-alone methods section in the dissertation, as methods are discussed in each manuscript. Each manuscript chapter also contains an introduction and conclusions section, so the traditional literature review and introduction (Chapter 1), as well as the overall conclusions are intentionally succinct, in an attempt to provide an overview of the entire dissertation and recapitulate and incorporate the results from the manuscript chapters.

REFERENCES

Amundson, R., Jenny, H., 1991. The place of humans in the state factor theory of ecosystems and their soils. Soil Science. 151 (1), 99-109.

Anderson, S.P., Dietrich, W.E., Brimhall, G.H., 2002. Weathering profiles, mass-balance analysis, and rates of solute loss: Linkages between weathering and erosion in a small, steep catchment. Geological Society of America Bulletin. 114 (9), 1143-1158.

Bern, C.R., Chadwick, O.A., Hartshorn, A.S., et al., 2011. A mass-balance model to separate and quantify colloidal and solute redistributions in soil. Chemical Geology. 282 (3-4), 113-119.

Berner, E.K., 1983. The natural geochemistry of our environment - Speidel, DH, Agnew, AF. American Scientist. 71 (3), 309-309.

Blouin, M., Hodson, M.E., Delgado, E.A., et al., 2013. A review of earthworm impact on soil function and ecosystem services. European Journal of Soil Science. 64 (2), 161-182.

Brimhall, G.H., Alpers, C.N., Cunningham, A.B., 1985. Analysis of supergene ore-forming processes and groundwater solute transport using mass balance principles. Economic Geology. 80 (5), 1227-1256.

Brimhall, G.H., Chadwick O.A., Lewis, C.J., et al., 1992. Deformational Mass-Transport and Invasive Processes in Soil Evolution. Science. 255 (5045), 695-702.

Chadwick, O.A., Brimhall, G.H., Hendricks, D.M., 1990. From a Black to a Gray Box - a Mass Balance Interpretation of Pedogenesis. Geomorphology. 3 (3-4), 369-390.

Chadwick, O. A., Kelly, E.F., Merritts, D.M., 1994. Carbon-dioxide consumption during soil development. Biogeochemistry. 24 (3), 115-127.

Egli, M., Fitze, P., Mirabella, A., 2000. Formulation of pedologic mass balance based on immobile elements: A revision. Soil Science. 165 (5), 437-443.

Ewing, S.A., Sutter, B., Owen, J., et al., 2006. A threshold in soil formation at Earth's arid-hyperarid transition. Geochimica et Cosmochimica Acta. 70 (21), 5293-5322.

Gislason, S. R., Oelkers, E.H., Eiriksdottir, E.S., et al. 2009. Direct evidence of the feedback between climate and weathering. Earth and Planetary Science Letters. 277 (1-2), 213-222.

Huggett, R.J., 1975. Soil landscape systems – model of soil genesis. Geoderma. 13 (1), 1-22.

Humphreys, G.S, Wilkerson, M.T., 2007. The soil production function: a brief history and its rediscovery. Geoderma. 139 (1-2), 73-78.

Jenny, H., 1941. Factors of soil formation; a system of quantitative pedology. New York, London, McGraw-Hill.

Jenny, H., 1980. The soil resource: origin and behavior. New York, Springer-Verlag.

Kump, L.R., 2000. What drives climate? Nature. 408 (6813), 651-652.

Likens, G. E., Bormann, F.H., Johnson, N.M., et al., 1967. Calcium magnesium potassium and sodium budgets for a small forested ecosystem. Ecology. 48 (5), 772-&.

Litaor, M.I., 1992. Aluminum mobility along a geochemical catena in an alpine watershed, Front Range, Colorado. Catena. 19 (1), 1-16.

Milne, G., 1935a. Some suggested units of classification and mapping, particularly for East African soils. Soil Research. 4, 183-198.

Porder, S., Clark, D.A., Vitousek, P.M., 2006. Persistence of rock-derived nutrients in the wet tropical forests of La Selva, Costa Rica. Ecology. 87, 594-602.

Ricklefs, R.E., 2010. The economy of nature. 6th ed. New York: W.H. Freeman.

Schaetzl, R.J., Anderson, S., 2005. Soils: genesis and geomorphology. Cambridge Press, Cambridge.

Schimel, D.S., Braswell, B.H., Holland, E.A., et al. 1994. Climatic, edaphic, and biotic controls over storage and turnover of carbon in soils. Global Biogeochemical Cycles. 8 (3), 279-293.

Schimel, D.S., Stiwell, M.A., Woodmansee, R.G., 1985. Biogeochemistry of C, N, and P in a soil catena of the Shortgrass Steppe. Ecology. 66 (1), 276-282.

Sommer, M., Schlichting, E., 1997. Archetypes of catenas in respect to matter- A concept for structuring and grouping catenas. Geoderma. 76 (1-2), 1-33.

Stallard, R.F., 1998. Terrestrial sedimentation and the carbon cycle: coupling weathering and erosion to carbon burial. Global Biogeochemical Cycles. 12 (2), 231-257.

Vitousek, P.M., 2004. Oceanic islands as model systems for ecological studies. Journal of Biogeography. 29 (5-6), 573-582.

Young, A., 1976. Tropical soils and soil survey: Cambridge University Press, Cambridge, 468 p.

CHAPTER 2

TOPOGRAPHIC INFLUENCES ON SOIL DEVELOPMENT IN HIGH ELEVATION CATENAS OF THE ROCKY MOUNTAINS, COLORADO, U.S.

2.1 Summary

It is necessary to link soil properties and their distribution across landscapes to develop a comprehensive understanding of the critical zone, in both natural and managed ecosystems (Brantley et al. 2006). However, quantifying and predicting soil properties in mountain ecosystems across broad scales is challenging due to the inherent topographic variation (including and driven by slope position, aspect, elevation, underlying geology, etc.) in these ecosystems. As such, mountain ecosystems contain a diverse representation of soil properties in part due to large local topographic variations. A soil-landform model for mountain hillslopes (Wysocki et al. 2000; Schoenberger et al. 2012) was evaluated for the first time using the relationships between topography and selected soil properties along eight hillslope catenas within the Fraser Experimental Forest, Colorado, USA. Soil pits and cores were excavated, pedons were described, and soil samples from each genetic horizon were analyzed for chemical and physical properties. Systematic variability in soil properties along these mountain hillslopes allowed for the development of a coupled pedogenic and hydrologic conceptual model. Hydrologic functioning is conditioned by local topographic conditions and has resulted in 1) mountaintop landscapes with thin, pedogenically young soils in erosional environments, 2) relatively thick mountainflank soils marked by elluvial horizons and clay and sesquioxide enrichment, and 3) mountainbase landscapes that contain wetland soils accompanying riparian corridors containing high concentrations of soil carbon held in relatively thick sequences of O

and A soil horizons. In these mountain ecosystems water originating from snowmelt translocates soluble constituents and soil material downslope through soil horizons of higher hydraulic conductivity creating observable linkages and patterns. Also, surprisingly high percentages of silt and clay were detected in surface horizons along soil catenas, corroborating the importance of the role of regional dust deposition in soil formation across landscapes at FEF. The conceptual model and soil data presented here demonstrate the utility of employing the mountain hillslope geomorphic model to critical zone and/or pedologic research efforts.

2.2 Introduction

Soil properties are a product of the relative contribution of the soil forming factors—climate, organisms, relief, parent material, and time (Jenny 1941; 1980). These factors are effectively independent from each other at the space and time scales usually considered for studies of soil development. However, the biological, physical and chemical components within ecosystems are highly interrelated, and the feedbacks among components can create complex soil patterns. The ability to classify soils into distinct units and to predict their properties based on these units has traditionally led to the ability to make predictions for land management effects, such as farming, ranching, silviculture, commercial development, and conservation. Soil properties are influenced by landscape features and ecosystem dynamics, and subsequently are susceptible to land use changes (both natural and anthropogenic). Ecosystem dynamics are regularly affected by land disturbances such as fire, development, and pine beetle infestation (Jenkins et al. 2014; Collins et al. 2011, Palik, et al. 2002). Computational models are used to predict soil evolution, soil moisture dynamics, and climate change; models are also used to drive land management decisions surrounding nutrient management and water quality (Thompson and Kolka, 2005; Cao, et al. 2006). Evaluating soil properties at the landscape scale allows scientists to assess the extent to which ecosystems respond to global change drivers across multiple scales, alas, attempts to integrate soils into global and regional simulation models emphasize the temporal and spatial complexities associated with these systems (Schimel et al., 1994).The ability to accurately predict soil forming processes, and hence, soil property variability, is critical to the accuracy of such models and continues to be a significant limitation (Opolot et al. 2015).

Soil-geomorphic associations of mountain landscapes are often poorly understood based on inherent hillslope scale and slope complexity. Mountainous regions owe much of the variability in soil properties to the wide range of topographic conditions that modify or alter other soil forming factors (Badia et al. 2012). For this reason, it becomes difficult to generalize soil properties in these environments, where soil forming factors do not operate independently of one another. Soil properties such as soil mineralogy, soil carbon, and/or soil hydraulic conductivity may be difficult to predict in mountain ecosystems due to variability in precipitation, temperature, geology, and land use (Loescher et al. 2014; Price et al. 2010). Topography (e.g., aspect, landscape position and landforms types) conditions the geologic template for the ecosystem and fundamentally modifies the relationship between hydrological and biogeochemical processes. The coupling of hydrological and biogeochemical processes is reflected in soil morphological, physical, and chemical properties along soil hillslopes (Moore et al. 1993; Birkeland 1999; Lozano-Garcia et al. 2014).

Mountainsides are often characterized by long and complex backslopes, steep slope gradients, diverse sediment mantles, and complex near-surface hydrology. A recent model of soil-landform relationships on mountain hillslopes identifies distinct geomorphic components relative to the slope position (Wysocki et al. 2000; Schoenberger et al. 2012). Landform positions classified with this hillslope model include a transition from a crest (or summit) at the highest elevations; to a mountain side slope (or flank) that is long, complex, and colluvium mantled; to a mountain base near the transition between colluvial and alluvial dominated material. While these landscape position descriptors have generally been accepted in the scientific community, little to no work has confirmed the soil-landform relationships of this mountain hillslope geomorphic model.

The goal of this study was to identify linkages within and among mountain landscapes by evaluating key soil properties that are closely coupled to variations in water flow within and among a continuum of soils representative of landscapes of mountain ecosystems. The specific objective of this research was to link soil property variations and local hydrologic processes to the geomorphic components presented by Wysocki and Schoenberger— with the intention of establishing a template for detailed pedologic and biogeochemical research and/or modeling in mountain ecosystems. Our ability to predict the distribution of soil properties in mountain ecosystems will benefit researchers and land managers into the future.

2.3 Methods

2.3.1 Study Site Description

The research was conducted at Fraser Experimental Forest (FEF), Grand County, Colorado (Figure 2-1). FEF was established by the USDA in 1937 and has been the subject of long-term hydrology and forest management research and monitoring. FEF is located 130 km northwest of Denver, Colorado and lies in the Sulfur Ranger District of the Arapahoe-Roosevelt National Forest. The mean annual temperature at FEF is 1ºC and ranges from -40ºC and 32ºC annually. Mean annual precipitation is 71-76 cm, with two thirds of the mean annual precipitation falling as snow (Alexander and Watkins 1977). The geology of FEF consists primarily of felsic to intermediate composition metamorphic and igneous rocks; sedimentary rocks are less extensive. Alpine land consists of a mixture of rock fields and vegetated areas consisting of grasses, shrubs, and willows. The forested lands consist of a mixture of Lodgepole pine, Engelmann spruce, subalpine fir, and quaking aspens. Treeline at FEF exists between 3300-3500 m. Riparian areas and their associated wetlands consist of a mixture of grasses, sedges, and willows, among others. The soils of FEF are generally young and weakly developed. Soil orders that have been previously identified in FEF include the Inceptisols, Entisols, Alfisols, and Histosols (Retzer 1962).

The topography is dominated by steep, high mountain slopes. Mountaintop areas are generally narrow and are somewhat round, as opposed to having an abrupt, sharp peak. The mountainflank landscape position is generally steep and variable in its degree of recent slope movement. Some of these areas are quite hummocky, most likely due to relic glacial features; while others have relatively smooth slopes. Mountainflank slopes can approach 60%; the majority of slopes are less than 40%. Mountainbase sites are relatively flat—the mean slope of sites in this study is 7%; slopes ranged from 0%-15% (Table 2-1).

2.3.2 Study Site Selection

The catenary sequences selected for study were identified within 4 watersheds in the Fraser Experimental Forest: Byers Creek, East St. Louis Creek, Fool Creek, and Iron Creek (Figure 2-1). For this study two catenas were established in each watershed. Each catena consisted of 5 sites (e.g. the geomorphic components presented by Wysocki and Schoenberger): starting in the higher elevation mountaintop position of a landscape and ending in a lower elevation slope or riparian wetland (Figure 2-2). The highest elevation site within each catenary sequence is located in such a manner that they are not considered to be modified by other topographic elements of the catena. Mountaintop landscapes within soil catenas at FEF were either in forest or in alpine vegetation. Mountainflank positions within each catenary sequence are for the most part in forest cover; the exception is site EU2, which is above treeline. The data along the mountainflanks are separated into thirds when presenting as such is appropriate (upper third, center third, lower third). The mountainbase positions are in landscapes with a combination of wetland grasses and forest vegetation. A total of 40 pedons were identified and characterized; 10 per watershed. Catenas were identified for study so that differences in lithology along the landscape were minimized; the dominant geology along the catenas was that of quartzo-feldspathic metamorphic rocks, such as hornblende and biotite gneiss.

2.3.3 Soil Sampling and Analysis

At each of the 32 upland sites, a soil pit was excavated to the maximum depth allowable by hand, and that was "that portion of a C or R horizon which is easily obtainable but reasonably distant" below the solum (Buol et al. 1997). Soils were described in the field and subsequently sampled by genetic horizon. Approximately 1-2 kg of soil was taken from each genetic horizon for laboratory characterization and analysis. The eight mountainbase landscape soils were sampled by hand coring; these cores were extracted and sealed in the field and transported to Colorado State University for further description, sampling, and analysis in the laboratory.

Laboratory analyses included determination of soil texture, pH, total carbon and nitrogen. Soil texture was determined using the hydrometer method (Gavlak et al. 2003). Total carbon and nitrogen were determined on a LECO Tru-Spec CN analyzer (Leco Corp., St. Joseph, MI, USA). The detection limit for C and N analysis was 0.01%. Soil pH was determined using the 1:1 water pH method (NRCS 2004). Mean soil pH, C, N, and C:N by genetic horizon and landscape position are presented.

A pedogenic index based on clay translocation and accumulation was used to estimate relative differences in soil development along the catenas (Harden 1982; Walker and Green 1976). Clays in weathered soil horizons were compared to the C horizon, assuming the C horizon represents unweathered parent material (Bilzi and Ciolkosz 1977a) using the following equation:

$$e = \left(\left(\frac{C_h}{C_p}\right) C_p\right) * 100$$

where e is the percent pedogenic enrichment, C_h is the maximum percent of clay in the weathered soil horizon, and C_p is the percent clay in the C horizon.

2.4. Results and Discussion

2.4.1 Soil Classification

Geomorphometric differences between sites contribute to a particular set of soil properties and, in turn, its classification. The subgroup classification of the soils along the catenas is given in table 2-1. Representative pedons according to the three major landscape elements along the soil catenas are shown in figure 2-3. Soils in mountaintop landscape positions were pedogenically young—the least developed; these soils belong to the great groups Haplocryepts, Cryorthents, or Ustorthents. Soils are better developed along catenas in lower landscape positions—Alfisols (Haplocryalfs and Hapludalfs) occur in the mountainflank positions only. Soils in the mountainbase landscape position, which are all from riparian corridor wetlands, belong to the great group Cryofibrists.

2.4.2 Morphological Properties

Total excavated soil profiles along the catenas varied in depth from 48-202 cm (Table 1-A-1). Soils in the higher landscape positions had thinner A horizons (Figure 2-4), and increased in thickness downslope. A horizon thicknesses ranged from 3-15 cm. Organic horizons also increased in thickness moving downslope. B horizons reached a maximum thickness in the lower third mountainflank position; this landscape position marks the maximum accumulation of soil material from upslope and maximum soil development along the catenas.

Mean weathered profile depth (A+B horizons) within mountaintop positions was 39 ± 9 cm (Figure 2-5). Mountaintop landscapes contain organic horizons varying in thickness from 1-5 cm when present (Table 1-A-1). Soils within these landscapes contained A horizons that varied in thickness from 3-13 cm. A horizons within the mountaintops were the thinnest among the landscape positions. Not only are these summit soils weakly developed due to low soil moisture, these data provide evidence of erosional processes contributing to their weak development (Birkeland 2003). C horizons begin at a highly variable depth of 10-90 cm below the ground surface.

The greatest degree of pedogenesis in soils along these catenas is exhibited in the mountainflank landscapes. Mountainflank landscapes contain organic horizons that vary in thickness from 1 cm to 8 cm (Table 1-A-1). Mean soil depth in mountainflank positions was 112 ± 6 cm (Figure 2-5). Elluvial (E) horizons (8-35 cm thickness) were only found in mountainflank positions. The lower elevation catenas in the Byers Creek and East St. Louis Creek watersheds contained sites with relatively well developed Bt horizons. That mountainflank subsoil horizons along the BU and EU catenas contained nearly enough clay to be classified as argillic. B horizon thickness increases as elevation decreases through the mountainflank landscapes (Figure 2-4).

Mountainbase landscape soils had the lowest total soil depths along the catenas (Figure 2-5), however, these soils contained thickest O horizons (up to 46 cm) (Table 1-A-1). (Figure 2-4). Generally, soils in the mountainbase landscapes consisted of sequences of O and A horizons underlain by gleyed B or C horizons. B horizons in the mountainbase landscapes are thinner than the upland landscapes immediately upslope from them, as these soil landscapes are young compared to the mountainflanks. Wetland soil ages in the mountainbase landscapes of FEF have been calculated to a maximum of 4,450 years (unpublished data). Soil ages in the uplands are conservatively based on the timing of most recent regional glacial retreat (12,000 years maximum).

The surface mineral horizons in upland soils color ranged from very dark brown (10 YR 3/3) to dark yellowish brown (10 YR 4/4) (Table 1-A-1). These A and horizons are high in organic matter relative to other mineral horizons, lending to their low color values. B horizons along mountaintop and mountainflank landscapes were similarly colored; the most common B horizon soil color in these landscapes was 10 YR 4/6 (Table 1-A-1). The yellowish color of these horizons is due to the presence of the Fe mineral goethite (FeOOH), which is a very effective pigmenter in soils. Goethite is stable in environments that are periodically saturated. Mountainflank landscape soils were the only landscapes that contained elluvial horizons—the E horizons are lighter than adjacent horizons, with the most common color being 10 YR 5/3 (Table 1-A-1). The soil horizon thicknesses and colors in the mountaintop and mountainflank landscapes are indicative of: SOM decreasing with soil depth and elevation, leaching of ions through soil water movement, and the accumulation of sesquioxides in B horizons.

Soils that are poorly drained and are saturated for an extended period of time are grey in color due to the reduction of Fe and loss of pigment—soil colors in these conditions mirror the color of the soil parent material. Each site in the mountainbase landscape position contained horizons with gleyed colors with (Table 1-A-1), although the Bw horizon of this site had a depleted matrix color (value of 2), indicating extended periods of saturation. This site was in a slope wetland, so episodic periods of saturation are expected. Sites I contained subsurface horizons with 5-20% 5 YR 5/6 redox concentrations. None of the upland sites contained horizons with gleyed colors, as all of these landscapes are well drained.

Soil structure was least developed in mountaintop landscapes. Mountainflank landscapes contained soils with better developed and larger soil structure (Table 1-A-1). The majority of A horizons along the catenas exhibited granular structure. This soil structure was formed where sufficient organic material has been added from biologic activity. Blocky soil structure was primarily found in the subsoil, mostly in B horizons, and occasionally in E horizons. These horizons are formed as particles are aggregated into blocky peds through the process of alternating wetting and drying of the profile, and are indicative of the most stable soil landscapes.

2.4.3 Soil Particle Size

Laboratory particle size analyses revealed that soil horizons were predominantly sandy clay loam (SCL) or clay loam (CL) (Table 1-A-1). The data show that many sites along the catenas had their highest relative clay percentage in the surface horizons. Along all upland landscapes, silt + clay % (Si+C) is higher in the surface mineral horizon than in the subsurface mineral horizons (Figure 2-6). Mountaintop landscapes show the largest difference in (Si+C) values between surface and subsurface mineral horizons. Mountainbase landscapes do not display the same disparity between surface / subsurface silt + clay % (surface—mean = 51 ± 3%; subsurface— mean = 50 ± 4%) as do mountaintop or mountainflank landscapes. The high percentage of clay in the surface horizons of soils was contrary to traditional expectations of clays being translocated down-profile and accumulating in B horizons. In other words, the B horizon often contains the highest percentage of clay within a soil profile. Conversely, soils at FEF are relatively weakly developed and, in turn, pedogenic processes have not resulted in well expressed argillic subsoil horizons. In the Soil Survey of Fraser Alpine Area (1962), Retzer points out that silt deposits are noticeable during winters here, that they vary in extent from year to year, and that it is not known to what degree these deposits influence soil development at FEF. The trends in (Si+C) values among landscapes presented here provides evidence that secondary depositional processes (e.g. lateral movement across landscapes or atmospheric deposition) may play an important role in soil formation (Rhoades et al. 2010; Retzer 1962; Eger et al. 2012).

2.4.4 Pedogenic Enrichment

I considered landscape positions that are above or below the mean pedogenic enrichment value (*e*) for a particular catena as a means to determine whether that site had experienced clay loss laterally or deep in the profile or clay gains from upslope. Pedogenic enrichment was highest in MT and CT (Figure 2-8). Mountaintop *e* values are surprisingly high, (82 ± 19%), as soils in this landscape position displayed the lowest amount of soil development based on morphological observations. Multiple sites in the mountaintop landscape position have soils that exhibit a large degree of pedogenic enrichment (Figures 2-7a and 2-7b). Dust events in FEF have been previously documented (Retzer 1962; Rhoades et al. 2010) and my soil textural data supports the idea that atmospheric deposition of fine soil particles is an important mechanism and must account for pedogenic enrichment in mountaintop and mountainflank landscapes. Mountainflank soils at FEF demonstrate the greatest degree of pedogenesis based presence of both albic and argillic horizons, B-horizon depth, and high pedogenic clay enrichment. Enrichment data suggests that mountainflank landscapes receive clay from upslope. Calculated pedogenic enrichment values in the mountainbases were the lowest among the landscapes. Mountainbase landscape elements are dominated by cumulative processes and the soils can be deep, although the sampling procedure did not allow for sampling the full depth of the parent material in these landscapes. Hence, the *e* values for the mountainbase landscapes may not be as revealing as for the upland landscape positions. The distribution of *e* values within soil profiles and along soil catenas suggests that lateral translocations of clay are an important mechanism for the redistribution of soil materials in FEF landscapes.

2.4.5 Soil Carbon and Nitrogen

C values in the mineral horizons ranged from 0.1% (BU2 C-horizon) to 18.3% (IU3 A-horizon) (Table 1-A-1). Total carbon in A horizons was highest in the mountainbase landscapes (mean = 13.2 ± 3.3%), and lower along the upland landscapes, with the exception of the center third mountainflank (mean = 13.2 ± 2.3%). The E horizons exhibit unsystematic increases and decreases in carbon with depth along the three mountainflank subdivisions. However, carbon increases in E horizons as elevation decreases along the catenas. Carbon in B horizons increases from the mountaintop to mountainbase landscapes. Total carbon in C horizons exhibits no strong trend moving down catena, though the C horizon contains the least amount of soil carbon within each landscape position.

Soil carbon concentrations are controlled by the balance between biomass production and decomposition. Carbon concentrations in FEF forests are comparable to published data (Baritz et al. 2010; Schulp et al. 2008). Rates of decomposition are low at lower temperatures and the relatively cold mountaintop landscapes favor soil C preservation. Soil C in mountaintop landscapes appears to be controlled by the %C in their A horizons, as %C did not vary within O horizons in this landscape. Carbon in upland landscapes has accumulated in O and A horizons due to these horizons having favorable conditions for microbial activity (Hernandez et al., 2009). The decrease in soil C with increasing soil depth is evidence for where C is being deposited (the surface). Soil carbon in B horizons along the catenas is likely related to the increases in clay % in these horizons. Landscape position along soil catenas affects soil moisture and effectively, the stock of soil C. Mountainbase landscapes owe their high soil C values to the input of below ground root systems associated with wetland grasses (Meersmans et al. 2009) and high soil moisture content—these soils are in the wettest moisture regime as evidenced by their soil morphology. Land cover and soil wetness likely exhibit a substantial control over soil C values at FEF.

As was the case with soil C, soil N values also decrease with increasing soil depth (Table 2-2). The highest soil N value, 2.3%, was recorded in the Oe horizon at FL5 (Table 1-A-1). Soil N along the catenas was highest in mountainbase landscapes and among all soil horizons highest in the O horizons (Table 2-2). The A horizons contained the highest mineral horizon soil N across the landscapes, with the exception of the E horizons in the lower third of mountainflanks (mean = 0.5 ± 0.4%). Soil nitrogen in B horizons along landscapes shows a slightly positive trend moving from mountaintop to mountainbase; this trend is evident in C horizons as well.

Nitrogen concentrations followed the same trend across landscapes as did soil carbon, as nitrogen in organic matter is the main source for soil N. The decrease in N with soil depth in soil profiles is due to increasing distance from the source of soil N. The increase in soil N with increasing distance down catena is due to increased soil moisture downslope. Increased and/or increased N deposition are plausible explanations for the higher soil N in alpine mountaintop surface horizons (Baron et al. 2000). The high soil N values in mountainbase landscapes is due to the stocks of N held in O and A horizons; these areas favor preservation due to the high moisture content of these wetland soils.

2.4.5 Soil Properties and Water Movement within Landscapes

Hydrologic pathways within hillslopes are controlled, in part, by soil properties (e.g. macropore connectivity, soil texture) and exhibit a large control on soil formation. I have created a conceptual model that represents the distribution of soils and inferred hydrologic flow paths across landscapes at FEF based on soil properties (Figure 2-11).

Water derived from snowmelt is the primary agent for both the physical and chemical weathering of primary minerals during pedogenesis at FEF; snowmelt accounts for greater than 95% of annual streamwater discharge at FEF (Troendle and King, 1985). Water is released from the snowpack as it melts and infiltrates the soil surface; the yellow color of Bt and Bw horizons in the mountaintop and mountainflank landscapes implies that these horizons are periodically saturated, supporting the idea that the timing of subsurface flow generated from snowmelt influences the color of these horizons. The soil colors along the upland landscapes suggest significant illuvial accumulation of sesquioxides into subsurface horizons (relative to surface horizons) with hues close to 7.5 YR.

Infiltrated water percolates vertically until reaching E horizons; I reason that the presence/absence of well-expressed E horizons is an indicator of landscape stability, as soil morphology along the catenas has revealed various states of elluvial horizon development. Elluvial horizons are underlain by Bt or Bw horizons, which behave as a sort of aquitard, so that soil water flow becomes anisotropic at this point. Studies have discovered significant subsurface lateral flow above argillic horizons due to decreases in saturated hydraulic conductivity

(McDaniel et al. 2008; Reuter et al. 1998). I propose that the E horizons at FEF landscapes create a preferred flowpath for this snowmelt-generated subsurface lateral flow due to differences in clay content and soil structure up-profile. Upon reaching the E horizons, water is transmitted laterally down catena via subsurface lateral flow. In this sense, the E horizons act as an aquifer, and water (along with fine particles and dissolved ions) travels downslope along this preferential flowpath. Elluvial horizons exist at FEF in part due to the pulse of snowmelt that moves rapidly through the hillslopes laterally; research has suggested that this snowmelt is transmitted to streams as shallow subsurface lateral flow (Stottlemyer 2001). Presumed lateral transfers of clay as evidenced by the pedogenic enrichment data along soil catenas provides additional evidence for the existence of subsurface lateral flow along catenas. The lighter colors of the E horizons provide evidence that fine soil particles and dissolved ions have been leached from the profile and transported into lower landscapes. My data suggests that horizontal translocation of materials occurs along the catenas and is likely the dominant method of soil material transport, as the mountainflank landscapes act as corridors for translocation of fine particles and ions in solution.

Moving into lower-elevation landscapes, it is expected that soil nutrients sinks coexist with the Cryofibrist soils in the mountainbase landscape positions where elluvial horizons have discontinued and deposition of soil fines and cations has occurred. The mountainbase landscapes are poorly drained and, thus, their biogeochemical processes are greatly influenced by periods of water saturated conditions. Observations of high concentrations of soil C and N in these landscapes support this suggestion. Additionally, soils sampled in slope wetlands contained redoximorphic concentrations at depth, indicating that the period of water saturation in the mountainbase landscapes varies. The mountainbase landscapes remain pedogenically unstable due to inputs from upper landscape elements.

The soils examined at FEF fit into the mountain hillslope model of soil distribution and their properties are an expression of hydrologic flow paths and landscape stability. The presence or absence of Bt horizons in mountainflank positions may indicate 1) slope stability/instability or 2) the time elapsed since slope failure (mass movement). The presence or absence of well-expressed elluvial horizons is an additional indicator of landscape stability at FEF. The expression of argillic and albic horizons in FEF landscapes demonstrates the transitory state of pedogenic processes at work. There is no clear line to be drawn between the existences of these horizons; rather, I have discovered snapshots of the gradual development of argillic and cambic horizons in conjunction with albic horizons in FEF landscapes.

2.5 Conclusions

Soils in the Fraser Experimental Forest demonstrate properties which are conditioned by multiple soil forming factors and are linked to the larger geomorphic processes operating in complex mountain landscapes. As such, soil properties within mountain landscapes can be difficult to generalize and/or predict. The model of soil-landform relationships on mountain hillslopes presented by Wysocki and Schoenberger provides a useful framework for designing and testing landscape-scale pedogenic studies and/or models. Key findings of this work include the following:

1- Mountainflank soil landscapes had the highest pedogenic enrichment values and showed the greatest degree of soil development and horizon differentiation within all catenary sequences.

2- Sublateral flow of water and landscape stability are significant contributors to soil formation, as their contributions are exhibited in soil physical and morphological properties.

3- Mountainflank soils with cambic horizons may have experienced mass wasting relatively recently; mountainflanks containing argillic horizons may have existed in a recently more stable environment to allow for the formation of Bt horizons.

4- The larger proportions of silt+clay in near-surface horizons suggest that regional atmospheric deposition of dust may play a significant role in soil development in soils along high elevation catenas, irrespective of landscape position.

Table 2-1: Site characteristics and subgroup classifications of the soils. The watersheds represented are Byers Creek, East St. Louis Creek, Fool Creek, and Iron Creek. Sites are associated with upper (U) or lower (L) catena within its respective watershed.

Site	*Decimal Longitude*	*Decimal Latitude*	*Elevation (m)*	*Geomorphic Position*	*Slope Shape*	*Slope (%)*	*Aspect*	*Vegetation*	*Subgroup Classification*
BL1	-105.914483	39.872067	3237	MT	VV	2	N	F	Typic Haplocryept
BL2	-105.913933	39.873683	3170	UT	LL	22	NE	F	Inceptic Haplocryalf
BL3	-105.911950	39.874617	3109	CT	VL	20	NE	F	Psammentic Hapludalf
BL4	-105.908217	39.875633	3048	LT	LV	20	N	F	Inceptic Hapludalf
BL5	-105.904700	39.876983	2975	MB	CL	10	E	W	Typic Cryofibrist
BU1	-105.927310	39.880299	3368	MT	VV	5	S	F	Typic Cryorthent
BU2	-105.925560	39.879895	3322	UT	VV	25	SE	F	Typic Haplocryept
BU3	-105.923586	39.879524	3261	CT	LL	20	SE	F	Typic Haplocryept
BU4	-105.921582	39.878521	3182	LT	VL	25	SE	F	Typic Haplocryept
BU5	-105.920333	39.877267	3133	MB	LL	0-5	SE	W	Typic Cryofibrist
EL1	-105.871533	39.875717	3237	MT	LV	2	W	F	Typic Haplocryept
EL2	-105.874000	39.877433	3136	UT	LL	22	W	F	Typic Haplocryept
EL3	-105.876621	39.879221	3018	CT	CV	15	N	F	Typic Cryorthent
EL4	-105.877542	39.881091	2969	LT	VC	20	N	F	Inceptic Haplocryalf
EL5	-105.877900	39.882867	2938	MB	CL	7	NE	W	Typic Cryofibrist
EU1	-105.855033	39.845983	3633	MT	VV	5	NW	A	Typic Ustorthent
EU2	-105.858617	39.848733	3578	UT	LC	10	NW	A	Inceptic Haplocryalf
EU3	-105.862900	39.850617	3493	CT	VV	20	N	F	Inceptic Haplocryalf
EU4	-105.866517	39.853600	3353	LT	VL	15	W	F	Psammentic Haplocryalf
EU5	-105.870283	39.856867	3243	MB	LL	2	W	W	Typic Cryofibrist
FL1	-105.855467	39.874167	3386	MT	VV	5	NW	F	Typic Cryorthent
FL2	-105.856049	39.875963	3328	UT	LV	15	NW	F	Typic Haplocryalf
FL3	-105.858833	39.877567	3228	CT	LV	20	NW	F	Typic Haplocryalf
FL4	-105.860867	39.879400	3139	LT	CL	25	NW	F	Typic Haplocryept
FL5	-105.862517	39.880350	3097	MB	LL	7	NW	W	Typic Cryofibrist
FU1	-105.863648	39.860738	3499	MT	VV	5	N	A	Typic Haplocryept
FU2	-105.863344	39.863237	3472	UT	LL	8	N	F	Typic Haplocryept
FU3	-105.867059	39.869917	3435	CT	LL	10	N	F	Typic Haplocryept
FU4	-105.865700	39.865876	3374	LT	CL	15	E	F	Typic Haplocryept
FU5	-105.864373	39.874137	3219	MB	CL	15	E	W	Typic Cryofibrist
IL1	-105.922133	39.870683	3350	MT	VV	5	SE	F	Typic Cryorthent
IL2	-105.920567	39.869050	3267	UT	LV	25	SE	F	Typic Cryorthent
IL3	-105.917317	39.866367	3170	CT	CL	15	S	F	Typic Haplocryept
IL4	-105.914017	39.863267	3078	LT	VL	20	S	F	Typic Cryorthent
IL5	-105.910131	39.860637	2926	MB	CL	10	SE	W	Typic Cryofibrist
IU1	-105.938832	39.866276	3551	MT	VV	8	E	A	Typic Haplocryept
IU2	-105.936184	39.863850	3484	UT	CL	20	E	F	Typic Haplocryept
IU3	-105.934092	39.861981	3365	CT	LL	30	SE	F	Typic Haplocryept
IU4	-105.931828	39.860506	3267	LT	LL	25	SE	F	Typic Cryorthent
IU5	-105.931230	39.858309	3170	MB	LL	2	E	W	Typic Cryofibrist

Table 2-2: Mean soil pH, C, N, and C:N by soil horizon within landscape positions along the catenas. Variance is represented by the standard error of the means. MT = mountaintop, UT = upper third mountainflank, CT = center third mountainflank, LT = lower third mountainflank, MB = mountainbase.

					pH					
Landscape	MT		UT		CT		LT		MB	
Horizon	**Mean**	StdErr	**Mean**	StdErr	**Mean**	StdErr	**Mean**	StdErr	**Mean**	StdErr
O	***	***	***	***	***	***	***	***	**4.7**	0.1
A	**4.7**	0.1	**4.4**	0.1	**4.7**	0.1	**4.7**	0.1	**5.2**	0.6
E	*	*	**4.5**	0.2	**4.6**	0.1	**4.7**	0.4	*	*
B	**4.8**	0.1	**4.6**	0.1	**4.9**	0.1	**4.9**	0.1	**5.1**	0.2
C	**4.9**	0.1	**5.0**	0.1	**5.1**	0.1	**5.0**	0.1	**4.6**	0.1
					Carbon (%)					
	MT		UT		CT		LT		MB	
Horizon	**Mean**	StdErr	**Mean**	StdErr	**Mean**	StdErr	**Mean**	StdErr	**Mean**	StdErr
O	**32.5**	3.9	**25.4**	4.9	**33.8**	3.9	**32.1**	5.9	**27.7**	2.0
A	**5.3**	0.1	**5.5**	0.9	**10.8**	2.7	**4.1**	1.4	**13.2**	3.3
E	*	*	**0.7**	0.4	**1.4**	0.3	**1.9**	0.8	*	*
B	**1.3**	0.3	**2.3**	0.9	**0.7**	0.1	**1.9**	0.2	**5.1**	1.1
C	**0.7**	0.1	**0.6**	0.2	**0.5**	0.1	**0.4**	0.1	**1.2**	0.2
					Nitrogen (%)					
	MT		UT		CT		LT		MB	
Horizon	**Mean**	StdErr	**Mean**	StdErr	**Mean**	StdErr	**Mean**	StdErr	**Mean**	StdErr
O	**1.2**	0.2	**1.0**	0.2	**1.2**	0.1	**1.3**	0.2	**1.3**	0.1
A	**0.6**	0.2	**0.4**	0.1	**0.6**	0.2	**0.4**	0.2	**0.7**	0.3
E	*	*	**0.0**	**	**0.2**	0.2	**0.5**	0.4	*	*
B	**0.2**	0.1	**0.2**	0.0	**0.2**	0.1	**0.1**	0.1	**0.3**	0.1
C	**0.1**	0.0	**0.0**	0.0	**0.0**	0.0	**0.1**	0.0	**0.3**	0.2
					Carbon : Nitrogen					
	MT		UT		CT		LT		MB	
Horizon	**Mean**	StdErr	**Mean**	StdErr	**Mean**	StdErr	**Mean**	StdErr	**Mean**	StdErr
O	**28.9**	3.8	**24.2**	5.6	**27.5**	0.9	**24.3**	2.1	**24.3**	2.7
A	**19.6**	4.1	**25.6**	5.7	**28.9**	5.7	**44.3**	18.1	**25.7**	15.6
E	*	*	**63.4**	**	**41.5**	13.8	**14.5**	5.9	*	*
B	**38.0**	14.4	**22.9**	4.9	**14.0**	4.3	**14.4**	4.9	**14.9**	0.6
C	**34.3**	15.8	**14.7**	1.2	**30.4**	4.2	**28.5**	12.0	**11.4**	2.6
*	Horizon not present within landscape position									
**	No variance calculated									
***	Horizons not analyzed									

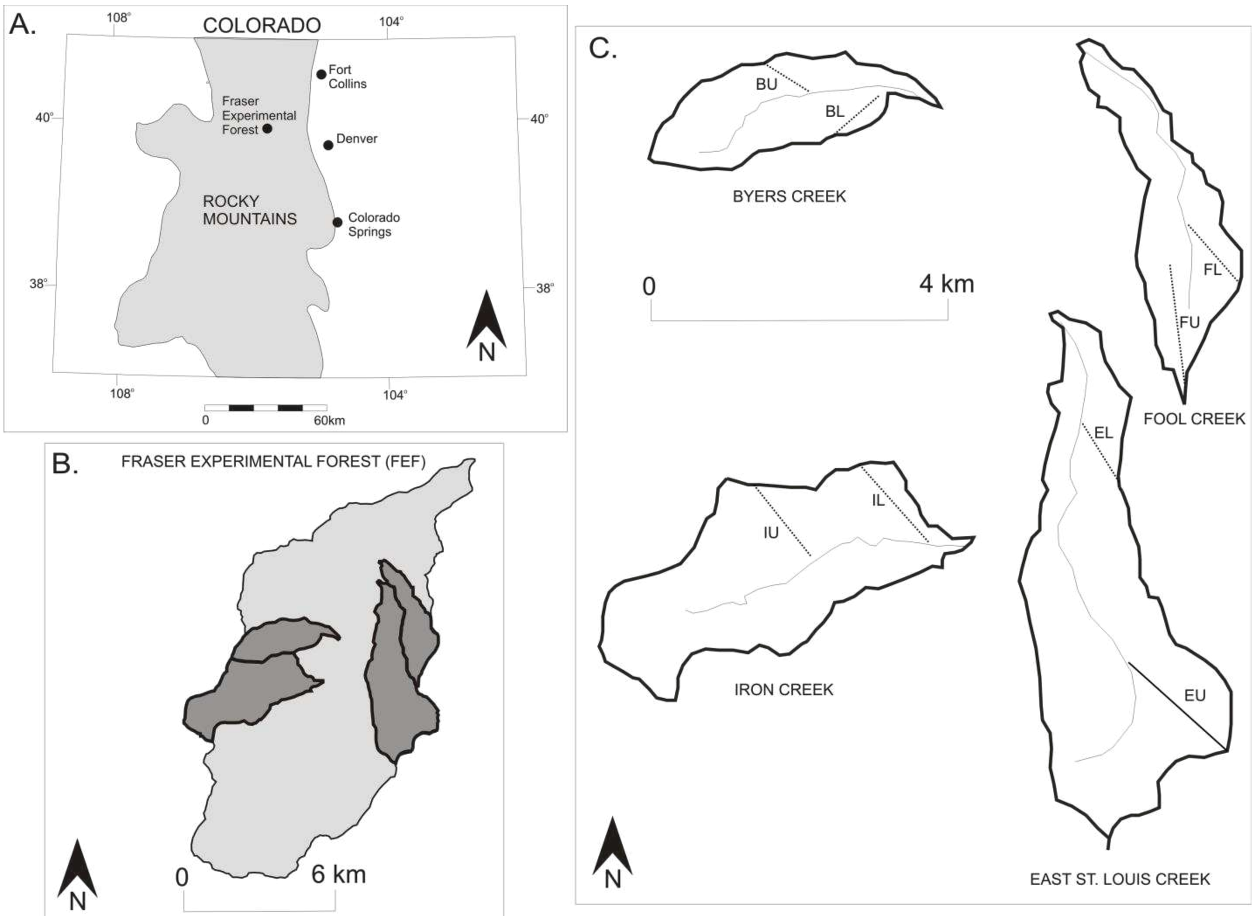

Figure 2-1. Location of the Fraser Experimental Forest, Grand County, Colorado (A). Soils were sampled from four watersheds within FEF (B). A total of eight catenas were sampled (C).

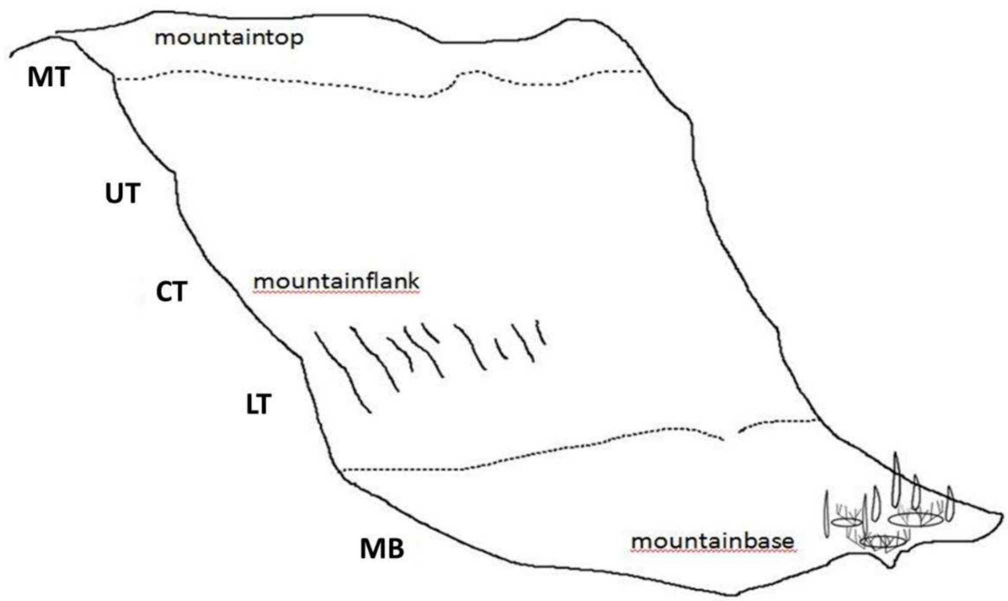

Figure 2-2. Geomorphic components for mountain landscapes. Five sites were located along each hillslope beginning in the mountaintop position and ending in the mountainbase position. MT = Mountaintop; UT = Upper Third Mountainflank; CT = Center Third Mountainflank; LT = Lower Third Mountainflank; MB = Mountainbase. Adapted from Wysocki et al., 2000.

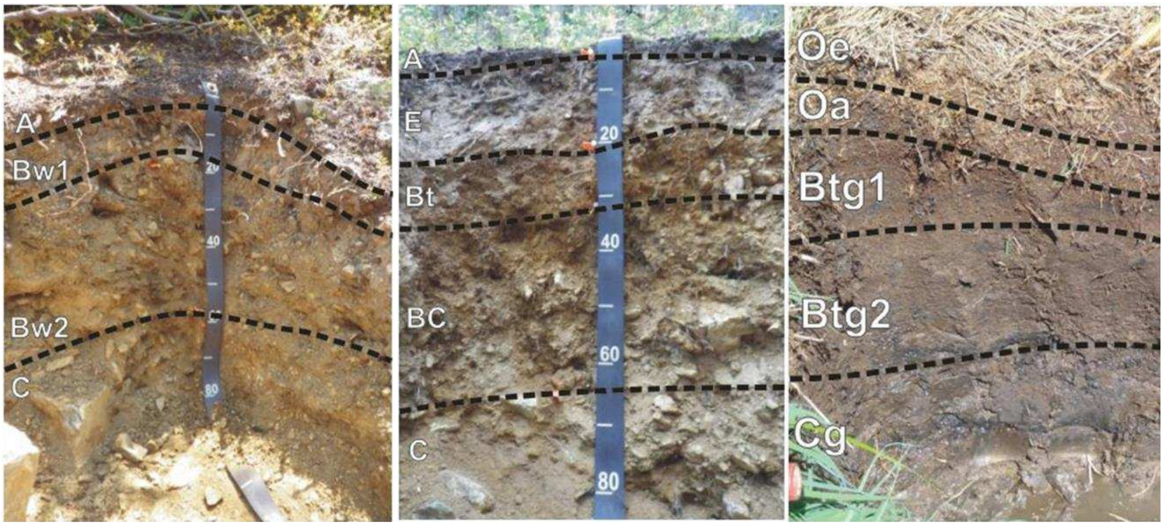

Figure 2-3. Profiles of representative pedons along the catenas. From left to right are pedons from the mountaintop, mountainflank, and mountainbase landscape positions. Mountaintop soils show minimal soil development and the shallowest among the upland landscapes. Mountainflank soils are colluvial-mantled and show the greatest degree of pedogenesis. Albic horizons are only found in this geomorphic component of the mountain slopes. Mountainbase soils exist near the boundary between colluvial and alluvial dominated landscapes. Soils in this geomorphic component contain thick, organic-rich horizons atop gleyed mineral horizons.

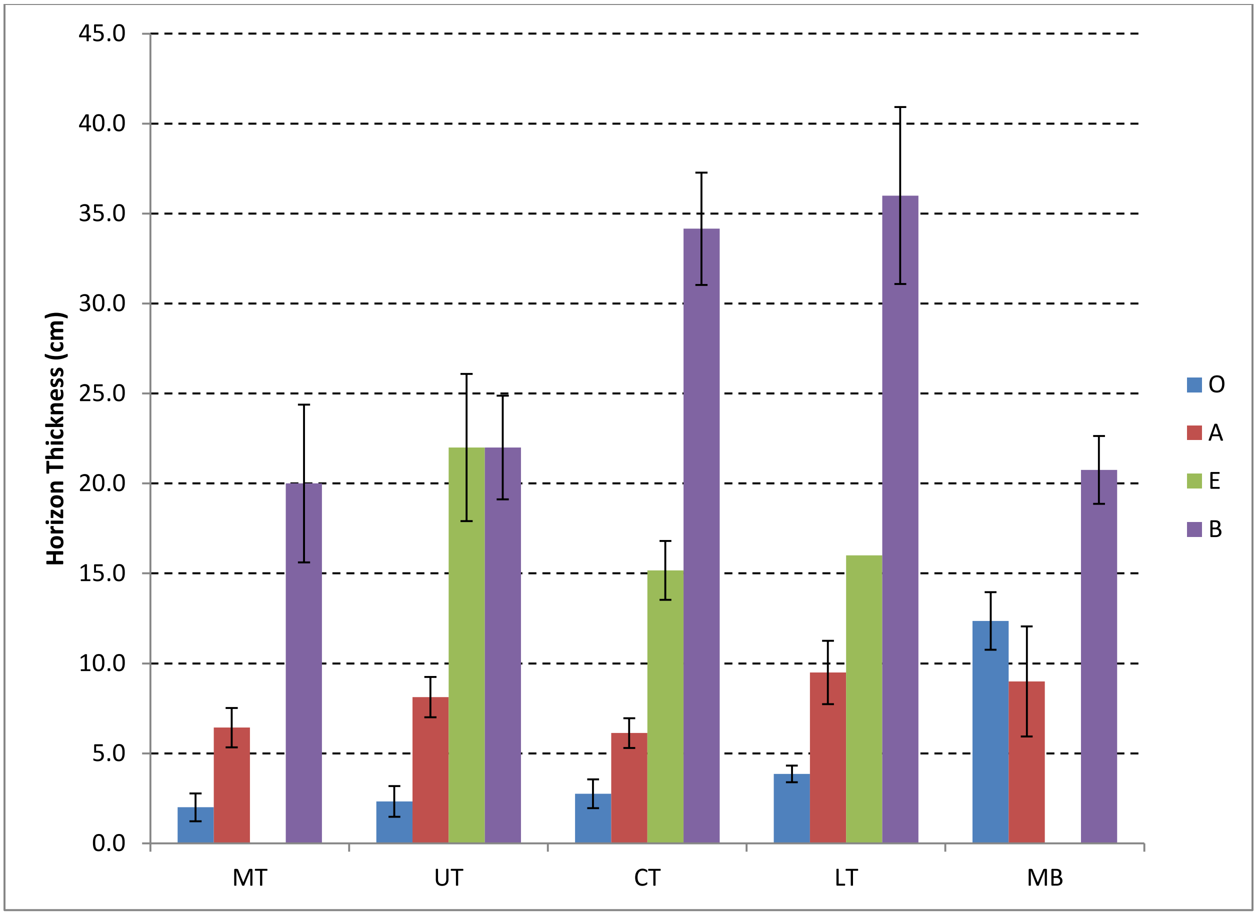

Figure 2-4. Mean horizon thicknesses across the catenas. MT = mountaintop, UT = upper third mountainflank, CT = center third mountainflank, LT = lower third mountainflank, MB = mountainbase. Error bars represent the standard errors of the mean.

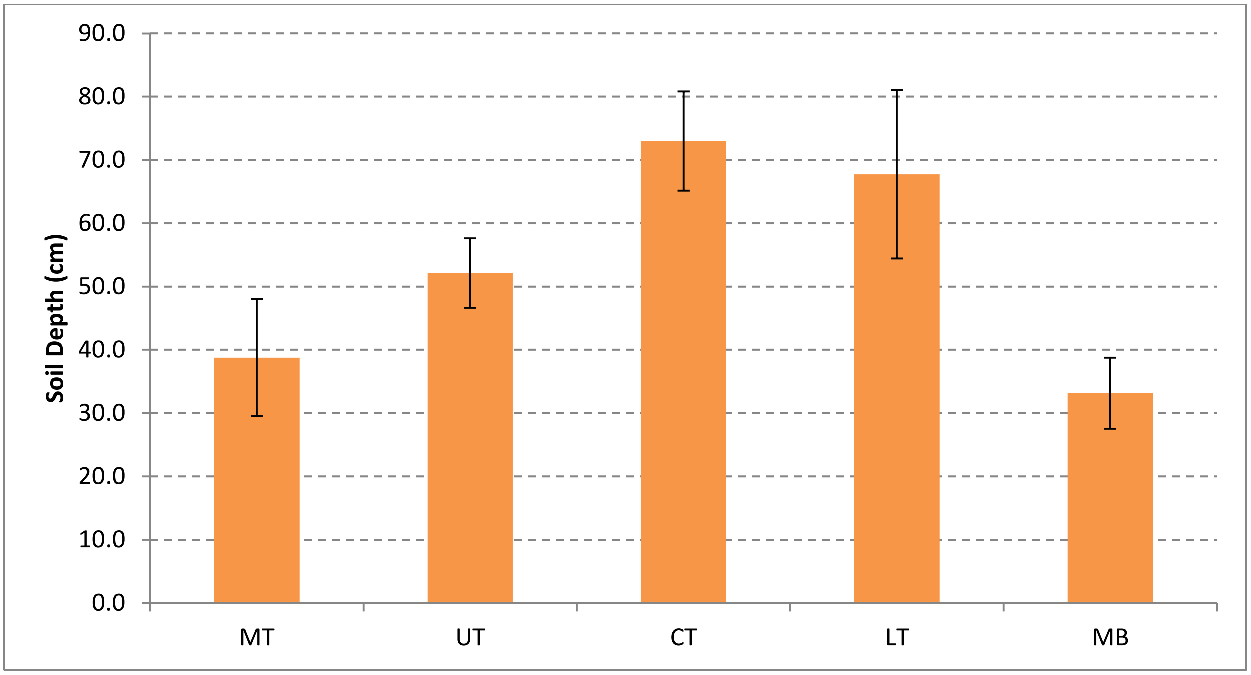

Figure 2-5. Mean soil depth along the catenas. Soil depth is reported to the top of the C horizon. MT = mountaintop, UT = upper third mountainflank, CT = center third mountainflank, LT = lower third mountainflank, MB = mountainbase. Error bars represent the standard errors of the mean.

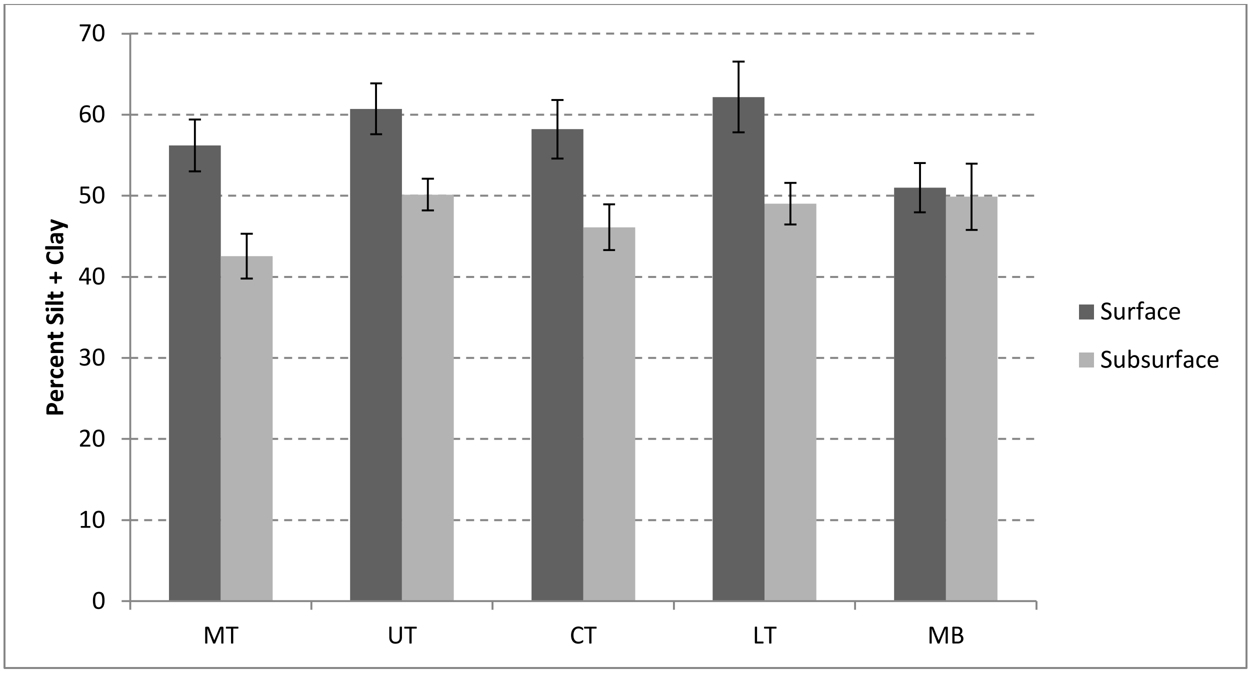

Figure 2-6. Mean percent silt + clay in surface and subsurface horizons along the catenas. MT = mountaintop, UT = upper third mountainflank, CT = center third mountainflank, LT = lower third mountainflank, MB = mountainbase. Surface horizons are the A horizons; subsurface horizons are all mineral horizons below the A horizon. Error bars represent the standard errors of the means.

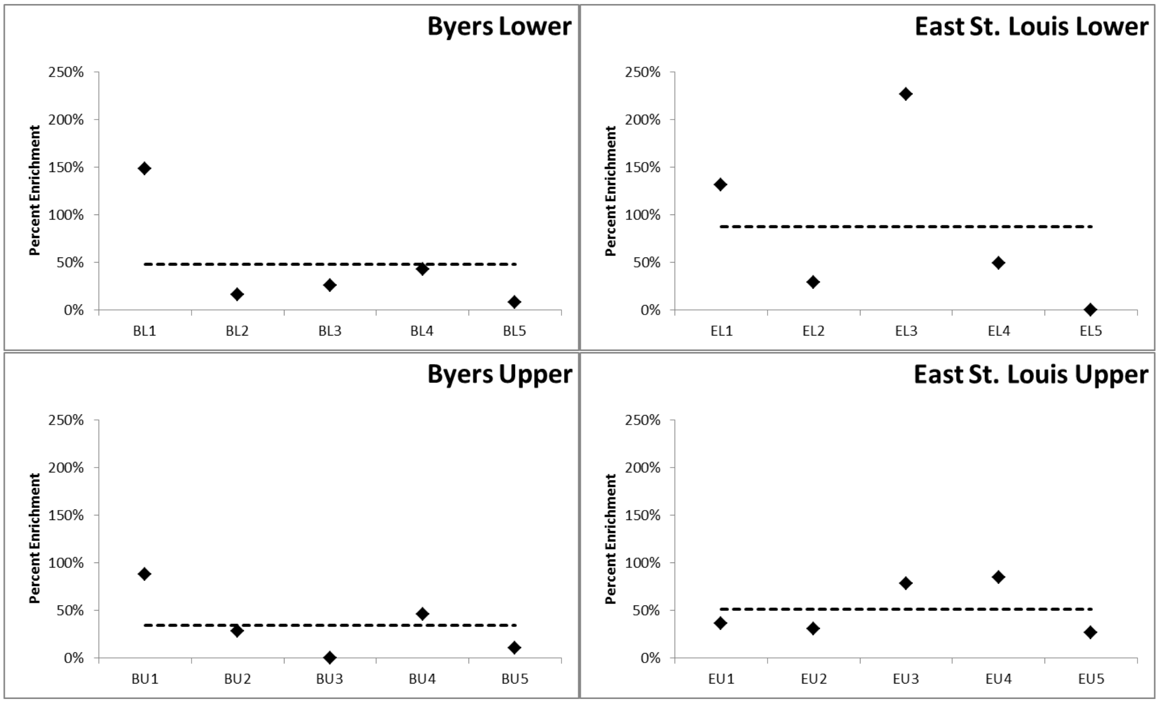

Figure 2-7a. Mean pedogenic enrichment values along the Byers Creek and East St. Louis catenas. The horizontal dashed line represents the mean pedogenic enrichment along its respective catena. Error bars represent the standard errors of the means.

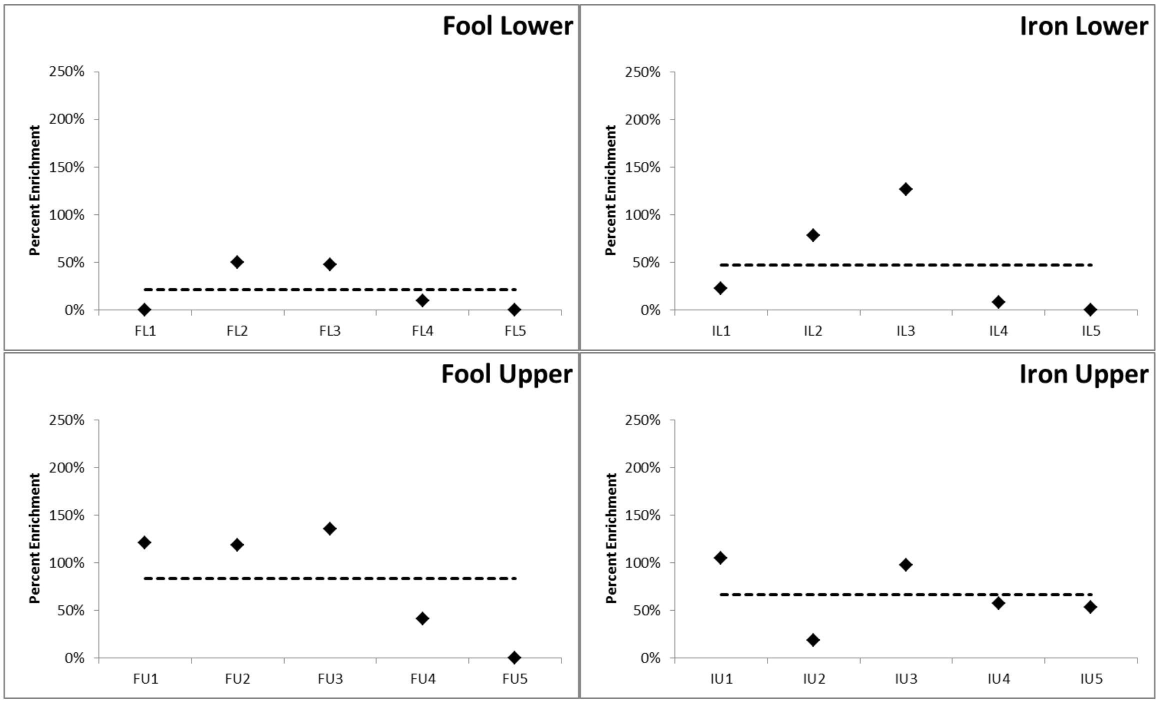

Figure 2-7b. Mean pedogenic enrichment values along the Fool Creek and Iron Creek catenas. The horizontal dashed line represents the mean pedogenic enrichment along its respective catena. Error bars represent the standard errors of the means.

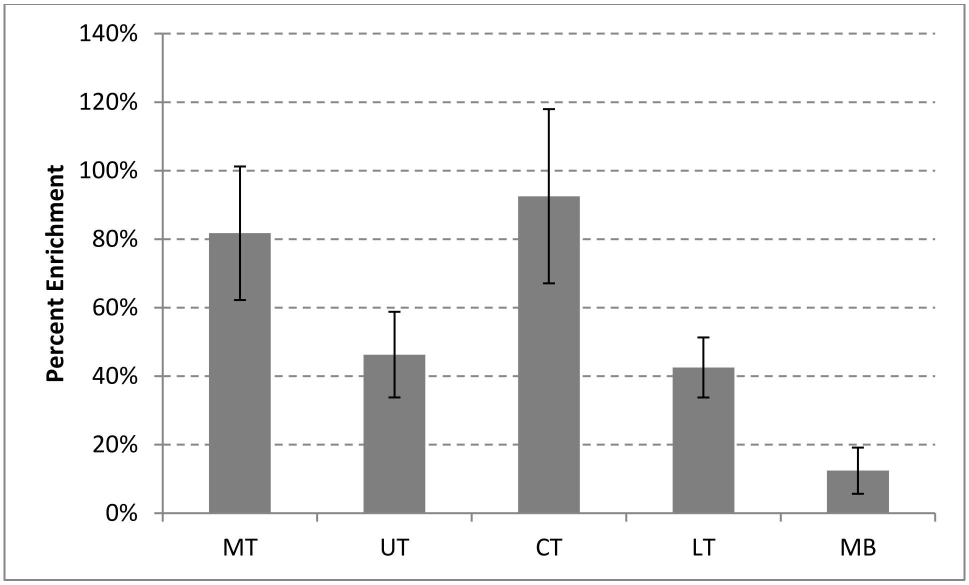

Figure 2-8. Mean pedogenic enrichment values within landscape positions along the catenas. MT = mountaintop, UT = upper third mountainflank, CT = center third mountainflank, LT = lower third mountainflank, MB = mountainbase. The mountainflank landscapes are comprised of the UT, CT, and LT positions. Error bars represent the standard errors of the means.

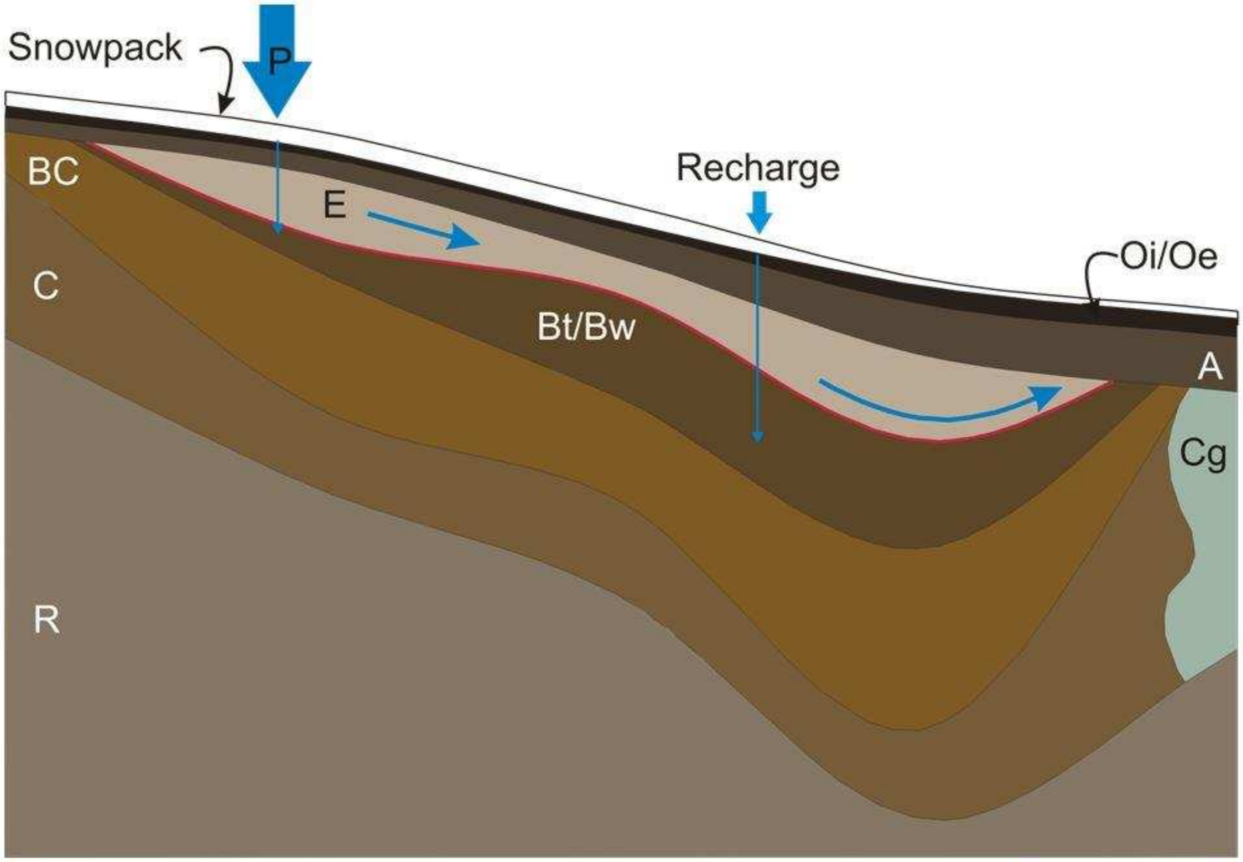

Figure 2-9. Soil-geomorphic associations and hydrology along a mountain slope at FEF. Mountaintop soils are young and weakly developed, mountainflank soils are better developed, composed of B horizons of varying states of evolution frequently overlain by E horizons. Mountainbase soils contain a large amount of soil C in their thick sequences of O and A horizons. Snowmelt, the dominant form of hydrologic recharge at FEF, infiltrates the soil surface until reaching E horizons, where subsurface lateral flow dominates the flow regime. B horizons act as aquitards and promote the anisotropic flow of groundwater in these soil systems. Wetlands and seeps occur where the E horizons terminate in the landscapes, where nutrient sinks likely exist in these ecosystems.

REFERENCES

Alexander, R.R., Watkins, R. K., 1977. The Fraser Experimental Forest, Colorado. Gen. Tech. Rep. RM-40. Fort Collins, CO: U.S. Department of Agriculture, Forest Service, Rocky Mountain Forest and Range Experiment Station. 32 p.

Badia, D., Marti, C., Aznar, J.M., et al., 2012. Influence of slope on soil genesis and classification in semiarid mountainous environments. Geoderma. 193, 13-21.

Baritz, R., Seufert, G., Montanarella, L., Van Ranst, E., 2010. Carbon concentrations and stocks in forest soils of Europe. Forest Ecology and Management. 260, 262-277.

Baron, J.S., Reuth, H.M., Wolfe, A.M., et al. 2000. Ecosystem Responses to nitrogen deposition in the Colorado Front Range. Ecosystems. 3, 532-568.

Bilzi, A.F., Ciolkosz, E.J., 1977. A field morphology rating scale for evaluating pedological development. Soil science. 124(1), 45-48.

Birkeland, P.W., 1999. Soils and geomorphology. 3rd ed. New York: Oxford University Press.

Birkeland, P.W., Shroba, R.R., Burns, S.F., et al., 2003. Integrating soils and geomorphology in mountains—and example from the Front Range of Colorado. Geomorphology. 55, 329-344.

Brantley SL, White TS, White AF, et al., 2006. Frontiers in Exploration of the Critical Zone, An NSF Sponsored Workshop. National Science Foundation, 30 pp.

Buol, S.W., Southard, R.J., Graham, R.C., McDaniel, P.A., 1997. Soil Genesis and Classification, fifth ed. Iowa State Press, Ames.

Cao, W., Bowden, W.B., Davie, T., Fenemor, A., 2006. Multivariable and multi-site calibration and validation of SWAT in a large mountainous catchment with high spatial variability. Hydrologic Processes. 20 (5), 1057-1073.

Collins, B.J., Rhoades, C.C., Hubbard, R.M., Battaglia, M.A., 2011. Tree regeneration and future stand development after bark beetle infestation and harvesting in Colorado lodgepole pine stands. Forest Ecology and Management. 261, 2168-2175.

Eger, A., Almond, P.C., Condron, L.M., 2012. Upbuilding pedogenesis under active loess deposition in a super-humid, temperate climate- quantification of deposition rates, soil chemistry and pedogenic thresholds. Geoderma. 189, 491-501.

Gavlak, R., Horneck, R., Miller, R.O., Kotuby-Amacher, J., 2003. Soil, Plant and Water Reference Methods for the Western Region. In: Soil, Plant and Water Reference Methods for the Western Region. WREP-125, pp. 129–134.

Harden, J.W., 1982. An index of soil development from field descriptions: examples from a chronosequences in central California. Geoderma. 28, 1-28.

Hernandez, V.A., Martinez, A.V., Perez, G.A., et al. 2009. Variation in soil carbon stocks in a toposequence. Agrociencia. 43, 457-464.

Jenkins, M.J., Runyon, J.B, Fettig, C.J., et al., 2014. Interactions among the mountain pine beetle, fires, and fuels. Forest Science. 60(3), 489-501.

Jenny, H., 1941. Factors of soil formation: a system of quantitative pedology. New York, McGraw-Hill Book Company, Inc.

Jenny, H., 1980. The soil resource: origin and behavior. New York, Springer-Verlag.

Loescher H., Ayres E., Duffy P., et al., 2014. Spatial variation in soil properties among North American ecosystems and guidelines for sampling designs. PLoS ONE 9(1): e83216. doi:10.1371/journal.pone.0083216

Lozano-Garcia, B., Parras-Alcantara, L., 2014. Variation in soil organic carbon and nitrogen stocks along a toposequence in a traditional Mediterranean olive grove. Land Degradation & Development. 25 (3), 297-304.

McDaniel, P.A., Regan, M.P., Brooks, E., et al., 2008. Linking fragipans, perched water tables, and catchment-scale hydrological processes. Catena. 73, 166-173

Meersmans, J., Van Wesemael, B., Van Molle, M., 2009. Determining soil organic for agricultural soils: a comparison between the Walkley & Black and the dry combustion methods (north Belgium). Soil Use and Management. 25 (4), 346-353.

Moore, I.D., Gessler, P.E., Nielsen, G.A., et al., Soil attribute prediction using terrain analysis. Soil Science Society of America Journal. 57 (2), 443-452.

NRCS, U., 2004. Soil Survey Laboratory Methods Manual No. 42.

Opolot, E., Yu, Y.Y., Finke, P.A., 2015. Modeling soil genesis at pedon and landscape scales: Achievements and problems. Quaternary International. 376, 34-46.

Palik, B.J., Mitchell, R.J., Hiers, J.K., 2002. Modeling silviculture after natural disturbance to sustain biodiversity in the longleaf pine (*Pinus palustris*) ecosystem: balancing complexity and implemtation. Forest Ecology and Management. 155 (1-3), 347-356.

Price, K., Jackson, C.R., Parker, A.J., 2010. Variation of surficial soil hydraulic properties across land uses in the southern Blue Ridge Mountains, North Carolina, USA. Journal of Hydrology. 383, (3-4) 256-268.

Retzer, J.L., 1962. Soil survey, Fraser alpine area, Colorado. Washington, D.C.: G.P.O.

Reuter, R.J., McDaniel, P.A., Hammel, J.E., et al., 1998. Solute transport in seasonal perched water tables in loess-derived soilscapes. Soil Science Society of America Journal. 62 (4), 977-983.

Rhoades, C., Elder, K., Greene, E., 2010. The influence of an extensive dust event on snow chemistry in the Southern Rocky Mountains. Arctic Antarctic and Alpine Research. 42 (1), 98-105.

Schimel, D.S., 1994. Climatic, edaphic, and biotic controls over storage and turnover of carbon in soils. Global Biogeochemical Cycles. 8(3), 279-293.

Schoeneberger, P.J., D.A. Wysocki, E.C. Benham, and Soil Survey Staff. 2012. Field book for describing and sampling soils, Version 3.0. Natural Resources Conservation Service, National Soil Survey Center, Lincoln, NE.

Schulp, C.J.E., Nabuurs, G., Verburg, P.H., de Waal, R.W., 2008. Effect of tree species on carbon stocks in forest floor and mineral soil and implications for soil carbon inventories. Forest Ecology and Management. 256, 482-490.

Stottlemyer, R., 2001. Processes regulating watershed chemical export during snowmelt, Fraser experimental forest, Colorado. Journal of Hydrology. 245 (1-4), 177-195.

Thompson, J.A., Kolka, R.K., 2005. Soil carbon storage estimation in a central hardwood forest watershed using quantitative soil-landscape modeling. Soil Science Society of America Journal. 69, 1086-1093.

Troendle, C.A., King, R.M., 1985. The effect of timber harvest on the Fool Creek Watershed, 30 years later. Water Resources Research. 21, 1915-1922.

Walker, P.H., Green, P., 1976. Soil trends in two valley fill sequences. Australian Journal of Soil Research. 14 (3), 291-303.

Wysocki, D.A., P.J. Schoeneberger, and H.E. LaGarry. 2000. Geomorphology of soil landscapes. p. E5–E39. In M.E. Sumner (ed.) Handbook of Soil Science. CRC Press, Boca Raton, FL.

CHAPTER 3

THE GENERATION AND REDISTRIBUTION OF SOIL CATIONS IN HIGH ELEVATION CATENARY SEQUENCES IN THE FRASER EXPERIMENTAL FOREST, COLORADO, U.S.

3.1 Summary

Pedogenic processes imprint their signature on soils over the course of thousands to millions of years in most soil systems. Variation in soil forming processes – such as parent material weathering, organic material additions, hydrologic processes, and atmospheric additions – account for the distribution and sourcing of cations in ecosystems, and hence exert a strong influence on ecosystem productivity. Soil nutrient dynamics of cations also provide an indication of the dominant soil forming processes at work in a particular system. To gain insight into the generation and distribution of the soil cation pool in the Fraser Experimental Forest (FEF), we combined geochemical mass balance techniques and isotopic analyses of soil geochemical data to pedons across eight soil catenas in complex mountain terrain typical of the central Rocky Mountains. We found that mass gains in FEF soils are primarily attributable to pedogenic additions of Ca to the soil mantle via atmospheric dust, and specifically that soil catenas on the summit landscapes were most enriched in Ca. Our data also show that atmospheric deposition contributions (calculated using Sr isotope ratios) to soils is as high as 82% (± 3% SD), and that this isotopic signature in A-horizons and subsurface soil horizons diverges along a soil catena, due to both vertical and lateral hydrologic redistribution processes. Our results suggest that long term soil development and associated chemical signatures at FEF are principally driven by the coupling of landscape scale cation supply processes, snow distribution, and snowmelt dynamics. Soil development models describing pedogenesis across catenas in montane ecosystems must

pay special attention to atmospheric inputs and their redistribution. Any changes to these dynamics will affect productivity and soil/water chemistry in such ecosystems as investigated here.

3.2 Introduction

Two major sources of base cations exist in terrestrial ecosystems—cations derived from parent materials (usually bedrock) and cations added via both wet and dry atmospheric deposition. Weathering processes makes nutrients, such as Ca^{2+}, biogeochemically available in terrestrial ecosystems and local bedrock weathering is a major source of nutrients for vegetation in a variety of ecosystems (Johnson, 1968; Walker and Syers, 1976). However, local weathering inputs alone may be inadequate to maintain soil fertility without the addition of exogenous cations (Capo and Chadwick, 1999; Zaccherio and Finzi, 2007). Indeed, long term additions of atmospherically-derived dust (both via dry and wet deposition) provides a key geochemical input for various terrestrial ecosystems (Stoorvogel et al., 1997; Capo and Chadwick, 1999; Okin et al., 2004) and the incorporation of dust into soil systems is an important factor in pedogenesis (Simonson, 1995; Porder et al., 2007; Lawrence et al., 2013).

Atmospheric dust has been found to contribute to soil nutrient pools in mountain ecosystems in the Mountain West and in Colorado (Clow et al., 1997, Mladenov, et al., 2012, Lawrence et al., 2013, Brahney et al., 2014). Dust may become trapped in soil crusts, exerting a pronounced influence on the concentrations of Ca, Na, K, and N at and near the soil surface (Reynolds et al., 2001; Blank et al., 1999). Human activities directly and indirectly impact dust production and, hence its potential influence in soil chemistry. It has been recognized for decades that drought conditions, in combination with agriculture and other landuses, markedly increase soil erosion and substantially contribute to airborne dust production (Middleton, 1985; Tegen et al., 1996). For instance, overgrazing by livestock has been shown to be a significant contributor to soil erosion and dust production (Niu et al., 2011; Su et al., 2005). Soil loss and production of airborne dust is also exacerbated by off-highway vehicles traveling on unpaved roads and trails (Padgett et al., 2008). It has also been suggested that wildfire may contribute to airborne dust production through the increase of wind erosion (Balfour et al., 2014; Santin et al., 2015).

Constituent mass balance techniques have been used to quantify soil weathering in a variety of ecosystems (Bern et al., 2011; Porder et al., 2007; Anderson et al., 2002) and the application of the constituent mass balance model allows for the identification of pedogenic gains that may indicate dust inputs (Chadwick et al., 1990; Egli and Fitze, 2000). This approach has been used traditionally to quantify soil development by estimating soil strain, volumetric gains or losses within a pedon (Brimhall et al., 1992). Recently, supplemental analytical techniques, such as the utilization of XRD and application of Sr isotopes have been combined with the mass balance approach to quantify soil weathering (Bern et al., 2011; Porder et al., 2007; Anderson et al., 2002).

Strontium (Sr) isotope ratios are regularly employed to determine the relative contribution of soil nutrients from differing weathering pools in ecosystems, including the importance of atmospheric processes (dust) in soil across a variety of ecosystems (Capo and Chadwick, 1999; Blum et al., 2002; Drouet et al., 2005; Chadwick et al., 2009; Reynolds et al., 2012). In studies based in arid climatic zones, where rates of soil development are strongly controlled by eolian dust (Gile et al., 1966; Gile 1979; Chadwick and Davis, 1990; McFadden et al., 1991), Sr isotopes were used to determine the provenance of Sr, and therefore Ca, available in the soil environment (Graustein and Armstrong, 1983; Capo et al., 1995). Strontium is a powerful isotopic tracer in terrestrial ecosystems is frequently used as a proxy for Ca due to their chemical similarities (Dasch, 1969; Brass, 1975). Numerous studies have demonstrated the potential of using stable Sr isotopes in quantifying atmospheric deposition in ecosystems (Graustein and Armstrong, 1983; Aberg et al., 1989; Gosz and Moore, 1989; Graustein, 1989), weathering and chemical processes in soil environments (Miller et al., 1993), and paleoenvironmental applications (Quade et al., 1995; Capo et al., 1995). Use of isotopic tracers has shown that some terrestrial ecosystems rely more on soil cations received from atmospheric deposition than from bedrock weathering (Drouet et al., 2005; Vitousek et al., 1999; Lawrence et al., 2013). To date, dust studies have been confined to alpine ecosystems, or to multiple, unconnected sites within various landscapes (Reynolds et al., 2006; Lawrence et al., 2010; Lawrence et al., 2013).

The goals of this research were to 1) determine whether landscape position along catenas imparts a control on the distribution and sourcing of soil cations in FEF and 2) evaluate the contribution of atmospherically-derived Ca to the soil cation pool in FEF soils. We focus on soil Ca here because of its chief role in ecosystem function. Soil Ca acts as a buffer to acid precipitation and surface waters, plays a main role in the base saturation of soils, and is an essential plant nutrient, exerting an important influence on the health of forest ecosystems (Richter et al., 1994, Schmitt and Stille, 2005, Groffman and Fisk, 2011). There is also recent interest in the effects of changing forest harvest practices on soil Ca stocks (Brandtbert and Olsson, 2012; Zetterberg et al., 2016). Prior studies conducted at the Fraser Experimental Forest (FEF) documented the occurrence of dust deposition events (Retzer, 1962; Rhoades et al., 2010), though dust's overall impact on soil functions at FEF remains undetermined. As done in many other studies, we will use Sr isotopic techniques in this effort, though what is innovative is that we employ Sr isotopes to characterize the contributions of dust to soil chemistry along soil catenas. To our knowledge, this is the first study to offer a comparison between dust and weathering additions along a topographic continua, and to describe how they contribute to pedogenesis along a soil catena. Mass balance calculations are presented for soils along catenary sequences in FEF, and Sr isotopes were analyzed to determine estimates of dust accumulation and contributions to the soil chemistry at FEF.

3.3 Methods

3.3.1 Study Site Description

The Fraser Experimental Forest (FEF), Grand County, Colorado, USA, is located in the central Rocky Mountains (Figure 3-1). Research in the fields of hydrology and forest dynamics has taken place in FEF since 1937. Contemporary research at FEF is primarily centered on water quantity and quality, and their relationship to forest management and vegetation, at different scales. Daily minimum and maximum temperatures at FEF range from -40 ^{o}C and 32 ^{o}C annually; the mean annual temperature is 1 ^{o}C. Mean annual precipitation is 71-76 cm, two thirds of which is snowfall (Alexander and Watkins, 1977). Metamorphic rocks dominate the FEF landscape, with sedimentary rocks a minor component. FEF geology consists mostly of felsic to intermediate composition gneiss and schist, with small amounts of granitic and intermediate composition igneous rocks (Theobald, 1965). Alpine landscapes are dominated by grasses and shrubs. The forested landscapes consist of a mixture of lodgepole pine, Engelmann spruce, subalpine fir, and quaking aspen. The soils of FEF are commonly young and poorly developed. Inceptisols and Entisols dominate the upper landscape positions; Alfisols with weakly developed illuvial horizons occur on the sideslope positions; and Histosols can be found along riparian corridors within slope and depression wetlands (unpublished data).

The topography of FEF is dominated by steep, high mountain slopes. The only portion of the landscape that approaches a zero slope are either high atop alpine grasslands or small areas adjacent to surface water corridors. Summit landscapes are generally narrow and are somewhat convex, rather than having abrupt, sharp peaks. These landscapes are also relatively stable and gently sloping, while sideslope landscapes along catenas are relatively unstable and steep. Some of these areas are quite hummocky, most likely due to relic glacial features, while others have relatively smooth slopes. The slopes along the catena shoulder, backslope, and footslope landscapes sampled in this study approached 20^{o}. Elevation of the sites within this study ranged from approximately 2,900 m (9,500 ft) to 3,550 m (11,600 ft) (Figure 3-1).

3.3.2 Catena Selection

The catenary sequences selected for sampling were located in FEF within 4 catchments: Byers Creek, East St. Louis Creek, Fool Creek, and Iron Creek (Figure 3-1). These catchments were chosen primarily based on accessibility and parent material geology. Two catenas were established in each catchment, for a total of 8 catenas. Each catena contained four sites within each from a summit, shoulder, backslope, and footslope landscape position, for a total of 32 sites. The shoulder, backslope, and footslope, collectively, are often referred to as the sideslope. The summit positions do not receive upslope inputs hydrologically; they are the highest elevation sites along the catenas. All sites along the sideslopes are hydrologically connected to adjacent landscape positions.

A single type of parent material was isolated across all of the catenas to hold that influence constant in the study. Catenas and their individual sites were located on areas of mineralogically-similar granodiorite, biotite gneiss, and biotite schist. Relatedly, no lithologic discontinuities along the catenas were identified. The parent materials identified in this study are consistent with previous geologic mapping conducted at FEF (Theobald, 1965; Eppinger et al., 1984; Shroba et al., 2010).

3.3.3 Soil Sampling and Analysis

At each of the 32 sites, a soil pit was excavated to the maximum depth allowable by hand, and that was "that portion of a C or R horizon which is easily obtainable but reasonably distant" below the solum (Buol et al., 1997). As such, parent material properties were obtained from the analysis of the deepest portion of the C horizons accessible in the soil pits or soil cores. Pedons were described and sampled by genetic horizon (Schoeneberger et al., 1998) and approximately 1-2 kg of soil was taken from each genetic horizon for laboratory and mineralogical characterization and analysis. All soil samples were bagged and sealed in the field, and transported to the Colorado State University (CSU) laboratory immediately.

Laboratory analyses included the determination of soil texture, total carbon, geochemistry, and bulk mineralogy. All laboratory work, except for X-ray diffraction (XRD), was performed at Colorado State University. Soil texture was determined using the hydrometer method (Gavlak et al., 2003). Total carbon was determined on a LECO Tru-Spec CN analyzer (Leco Corp., St. Joseph, MI, USA). Soil bulk density was determined empirically by the method outlined by Rawls (1983). Major elements were measured on a Perkin Elmer Optima 7300 CV inductively coupled plasma-optical emission spectrometer. Strontium isotopes were measured on a Perkin Elmer Sciex Elan CRC II inductively coupled plasma-mass spectrometer. ICP analysis followed total digestion of samples in HCl, HNO_3, and HF (Page et. al., 1982). Bulk mineralogical analyses were performed on samples of unweathered parent material (C horizon rock). XRD spectra were obtained for randomly oriented aggregate mounts between 2 and 65° 2Θ on a Scintag GBC MMA Diffractometer (University of Northern Colorado, Department of Earth Sciences) configured at: 35 kV, 28.5 mA, a step size of 0.02 at 2°/minute. Analysis of the obtained powder XRD patterns was performed using the RockJock program (Eberl, 2003).

3.3.4 Geochemical Mass Balance

Here, we employ the geochemical (constituent) mass balance approach to estimate weathering by calculating volume changes through a soil profile and parent material composition. Strain (ε), is a measure of soil volume change incurred during pedogenesis, and was calculated as follows: (Brimhall and Dietrich 1987; Chadwick et al., 1990; Brimhall et al., 1992)

$$\varepsilon_{i,w} = \frac{\rho_p C_{i,p}}{\rho_w C_{i,w}} - 1$$

where ρ is soil bulk density and C_i is the concentration of an immobile reference element in w the weathered soil horizon or p the soil parent material. The mobility of titanium and zirconium were evaluated by analyzing the relationship between their mass transfer function values and percent clay and sand, respectively. Titanium was selected as the immobile element for this study due to showing a low degree of mobility in FEF soils. Regression analysis showed that its mass transfer function value was not dependent upon percent clay, as the R^2 of the fitted regression line between the two variables was 0.07%. Essentially, its concentration was more uniform with depth. Strain is a unitless index; positive and negatives values indicate increasing or decreasing soil volume, respectively. Strain values calculated in this study are the sum of the depth-weighted contributions from each weathered soil horizon in its respective pedon.

The mass transfer coefficient, $\tau_{j,w}$, is used to evaluate element mobility within the soil (Brimhall and Dietrich 1987; Chadwick et al., 1990; Brimhall et al., 1992) as such:

$$\tau_{j,w} = \frac{\rho_w C_{j,w}}{\rho_p C_{j,p}}(\varepsilon_{i,w} + 1) - 1$$

where C_j is the concentration of a chemical species and $\varepsilon_{i,w}$ is volumetric strain. The mass transfer coefficient is used to compute elemental flux for a given soil horizon, in relation to the element's mass in the parent material.

The weathering mass flux from a soil profile using the following equation (Egli and Fitze, 2000):

$$\text{mass}_{j,flux} = \rho_p \Delta z_w \frac{1}{\varepsilon_{i,w} + 1} C_{j,p} \tau_{j,w}$$

where ρ is bulk density, w is the weathered soil horizon, p is parent material, and $C_{j,p}$ is the concentration of element j, and z is the thickness of the soil horizons. The mass fluxes from horizons contributing to a soil profile were summed to obtain a weathering mass flux for the entire soil profile. Mass flux values estimate elemental gain or loss of a mobile element from the soil profile.

3.3.5 Strontium Isotopes

Here, we express the isotopic composition of strontium as δ^{87}Sr, which is calculated by:

$$\delta^{87}Sr = \left(\frac{87_{Sr}/86_{Sr_{SAMPLE}}}{87_{Sr}/86_{Sr_{SEAWATER}}}\right)$$

Likewise, a two end member mixing model can be used to determine the relative contributions of two sources (Capo et al., 1998). We use such a model to calculate the relative contributions of atmospheric dust and in situ weathered mineral rock to summit soils as follows:

$$X(Sr)_1 = \frac{\left({}^{87_{Sr}}/_{86_{Sr}}\right)_{mix} - \left({}^{87_{Sr}}/_{86_{Sr}}\right)_2}{\left({}^{87_{Sr}}/_{86_{Sr}}\right)_1 - \left({}^{87_{Sr}}/_{86_{Sr}}\right)_2}$$

where $X(Sr)_1$ is the mass fraction of Sr derived from source 1. Subscripts 1 and 2 refer to the two sources, dust and rock. The mix subscript indicates the mixture (soil) component. The mean ^{87}Sr/^{86}Sr ratio from three rock (biotite gneiss) samples (δ^{87}Sr =41.66) from soil pits along the Byers Creek lower catena was used for the rock source isotopic signature. ^{87}Sr/^{86}Sr ratios of dust (δ^{87}Sr = 1.23) sampled from the Central Rocky Mountains (Neff, personal communication, October 17, 2013; Clow et al., 2005) for the dust source isotopic signature, as it has been suggested that the background dust signature across the Rocky Mountains is largely homogeneous (Munroe, 2014).

3.3.6 Statistical Calculations

Statistical tests were applied to multiple parameters, and results were calculated using the Minitab 17 software (Minitab, Inc., State College, PA). We used Welch's ANOVA test (α=0.05) to examine average values for mass transport coefficients and weathering mass flux along the catenas. When appropriate, average values are reported in the text as the data mean ± standard deviation.

3.4 Results

3.4.1 Pedogenic Gains and Losses along Catenas

Mass transfer function values (τ) were integrated over the entire weathered profile for each study site; the average masses of calcium gained or lost from soils over the course of soil formation are displayed in figure 3-3. The impetus for displaying results with respect to all six cations is to give the reader an idea of which landscapes have become elementally enriched or depleted, and which major cations may be accounting for said gains or losses.

Compared to their parent material, summit landscape soils were enriched in Ca, Na, K, Al, Fe, and Mg (Figure 3-2), although the most substantial gains were with respect to Ca and Na (Figure 3-2). Although the mean values for τ for K, Al, Fe, and Mg were slightly positive, it could be argued that as much of the data indicated losses as gains for these 4 elements. Likewise, the average τ for Ca in the summit landscape position was the highest among the landscapes, we found no statistical differences in τCa along the catenas due to the high variability in the data (Figure 3-2). Being the highest τ value among elements analyzed for along the catenas, Ca enrichment dominates the calculated elemental enrichment values in the summit landscape.

Soils along the catena shoulders were pedogenically enriched (experienced gains) with respect to two-thirds of the elements. Average τNa and τMg were positive; the median τ value for the remaining four elements was negative (Figure 3-2). The greatest elemental gains in the shoulder landscape were attributed to Ca; the τ value of this element was the most variable, as well. The lowest degree of elemental enrichment were observed with respect to Mg.

Backslope soils were pedogenically enriched with respect to only one element, Al. The data indicate that soils in this landscape position are depleted in Ca, Na, K, Fe, and Mg. The middle 50% of the τ data is most tightly bound for Al, Fe, and Mg in this landscape.

Footslope soils were pedogenically depleted (experienced losses) with respect to all elements; the median τ value for all elements is negative. Considering all the elements analyzed, elemental enrichment values in this landscape were more tightly constrained than in any other landscape position and the variability in τ values decreased with decreasing elevations.

Generally, summit landscapes experienced the highest degree of elemental enrichment; landscapes along catena sideslopes experienced losses or minimal gains of all elements except for Ca and Na (shoulder; Figure 3-2) during pedogenesis. Considering median τ values along the sideslope, the data suggest that soils are losing all major elements during pedogenesis, with the greatest losses having occurred in the lowest elevation of these sites (Figure 3-2).

3.4.2 Weathering Mass Flux of Calcium along Catenas

During preliminary data analysis it became clear that Ca enrichment may hold the most pedogenic importance to FEF soils, among the elements analyzed. Subsequently, mass flux values were integrated over the entire weathered profile for each study site; the average masses of Ca gained or lost from soils during pedogenesis are displayed in figure 3-3. Regardless of landscape position, individual Ca mass fluxes ranged from -20.4 kg m^{-2} to 6.6 kg m^{-2}. No statistical differences are reported with regard to average calcium flux along catenas, though the median calcium flux values are more likely to be positive in the upper landscapes, and negative in the lowest landscapes (Figure 3-3). Similarly, the average rate of calcium mass gain or loss during the period of soil formation was calculated using a maximum residence time of the soil.

The period of pedogenesis assumed is conservatively based on the timing of most recent regional glacial retreat (12,000 years maximum). The average mass flux for calcium for the four landscape positions moving down-catena follows; summit= 0.4 kg $ha^{-1}yr^{-1}$, shoulder= 0.1 kg $ha^{-1}yr^{-1}$, backslope= -1.6 kg $ha^{-1}yr^{-1}$, and footslope= -3.3 kg $ha^{-1}yr^{-1}$, respectively.

3.4.3 Strontium Isotopes along a Soil Catena

To examine the influence of landscape position on atmospherically-derived soil Ca stocks, $\delta^{87}Sr$ values were calculated along one catena with consistent forest species composition to minimize the effect of vegetation. Surface soil $\delta^{87}Sr$ values along the soil catena ranged between 6.12 ‰ and 14.02 ‰ (Figure 3-4). The average surface soil $\delta^{87}Sr$ value was 9.23 ± 3.0‰. Moving along the catena, these values remain relatively close to the to the $\delta^{87}Sr$ value of dust 1.23 ‰ collected at the Loch Vale Main Weather Station, Rocky Mountain National Park, elevation 3050 m (Clow et al., 1997). In subsurface soils $\delta^{87}Sr$ values trend toward the $\delta^{87}Sr$ of parent material (rock) moving down the catena. The $\delta^{87}Sr$ value of subsurface horizons along the catena ranged between 4.42 ‰ and 27.88 ‰. The average $\delta^{87}Sr$ value in subsurface soil horizons was 14.73 ± 9.3‰. There was less variation in surface than subsubsurface $\delta^{87}Sr$ values. Selected soil properties of the pedons along this soil catena are presented in Table 3-1.

3.4.4 Atmospheric Contributions to Soils

Atmospheric deposition contributions (ADC) to summit landscapes were calculated for both A (surface) horizons and whole soil profiles in order to examine the influence of vegetative cover on atmospherically-derived soil Ca stocks (Figure 3-5). The average ADC to soil Ca was higher in forested summit landscapes than in alpine summit landscapes. The mixing model calculations indicate that the ADC to alpine A horizon Ca was 68 ± 3%; the ADC to forest A horizon Ca was 76 ± 12%. Whole-profile ADC to alpine soil Ca was 74 ± 7%; whole-profile ADC to forest soil Ca was 82 ± 3%. Although the average ADC values are higher for forested vs. alpine landscapes, no statistical differences in ADC were found between the averages. Selected soil properties of the summit pedons are presented in Table 3-1.

3.5 Discussion

Studies have analyzed soil properties along soil catenas to gain insight into the dynamics of soil landscapes for over eighty years. Hillslopes were represented as a chain of soil profiles very early in the application of the catena model by P.H. Nye in a paper published in 1954. The catena model has been used in studying soil connectivity (Young, 1976), soil topographic relationships (Huggett, 1975), and biogeochemical properties across soil landscapes (Schimel et al., 1985; Litaor, 1992). To this day, the soil catena model continues to be used in pedologic-based research to describe the influence of the soil forming factors on the variation in soil properties across landscapes (Evans, 2014; Badia et al., 2015). There is a great amount of evidence that demonstrations the importance of atmospheric deposition as a soil input, however we are the first to use the catena model in describing relative importance of atmospheric deposition (cation sourcing) in soil formation.

We evaluated the degree of elemental enrichment with respect to six major cations in order to identify “hot spots” of elemental accumulations (or losses) along soil catenas. We discovered gains of all elements in the summit landscapes, of similar magnitude as reported by Lawrence et al. (2013), and progressive elemental losses in each successive lower elevation position along the catenas. We presented the mass balance data for all of these soil elements to point out, perhaps, the most noteworthy finding regarding the distribution of theses soil cations along the catenas—the high elemental enrichment of Ca. Our data suggest that landscapes higher in catenas have, on average, experienced pedogenic gains of Ca, while landscapes lower along catenas, on average, have experienced pedogenic losses of Ca (Figure 3-3). These Ca gains substantiate the importance of atmospheric deposition to the supply of base cations at FEF, as was previously suggested by others as precipitation inputs at FEF (Retzer, 1962; Rhoades et al., 2010). Indeed, the Ca ion is the most abundant element in the snowpack across Colorado (Stottlemyer and Troendle, 1992). It is likely that the pedogenic gains of Na and Mg, especially in summit landscape positions, are largely influenced by atmospheric deposition as well. Our findings demonstrate how atmospheric deposition and elemental transfers fit into the model of pedogenesis at FEF.

The base cation reserve (stocks) contained in soil, including Ca, is mostly dependent upon the flux of elements moving in and out the soil and controlled by weathering and element supply rates. The isotopic signature of a soil horizon or profile, specifically its δ^{87}Sr value, is dependent upon the degree to which certain processes contribute to flux. In this paper, the contributions of parent material and atmospheric deposition to the Ca reserve held in the soil along a forested catena is presented. It is clear that the δ^{87}Sr values of surface soil horizons and subsurface soil horizons diverged moving down this catena (Figure 3-4), and there appears to be a geochemical knickpoint, below which the surface (A-horizons) and subsurface soils are most isotopically dissimilar. These data suggest that a chief ecosystem input of Ca at FEF is being deposited via precipitation and/or dry dust deposition, and that this signature is strong in A horizons regardless of landscape position along catenas. Moving down-catena, this Ca signal becomes somewhat muted in subsurface soil horizons, as δ^{87}Sr values approached values of the geological substrate on which these soils have formed. The wider range of $\delta^{87}Sr$ values in subsurface horizons along this catena indicate that atmospherically-derived Ca have been variably incorporated into the soil mantle during pedogenesis through mixing processes such as bioturbation and other disturbances. Mammals, such as pocket gophers, contribute to the mixing of soil in mountain ecosystems (Zaitlin and Hayashi, 2012) and wind disturbances resulting in tip up mounds were observed along the catenas and have been documented in similar ecosystems (Kulakowski and Veblen, 2003).

Our statistical analysis suggests that the degree of mass flux for Ca is not dependent upon the position of soils in the landscape. This finding is not surprising, as the differences in soil temperature and precipitation across these catenas are likely not sufficient to impart differences in the chemical weathering rate of soils. It is interesting, however, that average τCa and average Ca flux indicate additions in the summit landscape followed by progressive losses along the catenas. Relatedly, the magnitude of soil Ca mass flux presented here is comparable to Ca flux reported in streams (7.9-59.8 kg m^{-2} yr^{-1}) by Barnes et al. (2014) and in soil (-7.1 ± 2.1 kg m^{-2}) by Lawrence et al. (2013) in similar ecosystems in Colorado. In this study, when evaluating the mass flux (per year) for Ca along catenas, it can be argued that the magnitude of Ca flux is consistent, irrespective of landscape position, although there is a high degree of variability in the data. Nutrient budget modeling efforts may benefit from this finding that the location within or along upland soil landscapes may not affect the degree of Ca weathering—Ca is normally considered a nutrient most at risk of depletion through forest harvest or acid deposition, and thus, one of the base cations that is often a focus of study in harvest intensity studies. It is likely that any real differences in soil Ca flux would be attributed to biomass uptake or atmospheric deposition.

Our atmospheric-deposition contribution (ADC) calculations are on par with similar studies that have addressed soil element origins in regions where dust deposition is prevalent. Graustein and Armstrong (1983) demonstrated that weathering of parent material contributes less than 20% of Sr to soil of the Sangre de Cristo Mountains in New Mexico; the remainder is supplied by atmospheric sources. More recently, Clow et al., (1997) found that ADC to A and B horizons of soils at Loch Vale, Colorado, ranged between 53% and 68%. Drouet et al., (2005) demonstrated that two forest soils in Belgium attribute 75%-78% of their soil Ca to atmospheric inputs. Data, based on Sr isotope ratios, indicating high (90%) eolian influence on gneiss-derived soils in New Mexico has been presented by A.C. Reynolds et al., (2012). Dust inputs must be accounted for when carrying out geochemical modeling and/or the prediction/calculation of soil buffering capabilities are important (as in acidified landscapes). The relative importance may be a function of both where soils exist in the landscape and the assumed thickness of the solum.

In addition to shedding light on the proportion of atmospheric contributions to FEF soils, Sr isotope data from summit landscapes demonstrate the preservation of atmospherically-derived Ca into the soil mantle. This variability is especially evident in the A-horizons of forested summit soils, although variability in the summit data is high, regardless of vegetative cover or soil section examined (A horizon vs. whole soil profile). Forest canopies intercept a large portion of snowfall in Colorado Mountains (Schmidt et al., 1998; Montesi et al., 2004; Troendle and King, 1985; Troendle and Reuss, 1997); dust that falls in these environments is also intercepted by the forest canopy. In fact, complementary research at FEF found a lower dust signature under trees than in adjacent openings, demonstrating dust interception by the canopy (Rhoades et al., 2010). Data from our current study indicate that dust inputs have a greater impact on the geochemistry of forested summit soils as compared to alpine summit soils. Similarly, Clow et al.,

(1997) found that forest soil exhibited a higher atmospheric-deposition contribution in surface and subsurface mineral horizons as compared to alpine soil.

The distribution of atmospherically derived soil Ca in summit landscapes at FEF is coupled to the dynamics of snowmelt runoff processes in these mountain ecosystems. The timing of snowmelt is more synchronous and rapid in the alpine ecosystems than in subalpine forests, as incoming solar radiation which drives snowmelt generation is more uniform in alpine ecosystems. In contrast, the timing of snowmelt can be especially variable in forests of differing densities (Guan et al., 2013; Molotch et al., 2009). Sr isotope data indicate that atmospherically derived dust (and its chemical constituents) that falls in alpine summit landscapes in FEF is incorporated into the soil and subsequently leached downslope into lower landscapes through a pulse of snowmelt-derived subsurface lateral flow. Baron, et al. (1992) describe that early season snowmelt flushes the accumulated by-products of “8 months of soil weathering and decomposition” as soil water infiltrates soil horizons. Contrary to the alpine landscapes, snowmelt in FEF forest landscapes infiltrates the soil at a more variable rate and in a more variable spatial pattern. Ca derived from both in-situ weathering and atmospheric deposition in forest landscapes is not subject to this “cationic flushing”. Our data provide evidence that this cationic flush influences the chemistry of FEF summit soils. On a similar note, this mechanism is coupled to the occurrence of greater dust (snow) interception in forest canopies that is temporarily stored and washed down later via melt and/or throughfall, leading to a pedologically key chemical signature (higher ADC values) regarding the degree of atmospheric dust contributions to these forested landscapes.

It was surprising to find that the contribution of dust to the whole soil profile was as great as or greater than the contribution of dust in the soil surface (A) horizons. Physical soil data revealed high silt size fractions in subsoil horizons, and we interpret this as evidence for the movement of atmospherically derived dust deep into the soil profiles. Silt is by far the dominant particle size fraction found in Colorado dust (Lawrence et al., 2010), and it follows that soils which are heavily influenced by dust deposition would contain high quantities of silt. Our data revealed a higher percentage of silt in our forested summit soil horizons as opposed to alpine summit soil horizons (Table 3-1). Similarly, the mean Sr87/Sr86 value for forested summit soil horizons is closer to the isotopic dust signature than their alpine counterparts, indicating that their chemistry is more heavily influenced by dust than by their underlying parent material. This chief input is traditionally understated when considering or defining parent material contributions to soil formation, especially when generalizing the development of soils along catenas. Historically, parent materials are highlighted as being sourced from, for example, bedrock, glacial till, alluvium, eolian sand, and loess deposits. Bedrock geology is usually the presumed parent material for a given soil, unless the soil formed on top of sediment. Typical soil development models may overestimate the relative importance of soil elements derived from bedrock geology, and underestimate the importance of elements derived from elsewhere (e.g. atmospheric sources). It has been shown that older landscapes depend almost entirely on exogenous sources for their soil base cation stocks (Kennedy et al., 1998; Chadwick et al., 1999) and it is well known that ecosystems in the Amazon rainforest depend on dust inputs. The base cation stocks of even relatively young soils can be highly dependent upon atmospheric inputs. We have shown that these inputs fit into the catena model of soil formation—in that the degree of atmospheric influence with respect to soil Ca depends on topographic position, and that this geochemical signal is linked to adjacent hillslope positions. We argue that with respect to soil development models, atmospheric-derived constituents may often be a better label of "parent material", than the underlying bedrock, whether it be of crystalline or sedimentary origin.

3.5 Conclusions

Over time, the chemical signature of soils is shaped by the relative contributions of weatherable materials from sources such as bedrock and atmospheric dust. Most of recent dust-related studies have focused on high-elevation alpine catchments; here, we broadened the focus to include multiple landscapes along soil catenas, essentially evaluating weathering along hillslopes. Evaluation of elemental gains and losses by landscape position pointed to noteworthy additions of Ca to summit and mountainbase landscapes, as hillslope processes enable progressive losses of soil Ca that accumulate in mountainbase wetland soils. Surface soil horizons in summit landscapes are more strongly coupled to the influence of atmospheric deposition than subsurface horizons—and this disparity increases with decreasing elevation. We display geochemical evidence that atmospherically-derived additions contribute to the Ca stocks in FEF soils and that these atmospheric contributions to the soil chemistry at FEF are pedologically significant. This study also suggests that the chemical signature of soils in snowfall-dominated mountain ecosystems with significant dust inputs may be coupled to snowmelt runoff processes. Increasing rates of dust deposition due to land use change in the region and changing precipitation dynamics due to climate change (i.e. snow vs. rain) will continue to influence soil formation at FEF analogous environments; it remains to be seen how these montane ecosystems are to be affected by these changing dynamics. We conclude that atmospheric deposition plays an important role in soil development at FEF, and its contributions to soil development at FEF are entwined with landscape position, vegetation cover, and snowfall dynamics. We have shown how certain soil geochemical properties change along catenas in complex mountain catenas. Typical soil development models along catenas include the underlying parent material contributions but largely exclude this atmospheric input-- we should always consider the importance this additional input when describing pedogenesis along catenas. We have provided a foundational framework for how these inputs express themselves geochemically along soil catenas. Future work must focus on further unraveling these complex relationships.

Table 3-1: Selected soil properties for all sites along the Byers Lower Catena and all summit position sites in the study. Site names are coded as follows: Catena Name – Landscape Position – Vegetative Cover. BL = Byers Lower; BU = Byers Upper; EL = East St Louis Lower; EU = East St Louis Upper; FL = Fool Lower; FU = Fool Upper; IL = Iron Lower; IU = Iron Upper. SU = summit; SH = shoulder;BS = backslope; FS = footslope. F = Forest; A = Alpine.

Site	Horizon	Interval (cm)	Silt (%)	Clay (%)	Sr87/Sr86	Ca (ppm)	Silt/Clay
BL-SU-F							
	A	0-5	26	25	0.7135	12210	1.06
	Bw1	5-18	35	26	0.7157	20210	1.33
	Bw2	18-58	20	20	0.7123	12020	0.99
	C	58-85	18	10	0.7142	3180	1.83
BL-SH-F							
	A	0-10	31	29	0.7162	3748	1.06
	Bw	10-35	25	31	0.7165	3929	0.82
	BC	35-75	14	27	0.7134	4384	0.53
	C	75-100	25	24	0.7121	5196	1.06
BL-BS-F							
	A	0-10	26	30	0.7155	11120	0.85
	E	10-20	28	27	0.7167	10810	1.02
	Bw	20-82	10	24	0.7144	13080	0.44
	BC	82-122	25	23	0.7150	11920	1.08
	C	122-140	19	23	0.7156	9320	0.81
BL-FS-F							
	A	0-13	34	33	0.7191	4665	1.04
	Bw	13-24	32	34	0.7161	6438	0.93
	C1	24-67	17	29	0.7171	7090	0.58
	C2	67-95	12	23	0.7236	9782	0.54
BU-SU-F							
	A	0-5	19	30	0.7143	6935	0.63
	Bw1	5-10	22	21	0.7175	878	1.04
	Bw2	10-50	16	16	0.7151	931	1.03
EL-SU-F							
	A	0-5	21	28	0.7151	4231	0.76
	Bw	5-18	22	20	0.7160	4557	1.09
	C	18-60	13	12	0.7141	894	1.08
EU-SU-A							
	A	0-10	20	37	0.7176	3455	0.54
	BC	10-25	18	20	0.7139	2050	0.92
	C	25-50	15	27	0.7138	786	0.56
FL-SU-F							
	A	0-4	27	24	0.7210	5404	1.13

	BC	4-15	38	17	0.7124	20720	2.24
	C	15-60	26	28	0.7119	25560	0.92
FU-SU-A							
	AB	0-10	33	33	0.7206	3871	1.01
	Bw	10-61	10	20	0.7176	1000	0.49
	BC	61-90	17	18	0.7180	751	0.95
	C	90-110	27	15	0.7239	745	1.80
IL-SU-F							
	A	0-3	41	29	0.7200	4979	1.42
	BC	3-17	36	24	0.7150	4407	1.51
	C	17-90	41	24	0.7141	3754	1.72
IU-SU-A							
	A	0-8	32	28	0.7189	2871	1.15
	Bw	8-31	23	31	0.7125	2789	0.73
	BC	31-37	16	25	0.7234	3834	0.62
	C1	37-60	22	30	0.7189	5485	0.74
	C2	60-100	11	15	0.7147	5916	0.75

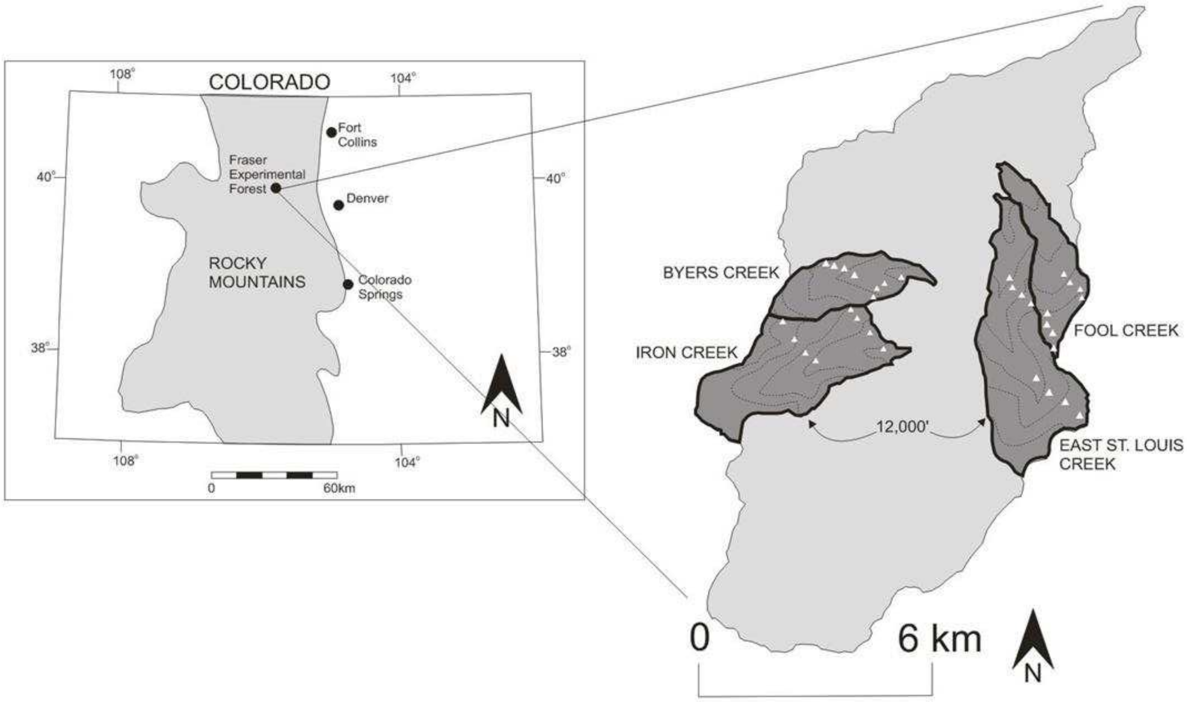

Figure 3-1. The location of the Fraser Experimental Forest, Colorado. Soils were sampled along eight catenas in four catchments (dark gray) within the larger St. Louis Creek catchment (light gray). Sample points along the catenas are indicated by white triangles. Contour lines for elevation (countour interval = 500') are represented by hachured lines; the highest contour line shown (12,000') is labeled, for ease of reference.

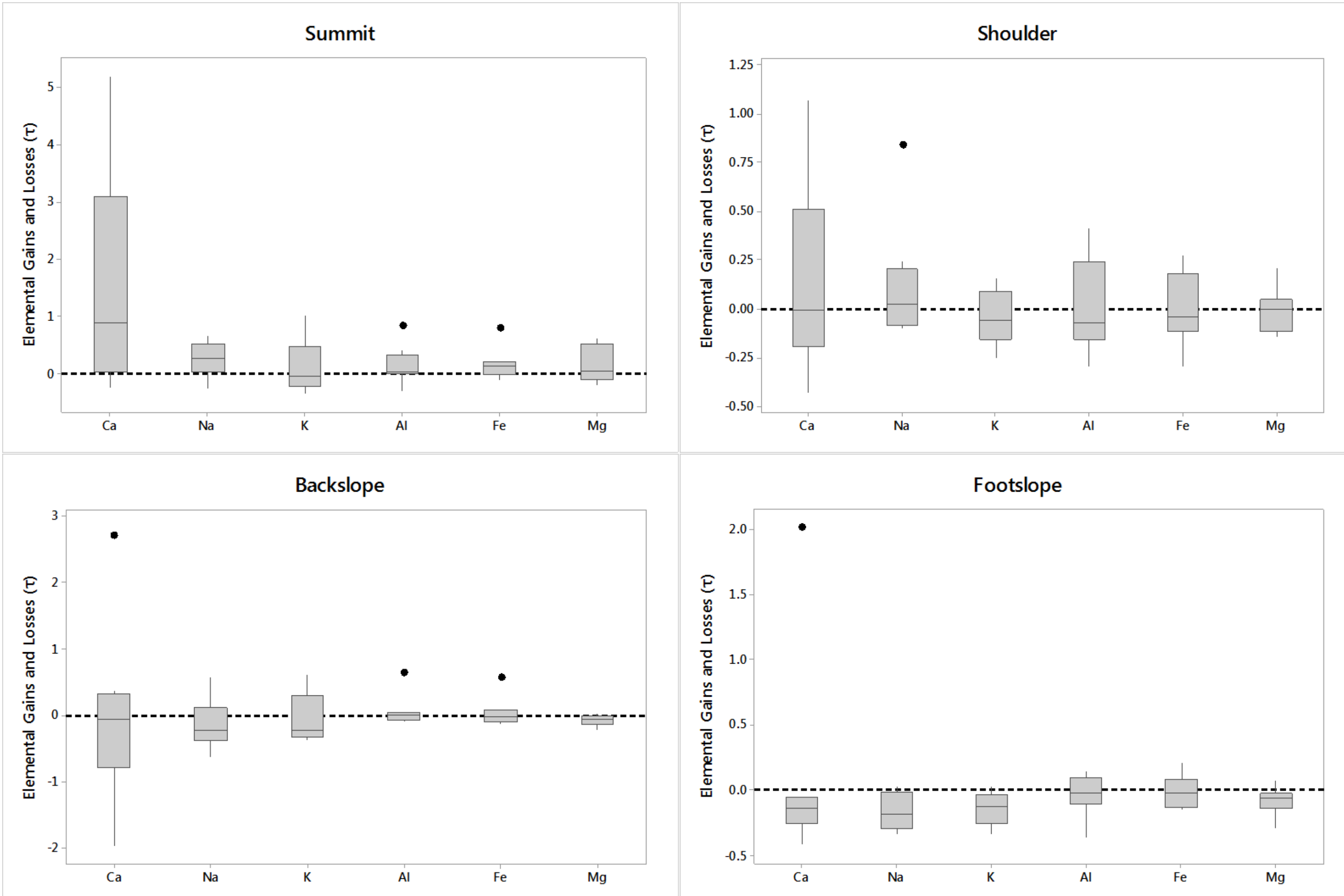

Figure 3-2. Elemental gains and losses for whole soil profiles by landscape position (n=8). Box plots show depth-weighted median mass transfer function values (horizontal line), middle 50% (box), upper and lower 25% (bars), and outliers (filled circles). Note the y-axis scale changes between panels. Values which fall on the dashed horizontal line displayed no change in median τ.

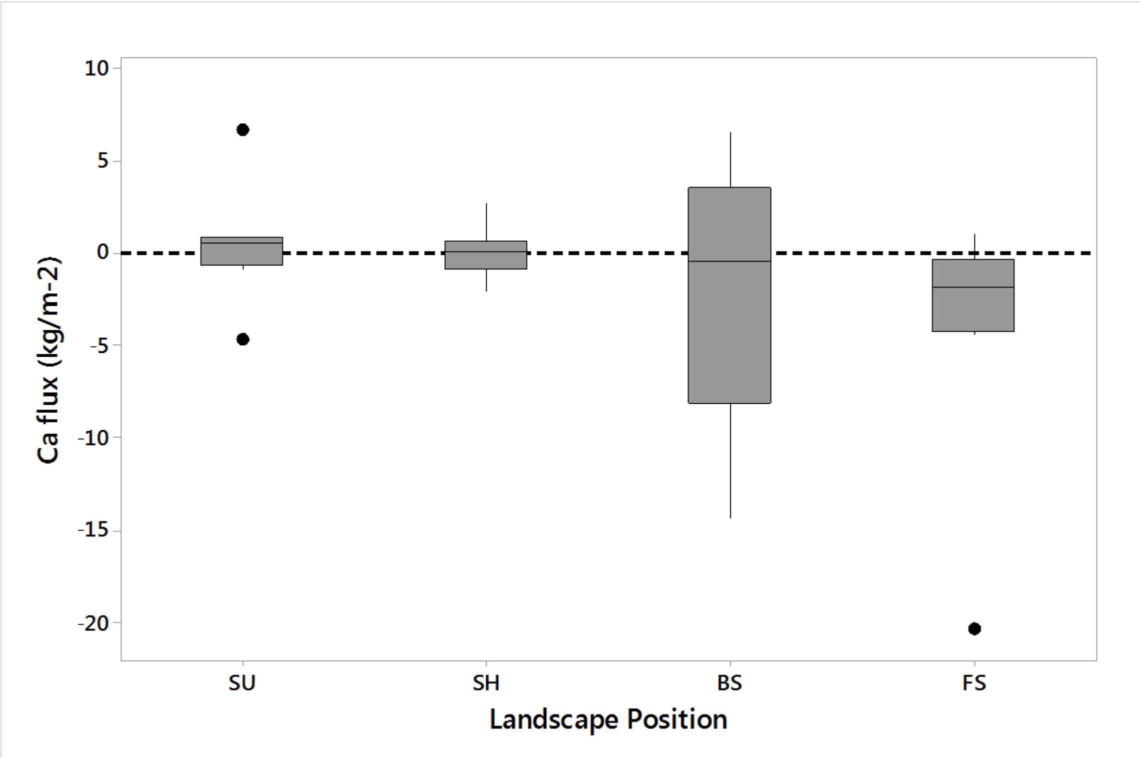

Figure 3-3. Average weathering mass flux of calcium across soil landscapes over the period of pedogenesis (12,000 yrs). Data are the average of Ca mass flux integrated over entire soil profiles along the five landscape position (n=8). Box plots show depth-weighted median mass transfer function values (horizontal line), middle 50% (box), upper and lower 25% (bars), and outliers (filled circles). Values which fall on the dashed horizontal line displayed no change in median flux. SU = summit; SH = shoulder; BS = backslope; FS = footslope.

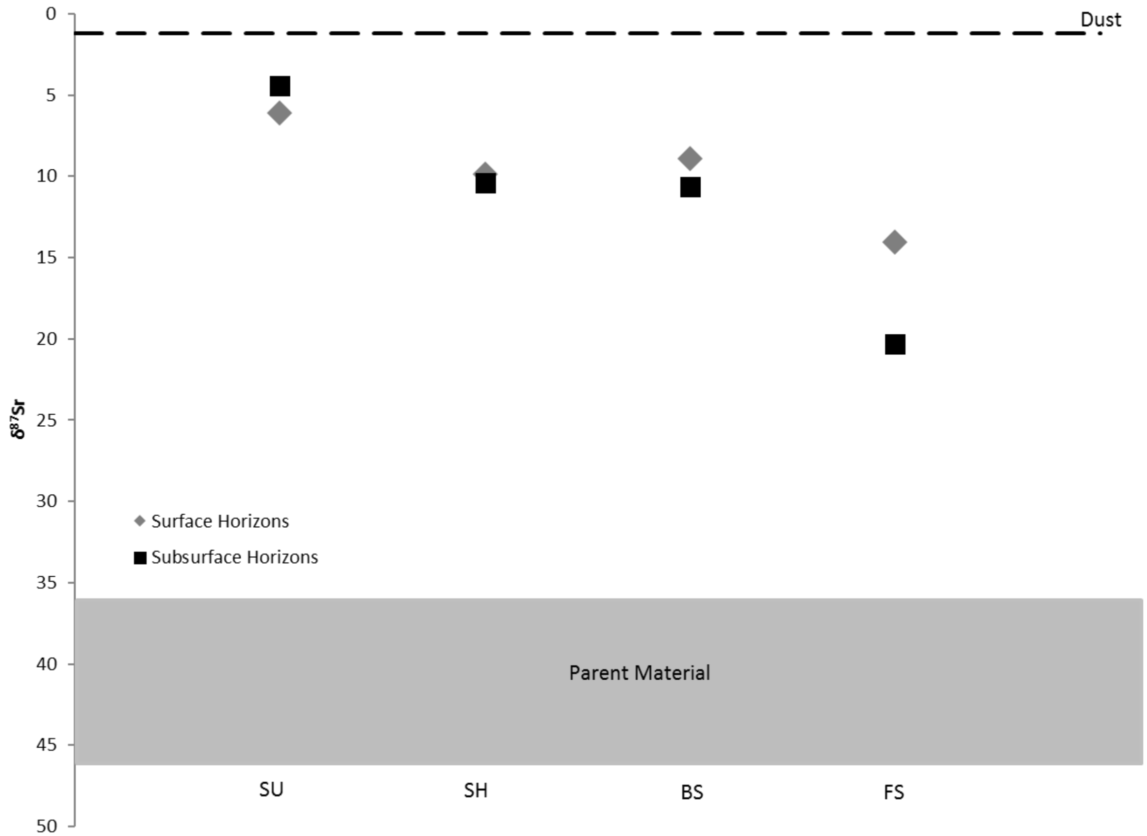

Figure 3-4. Plot of δ87Sr for surface soil horizons and subsurface soil horizons along one soil catena. Moving down-catena from the summit to mountainbase landscape position, surface horizon values remain relatively close to δ87Sr dust values reported in similar ecosystems in Colorado, while subsurface horizon values trend towards the δ87Sr for the range (n=3) of parent material along this catena. SU = summit; SH = shoulder; BS = backslope; FS = footslope.

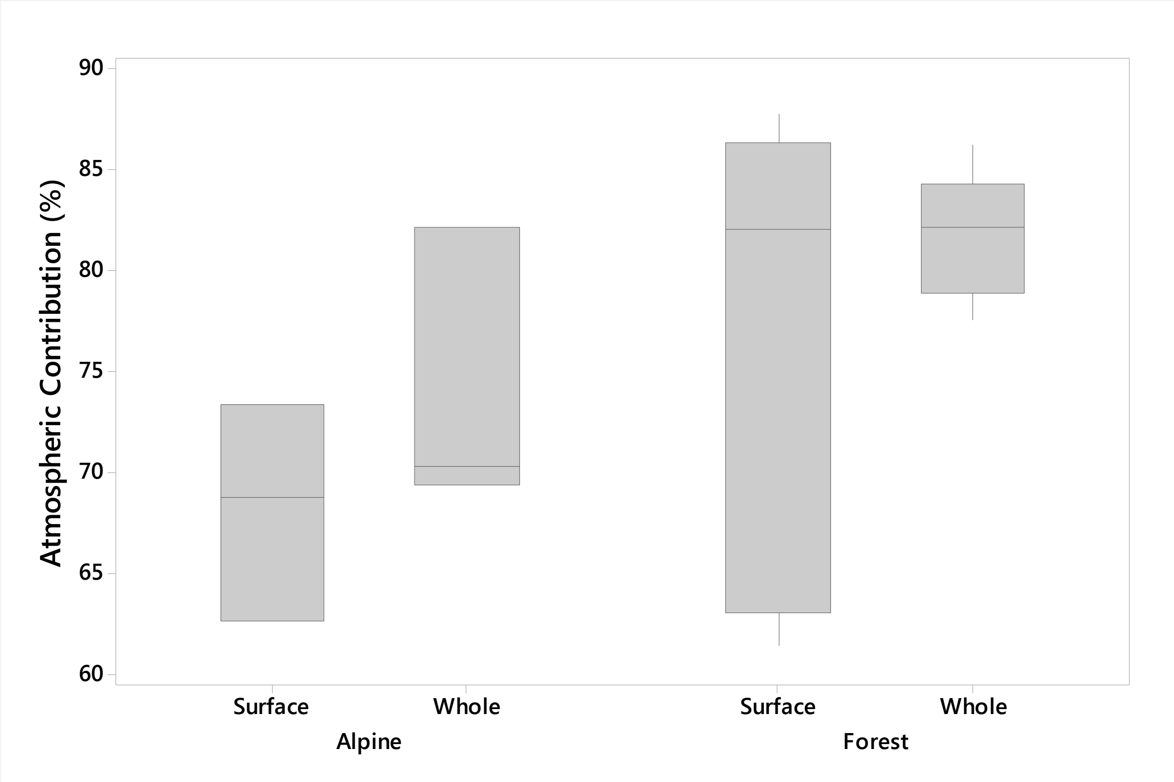

Figure 3-5. Atmospheric deposition contribution to FEF summit soils associated with alpine (n=3) and forest vegetation (n=5). Box plots show depth-weighted median mass transfer function values (horizontal line), middle 50% (box), and upper and lower 25% (bars). There were no outliers to report. Surface = surface mineral horizon; Whole = whole soil profiles.

REFERENCES

Aberg, G., Jacks, G., Hamilton, P.J., 1989. Weathering rates and 87Sr/86Sr ratios: An isotopic approach. Journal of Hydrology. 109, 65-78.

Alexander, R.R., Watkins, R. K., 1977. The Fraser Experimental Forest, Colorado. Gen. Tech. Rep. RM-40. Fort Collins, CO: U.S. Department of Agriculture, Forest Service, Rocky Mountain Forest and Range Experiment Station 32 p.

Anderson, S.P., Dietrich, W.E., Brimhall, G.H., 2002. Weathering profiles, mass-balance analysis, and rates of solute loss: Linkages between weathering and erosion in a small, steep catchment. Geological Society of America Bulletin. 114 (9), 1143-1158.

Badia, D., Orus, D., Doz, J.R., Garcia-Gonzalez, M.T., 2015. Vertic features in a soil catena developed on Eocene marls in the Inner Depression of the Central Spanish Pyrenees. Catena. 129. 86-94.

Balfour, V.N., Doerr, S.H., Robichaud, P.R., 2014. The temporal evolution of wildfire ash and implications for post-fire infiltration. 23 (5) 733-745.

Barnes, R.T., Williams, M.W., Parman, J.N., Hill, K., Caine, N., 2014. Thawing glacial and permafrost features contribute to nitrogen export from Green Lakes Valley, Colorado Front Range, USA. Biogeochemistry. 117 (2-3), 413-430.

Baron, J., et al., 1992. Biogeochemistry of a Subalpine Ecosystem: Loch Vale Watershed. Springer-Verlag, New York.

Bern, C.R., Chadwick, O.A., Hartshorn, A.S., Khomo., L.M., Chorover, J., 2011. A mass-balance model to separate and quantify colloidal and solute redistributions in soil. Chemical Geology. 282 (3-4), 113-119.

Blank, R.R., Young, J.A., Allen, F.L., 1999. Aeolian dust in a saline play environment, Nevada, USA. Journal of Arid Environments. 41 (4), 365-381.

Blum, J.D, Klaue, A., Nezat, C.A., Driscoll, C.T., Johnson, C.E., Siccama, T.G., Eagar, C., Fahney, T.J., Likens, G.E., 2002. Mycorrhizal weathering of apatite as an important calcium source in base-poor forest ecosystems. Nature. 417 (6980), 729-731.

Brahney, J., Ballantyne, A.P., Kociolek, P., Spaulding, S., Out, M., Porwoll, T., Neff, J.C., 2014. Dust mediated transfer of phosphorus to alpine lake ecosystems of the Wind River Range, Wyoming, USA. Biogeochemistry. 120 (1-3), 259-278.

Brass, G.W., 1975. The effect of weathering on the distribution of strontium isotopes in weathering profiles. Geochimica et Cosmochimica Acta. 40, 721-730.

Brandtbert, P.O., Olsson, B.A., 2012. Changes in the effects of whole-tree harvesting on soil chemistry during 10 years of stand development. Forest Ecology and Management. 277, 150-162.

Brimhall, G.H., Dietrich, W.E., 1987. Constitutive Mass Balance Relations between Chemical-Composition, Volume, Density, Porosity, and Strain in Metasomatic Hydrochemical Systems - Results on Weathering and Pedogenesis. Geochimica et Cosmochimica Acta. 51 (3), 567-587.

Brimhall, G.H., Chadwick O.A., Lewis, C.J., Compston, W., Williams, I.S., Danti, K.J., Dietrich, W.E., Power, M.E., Hendricks, D., Bratt, J., 1992. Deformational Mass-Transport and Invasive Processes in Soil Evolution. Science. 255 (5045), 695-702.

Buol, S.W., Southard, R.J., Graham, R.C., McDaniel, P.A., 1997. Soil Genesis and Classification, fifth ed. Iowa State Press, Ames.

Capo, R.C., Hsieh, J.C.C., Chadwick, O.A., 1995, Pedogenic origin of dolomite and calcite in a basaltic weathering profile, Kohala Peninsula, Hawaii. Abstracts International Goldschmidt Conference. p. 34.

Capo, R.C., Stewart, B.W., Chadwick, O.A., 1998. Strontium isotopes as tracers of ecosystem processes: theory and methods. Geoderma. 82 (1-3), 197-225.

Capo, R.C., Chadwick, O.A., 1999. Sources of strontium and calcium in desert soil and calcrete. Earth and Planetary Science Letters. 170 (1-2), 61-72.

Chadwick, O.A., Derry, L.A., Vitousek, P.M., Huebert, B.J., Hedin, L.O., 1999. Changing sources of nutrients during four million years of ecosystem development. 397, 491-497.

Chadwick, O.A., Brimhall, G.H., Hendricks, D.M., 1990. From a Black to a Gray Box - a Mass Balance Interpretation of Pedogenesis. Geomorphology. 3 (3-4), 369-390.

Chadwick, O.A., Davis, J.O., 1990, Soil-forming intervals caused by eolian sediment pulses in the Lahontan basin, northwestern Nevada. Geology. 18, 243-246.

Chadwick, O.A., Derry, L.A., Bern, C.R., Vitousek, P.M., 2009. Changing sources of strontium and ecosystems across the Hawaiian Islands. Chemical Geology. 267, 64-47.

Clow D., Mast, M.A., Bullen, T.D., Turk, J.T., 1997. Strontium 87/strontium 86 as a tracer of mineral weathering reactions and calcium sources in an alpine/subalpine watershed, Loch Vale, Colorado. Water Resources Research. 33 (6), 1335-1351.

Dasch, E.J., 1969. Strontium isotopes in weathering profiles, deep-sea sediments and sedimentary rocks. Geochimica et Cosmochimica Acta. 33, 1521-1552.

Drouet, T., Herbauts, J., Gruber, W., Demaiffe, D., 2005. Strontium isotope composition as a tracer of calcium sources in two forest ecosystems in Belgium. Geoderma. 126, 203-223.

Eberl, D.D., 2003. User's guide to RockJock—a program for determining quantitative mineralogy from x-ray diffraction data. Open File Report 03-78. Washington, DC: United States Geologic Survey.

Egli, M., Fitze, P., Mirabella, A., 2000. Formulation of pedologic mass balance based on immobile elements: A revision. Soil Science. 165 (5), 437-443.

Eppinger, R., Theobald, P., Carlson, R., 1984. Preliminary geologic map of the Western and Southern parts of the Byers Peak, the Northwestern part of the Loveland Pass, and the Eastern part of the Ute Peak 7 1/2 –minute quadrangles, Clear Creek and Grand Counties, Colorado: U.S. Geological Survey. Open-File Report OF-84274, scale 1:24,000.

Evans, D.M., Hartemink, A.E., 2014. *Terra Rossa* catenas in Wisconsin, USA. Catena. 123. 148-152.

Gavlak, R., Horneck, R., Miller, R.O., Kotuby-Amacher, J., 2003. Soil, Plant and Water Reference Methods for the Western Region. In: Soil, Plant and Water Reference Methods for the Western Region. WREP-125, 129-134.

Gile, L.H.,Peterson, F.F., Grossman, R.B., 1966. Morphological and genetic sequences of carbonate accumulation in desert soils. Soil Science. 101, 347-360.

Gile, L.H., 1979, The desert project soil monograph. SCS-USDA, Washington, DC, 984 pp.
Gosz, J. R., Moore, D.I., 1989, Strontium isotope studies of atmospheric inputs to forested watersheds in New Mexico. Biogeochemistry. 8, 113-134.

Grausetin W.C., Armstrong, R.L., 1983. The use of 87Sr/86Sr to measure atmospheric transport into forested watersheds. Science. 219, 289-292.

Graustein, W.C., 1989. 87Sr/86Sr ratios measure the sources and flow of strontium in terrestrial ecosystems, in Rundel, P. W., Ehleringer, J. R., and Nagy, K. A., eds., Stable isotopes in ecological research: New York, Springer-Verlag 491-512.

Groffman, P.M., Fisk, M.C., 2011. Calcium constrains plant control over forest ecosystem nitrogen cycling. Ecology. 92 (11), 2035-2042.

Guan, B., Molotch, N.P., Waliser, D.E., Jepsen, S.M., Painter, T.H., Dozier, J., 2013. Snow water equivalent in the Sierra Nevada: Blending snow sensor observations with snowmelt model simulations. Water Resources Research. 49 (8), 5029-5046.

Huggett, R.J., 1975. Soil landscape systems – model of soil genesis. Geoderma. 13 (1), 1-22.

Kennedy, M.P., Chadwick, O.A., Vitousek, P.M., Derry, L.A., Hendricks, D.M., 1998. Replacement of weathering with atmospheric sources of base cations during ecosystem development, Hawaiian Islands. Geology. 26, 1015-1018.

Kulakowski, D., Veblen, T.T., 2003. Influences of fire history and topography on the pattern of severe wind blowdown in a Colorado subalpine forest. Journal of Ecology. 90 (5), 806-819.

Lawrence, C.R., Painter, T.H., Landry, C.C., Neff, J.C., 2010. Contemporary geochemical composition and flux of aeolian dust to the San Juan Mountains, Colorado, United States. Journal of Geophysical Research, 115, 1-15.

Lawrence, C.R., Reynolds, R.L., Ketterer, M.E., Neff, J.C., 2013. Aeolian controls of soil geochemistry and weathering fluxes in high-elevation ecosystems of the Rocky Mountains, Colorado. Geochimica et Cosmochimica Acta. 107, 27-46.

Johnson, N.M., Likens, G.E., Bormann, F.H., Pierce, R.S., 1968. Rate of chemical weathering of silicate minerals in New Hampshire. Geochimica et Cosmochimica Acta. 32 (5), 531.

Litaor, M.I., 1992. Aluminum mobility along a geochemical catena in an alpine watershed, Front Range, Colorado. Catena. 19 (1), 1-16.

McFadden, L.D., Amundson, R.D., Chadwick, O.A., 1991. Numerical modeling, chemical, and isotopic studies of carbonate accumulation in soils or arid regions. In: Nettleton, W.D. (Ed.), Occurrence, Characteristics and Genesis of Carbonate, Gypsum, and Silica Accumulations in Soils. Soil Science Society of America Special Publication. 26. 17-35.

Middleton, N.J., 1985. Effect of drought on dust production in the Sahel. Nature. 316, 431-434.

Miller, E.K., Blum, J.D., Friedland, A.J., 1993. Determination of a soil exchangeable-cation loss and weathering rates using Sr isotopes. Nature. 362, 438-441.

Mladenov, N., Williams, M.W., Schmidt, S.K., Cawley, K., 2012. Atmospheric deposition as a source of carbon and nutrients to an alpine catchment of the Colorado Rocky Mountains. Biogeosciences. 9 (8), 3337-3355.

Molotch, N.P., Brooks, P.D., Burns, S.P., Litvak, M., Monson, R.K., McConnell, J.R., Musselman, K., 2009. Ecohydrological controls on snowmelt partitioning in mixed-conifer sub-alpine forests. Ecohydrology. 2 (2), 129-142.

Montesi, J., Elder, K., Schmidt, R.A., Davis, R.E., 2004. Sublimation of intercepted snow within a subalpine forest canopy at two elevations. Journal of Hydrometeorology. 5, 763-773.

Munroe, J.S, 2014. Properties of modern dust accumulating in the Uinta Mountains, Utah, USA, and implications for the regional dust system of the Rocky Mountains. Earth Surface Processes and Landforms. 39, 1979-1988.

Niu, D., Hall, S.J., Fu, H., Kang, J., Qin, Y., Elser, J.J., 2011. Grazing exclusion alters ecosystem carbon pool in Alxa desert steppe. New Zealand Journal of Agricultural Research. 54 (3), 127-142.

Okin, G.S., Mahowald, N., Chadwick, O.A., Artaxo, P., 2004. Impact of desert dust on the biogeochemistry of phosphorus in terrestrial ecosystems. Global Biogeochemical Cycles 18 (2), 1-9.

Padgett, P.E., Meadows, D., Eubanks, E., Ryan, W.E. 2008. Monitoring fugitive dust emissions from off-highway vehicles traveling on unpaved roads and trails using passive samplers. Environmental Monitoring and Assessment 144 (1-3), 93-103.

Page, A.L., Miller, R.H., Keeney, D.R., 1982. Methods of Soil Analysis, Part 2: Chemical and Microbiological Properties, 2nd ed. American Society of Agronomy, Madison, WI.

Porder, S., Clark, D.A., Vitousek, P.M., 2007. Persistence of rock-derived nutrients in the wet tropical forests of La Selva, Costa Rica. Ecology. 87, 594-602.

Quade, J., Chivas, A.R., McCulloch, M.T., 1995, Strontium and carbon-isotope tracers and the origins of soil carbonate in South Australia and Victoria. Palaeogeography, Palaeoclimatology, Palaeoecology. 113 (1), 103-117.

Rawls, W.J., 1983. Estimating soil bulk density from particle size analysis and organic matter content. Soil Science 135 (2), 123-125.

Retzer, J.L., 1962. Soil survey, Fraser alpine area, Colorado. Washington, D.C.: G.P.O.

Reynolds, R., Belnap, J., Reheis, M., Lamothe, P., Luiszer, F., 2001. Aeolian dust in Colorado Plateau soils: Nutrient inputs and recent change in source. Proceedings of the National Academy of Sciences of the United States of America. 98 (13), 7123-7127.

Reynolds, R.L., Reheis, M., Yount, J., Lamothe, P., 2006. Composition of aeolian dust in natural traps on isolated surfaces of the central Mojave Desert - Insights to mixing, sources, and nutrient inputs. Journal of Arid Environments. 66 (1), 42-61.

Reynolds, A.C., Quade, J., Betancourt, J.L., 2012. Strontium isotopes and nutrient sourcing in a semi-arid woodland. Geoderma. 189, 574-584.

Rhoades, C., Elder, K. Greene, E., 2010. The influence of an extensive dust event on snow chemistry in the Southern Rocky Mountains. Arctic Antarctic and Alpine Research. 42 (1), 98-105.

Richter, D.D., Markewitz, D., Wells, C.G., Allen, H.L, April, R., Heine, P.R., Urrego, B., 1994. Soil chemical-change during 3 decades in an old-field loblolly-pine (pinus-taeda l) ecosystem. Ecology. 75 (5), 1463-1473.

Santin, C., Doerr, S.H., Otero, X.L., et al., 2015. Quantity, composition and water contamination potential of ash produced under different wildfire seventies. Environmental Research. 142, 297-308.

Schimel, D.S., Stiwell, M.A., Woodmansee, R.G., 1985. Biogeochemistry of C, N, and P in a soil catena of the Shortgrass Steppe. Ecology. 66 (1), 276-282.

Schmitt, A.D.S., Stille, P. 2005. The source of calcium in wet atmospheric deposits: Ca-Sr isotope evidence. Geochimica et Cosmochimica Acta. 69 (14), 3463-3468.

Schmidt, R.A., Troendle, C.A., and Meiman, J.R., 1998. Sublimation of snowpacks in subalpine conifer forests. Canadian Journal of Forest Research. 28 (4), 501-503.

Schoeneberger, P.J., Wysocki D.A.,, Benham, E.C., Broderson, W.D., 1998. Field Book for Describing and Sampling Soils. National Soil Survey Center Natural Resources Conservation Service U.S. Dept. of Agriculture, Lincoln, Nebraska.

Shroba, R.R., Bryant, B., Kellogg, K.S., Theobald, P.K, Brandt, T.R., 2010. Geologic map of the Fraser 7.5-minute quadrangle, Grand County, Colorado: U.S. Geological Survey, Scientific Investigations Map SIM-3130, scale 1:24,000.

Simonson, R.W., 1995. Airborne dust and its significance to soils. Geoderma. 65 (1-2), 1-43.

Stoorvogel, J.J., VanBreemen, N., Janssen, B.H., 1997. The nutrient input by Harmattan dust to a forest ecosystem in Cote d'Ivoire, Africa. Biogeochemistry. 37 (2), 145-157.

Stottlemyer, R., Troendle, C.A., 1992. Nutrient concentration patterns in streams draining alpine and subalpine catchments, Fraser Experimental Forest, Colorado. Journal of Hydrology. 140 (1-4), 179-208.

Su, Y.Z., Li, Y.L, Cui, J.Y., Zhao, W.Z., 2005. Influences of continuous grazing and livestock exclusion on soil properties in a degraded sandy grassland, Inner Mongolia, northern China. Catena. 59 (3), 267-278.

Tegen, I., Lacis, A.A, Fung, I., 1996. The influence on climate forcing of mineral aerosols from disturbed soils. Mature. 380, 419-422.

Theobald, P.K., 1965. Preliminary geologic map of the Berthoud Pass quadrangle, Clear Creek, and Grand Counties, Colorado: U.S. Geological Survey, Miscellaneous Geologic Investigations Map I-443, scale 1:24,000.

Troendle, C.A., King, R.M., 1985. The effect of timber harvest on the Fool Creek Watershed, 30-years later. Water Resources Research. 21, 1915-1922.

Troendle, C.A., Reuss, J.O., 1997. Effect of clear cutting on snow accumulation and water outflow at Fraser, Colorado. Hydrology and Earth Systems Sciences. 1 (2), 325-332.

Vitousek, P.M., Kennedy, M.J., Derry, L.A., Chadwick, O.A., 1999. Weathering versus atmospheric sources of strontium in ecosystems on young volcanic soils. Oecologia. 121 (2), 255-259.

Walker, T.W., Syers, J.K. 1976. The fate of phosphorus during pedogenesis. Geoderma. 15, 1-19.

Young, A., 1976. Tropical soils and soil survey: Cambridge University Press, Cambridge, 468 p.

Zaccherio, M.T., Finzi, A.C., 2007. Atmospheric deposition may affect northern hardwood forest composition by altering soil nutrient supply. Ecological Applications. 17, 1929-1941.

Zaitlin, B., Hayashi, M. 2012. Interactions between soil biota and the effects on geomorphological features. Geomorphology. 157 (SI), 142-152.

Zetterberg, T., Olsson, B.A., Bengt, A., Lorgren, S., Hyvonen, R., 2016. Long-term soil calcium depletion after conventional and whole-tree harvest. Forest Ecology and Management. 369, 102-115.

CHAPTER 4

SUMMARY AND CONCLUSIONS

4.1 Summary and Conclusions

The principal goal of this work was to characterize soil landscapes at Fraser Experimental Forest (FEF) by evaluating the linkages of soil properties and contributors to and effects of pedogenesis along catenas. Insight gained into the behavior of soil landscapes at FEF is applicable to similar ecosystems across the U.S. Mountain West. More specifically, this research 1) linked the systematic variation in soil morphological, physical, and biogeochemical properties across landscapes to long term hydrologic processes that regulate soil formation within Mountain Ecosystems of the Western U.S., 2) evaluated the effects of topography and parent material on the distribution of major elements within soils of Mountain Ecosystems of the Western U.S., and 3) evaluated the internal and external inputs to soil formation within soils of Mountain Ecosystems of the Western U.S. These objectives allowed me to develop a model of pedogenesis and linkages across landscapes within soil catenas by evaluating morphological, physical, and chemical soil characteristics.

To address these aforementioned objectives, I characterized and sampled pedons across eight catenas in four watersheds (Byers Creek, East St. Louis Creek, Fool Creek, and Iron Creek) at FEF (Chapter 2) to assess the systematic variability in and soil morphology, chemistry, and physical properties to infer the degree of coupling between pedogenesis and hydrologic processes operating across landscapes. I then evaluated the distribution of the soil nutrient (base cation) reserve and the state of soil weathering along these eight catenas (Chapter 3) to determine and account for hot spots of soil nutrient accumulation and loss in these mountain landscapes.

Strontium isotopic data from various cation reserves (soil, rock, and dust) were utilized to determine the specific contributions of atmospheric dust deposition to the soil nutrient (Ca) reserve, and also, as a proxy for soil weathering at FEF. What follows is a brief summary that addresses the objectives as they are described above.

4.2 Chapter 2

The results from this chapter demonstrate that soil properties behave predictably across mountain hillslopes at FEF. Eight toposequences (soil catenas) were selected in the following four watersheds (two catenas per watershed)—Byers Creek, East St. Louis Creek, Fool Creek, and Iron Creek. Through the analysis of these soil catenas located in four watersheds in FEF I showed that distinct and interconnected soil morphologies, soil chemical properties, and soil physical properties are linked to landscape positions along these catenas and the local hydrologic system.

Results presented in chapter 2 show that pedogenesis has resulted in poorly developed soils along mountaintop landscapes that transition to more well developed soils along the relatively steep mountainflank landscape positions. The mountainflank soils exhibit high pedogenic enrichment values and contain an argillic or slightly less well-developed B horizons underneath elluvial horizons in various states of formation. The elluvial horizons act as a conduit that permits the movement of infiltrated snowmelt via subsurface lateral flow. Landscape stability and subsurface lateral flow are important drivers of soil development along the mountainflanks. Mountainflank landscapes terminate into more level mountainbase landscapes characterized by organic-rich soils corresponding with slope wetlands and depressional wetlands along riparian corridors. The soil material that is translocated downslope along soil catenas is deposited in the mountainbase landscapes, completing a key biogeochemical linkage along catenas in FEF. In addition, analysis of soil texture data revealed a surprising amount of fine soil material in upper soil horizons across the entire soil catenas. This noteworthy finding from data analyzed in this chapter led to the suggestion that atmospheric deposition of dust likely plays a vital role in soil formation across all landscape positions at FEF.

4.3 Chapter 3

By applying constituent mass balance model techniques to chemical data acquired along the eight catenas at FEF I was able to assess the state of soil weathering in terms of their soil strain and net elemental flux and, in turn, evaluate the distribution of soil nutrients in various landscape positions. The majority of soils at FEF experienced mass gains during pedogenesis and soil strain values were unexpectedly high in the summit landscapes. Estimates of soil strain were higher in the surface horizons than in the subsurface horizons, across all landscapes. Depth-weighted strain values indicated that 75% of soil profiles within mountaintop landscapes, 71% of soil profiles within mountainflank landscapes, and 100% of soil profiles within mountainbase landscapes were pedogenically dilated. Constituent mass balance data suggest that soils in summit landscapes are enriched in Ca, Na, K, Al, Fe, and Mg, although Ca was by far the most extensively gained major element. Sideslopes at FEF are depleted in Na, K, and Mg and enriched in Al and Fe. However, the magnitude and direction of soil nutrient flux in these landscapes is not easily predictable due to the amount of variability in soil properties along theses landscapes. The sideslope landscapes are the most transient in nature, lending to this variability in soil properties. That withstanding, the data suggests that Ca gains in the summits are progressively lost along the upland positions of the soil catenas, until being deposited in the footslope landscapes. The footslope landscapes at FEF are composed of soils that act as a biogeochemical sink for the deposition of nutrients, and act as a sort of biologic buffer to the local hydrologic systems. These footslope landscapes are pedogenically enriched in all major elements analyzed in the following order: Ca > Al > Na = K = Mg > Fe.

The chemical and physical data indicated that soils had undergone significant volumetric and elemental gains during pedogenesis and that atmospheric contributions were likely a key player in soil formation at FEF. Chemical data demonstrated that calcium was the most extensively gained element during pedogenesis across the soil catenas, regardless of landscape position. Strontium isotopes, used as a proxy for Ca provenance, were analyzed for soils along one catena and for all summit landscape sites in the study. Strontium isotope ratios ($^{87}Sr/^{86}Sr$) and $\delta^{87}Sr$ values were calculated in order to determine the relative contribution of atmospheric dust to pedogenesis at FEF.

Strontium isotope data presented in chapter 3 suggest that the isotopic signatures of soil A horizons and subsoil horizons behave differently moving along the Byers Creek soil catena from summit to footslope landscape positions. Sr isotope data from soil A horizons indicate that their chemical signature remains relatively close to that of the atmospheric dust signature, regardless of landscape position. On the other hand, subsoil horizons carry an isotopic signature that drifts closer to the value of soil parent material (rock) moving from the summit to lower elevation landscape positions.

The analysis of summit landscape soil Sr isotope data provided insight into the subtleties of atmospheric dust contributions in these high-elevation landscape positions at FEF. The vegetation structure and, consequently, snow hydrology dynamics control the isotopic signature of soils in the summit landscapes at FEF. Data from this study demonstrate a more marked contribution of atmospheric dust to forested summit soils; dust contributions to alpine summit soils are not preserved in the same manner. It is evident that atmospheric contributions and snowmelt hydrology play a significant role in pedogenesis and the soil cation reserve held at FEF and that any shifts in this cation supply may affect the productivity of these mountain ecosystems.

Appendix 1-A

1.A.1 Summary

Soil pits were excavated in all upland landscape positions (mountaintop and mountainflanks) using shovels and pick axe to a depth where below which the material was too competent for removal without mechanical means, that would allow descriptions of the full profile and sampling of the deep C horizons. Following this summary are the horizon-by-horizon morphological, physical, and chemical data along each soil catena (Table 1-A-1). Also included in this appendix are pictures of the soil profiles in all 32 upland sites and their USDA Subgroup taxonomic classification (Figures 1-A-1 through 1-A-16).

Mountainbase wetland soils were sampled using a steel corer (Giddings Machine Company, CO) with an inner, removable plastic liner. The steel corer was 1.5 m in length and allowed for, at best, recovery of 0.90 m of soil. Soil cores were extracted from each mountainbase site, capped and sealed in the field, and immediately transported to Colorado State University for characterization and sampling. No pictures of the soil cores from this project exist, however, included in this section is a picture of the typical wetland soil found in this landscape (Figure 1-A-17).

Following the soil pictures are graphical representations of the soil pedons along each catena (Figures 1-A-18 through 1-A-25). Included in these figures are the starting and ending elevations of each catena, dominant vegetation along the catena (alpine, forest, wetland), and a cross section of the hillslopes with genetic horizons labeled and appropriate thicknesses.

1.A.2 TABLES AND FIGURES

Table 1-A-1. Morphological, physical, and chemical properties of the soils in the study.

Site	*Interval (cm)*	*Genetic Horizon*	*PSD (%) Clay %*	*Silt %*	*Sand %*	*Textural Class*	*Structure* [a]	*Color (moist)*	*Gravel (%)*	*Bulk Density* [b] *(g/cm^3)*	*pH*	*C (%)*	*N*	*C/N*
BL1	0-5	A	25.2	26.5	48.4	Sandy Clay Loam	1 vf,f gr	10 YR 3/3	25-50	1.17	4.5	5.2	0.2	29.3
	5-18	Bw1	26.0	34.7	39.4	Loam	1 vf,f gr	10 YR 5/2	50	1.41	4.4	0.9	0.0	108.9
	18-58	Bw2	20.0	19.8	60.2	Sandy Clay Loam	1 vf gr,abk	10 YR 4/6	75	1.55	5.1	0.5	0.0	108.6
	58-85	C	10.5	18.3	71.2	Sandy Loam	sg	10 YR 3/3	>75	1.56	5.2	0.3	*	**
BL2	4-0	Oi	-	-	-	-	-	-	-	-	-	38.1	1.4	27.7
	0-10	A	28.8	30.9	40.3	Clay Loam	1 vf,f gr	10 YR 4/3	10	1.24	4.0	3.6	0.1	50.4
	10-35	Bw	31.3	25.5	43.3	Clay Loam	1 vf,f abk	10 YR 4/4	35	1.45	4.0	0.8	0.0	44.5
	35-75	BC	26.8	14.4	58.8	Sandy Clay Loam	sg	10 YR 4/6	>75	1.57	4.8	0.5	0.0	153.9
	75-100	C	24.4	25.5	50.1	Sandy Clay Loam	sg	10 YR 3/4	50	1.53	5.0	0.3	*	**
BL3	8-0	Oi	-	-	-	-	-	-	-	-	-	52.4	1.7	31.3
	0-10	A	30.2	25.6	44.2	Clay Loam	1 vf,f gr	10 YR 3/3	<10	1.23	4.1	4.3	0.1	40.0
	10-20	E	26.6	27.7	45.7	Sandy Clay Loam	1 vf,f gr	10 YR 5/3	10-25	1.41	4.5	1.4	0.0	47.1
	20-82	Bw	23.9	10.5	65.7	Sandy Clay Loam	1 vf,f abk	10 YR 4/6	50	1.62	5.1	0.2	*	**
	82-122	BC	23.4	24.7	51.8	Sandy Clay Loam	1 f abk	10 YR 5/4	15-20	1.52	5.9	0.3	*	**
	122-140	C	22.7	18.6	58.7	Sandy Clay Loam	sg	10 YR 5/8	10	1.56	5.5	0.2	*	**
BL4	4-0	Oi	-	-	-	-	-	-	-	-	-	43.9	1.4	31.4
	0-13	A	33.0	34.3	32.7	Clay Loam	1 vf,f gr	7.5 YR 3/3	<10	1.35	4.3	1.4	0.0	91.3
	13-24	Bw	33.5	31.8	34.7	Clay Loam	1 vf,f gr 1 f,m abk	7.5 YR 4/3	10	1.42	5.7	0.6	0.0	18.0
	24-67	C1	28.6	16.8	54.6	Sandy Clay Loam	sg	10 YR 4/4	50-75	1.54	5.1	0.8	*	**
	67-95	C2	23.5	12.4	64.1	Sandy Clay Loam	sg	7.5 YR 4/6	75	1.60	5.1	0.3	*	**
BL5	0-13	Oe	-	-	-	-	-	-	-	0.41	4.5	40.6	1.3	30.2
	13-20	Oa	-	-	-	-	-	-	-	0.62	5.3	25.5	1.0	25.4
	20-40	Bg1	29.2	26.8	44.0	Clay Loam	sg	GLEY 1 5/5 GY	<10	1.46	4.7	0.8	*	**
	40-60	Bg2	27.0	18.4	54.7	Sandy Clay Loam	sg	5-15%	<10	1.52	5.3	1.7	0.1	15.7

Site	Interval	Genetic	PSD (%)			Textural	Structure [a]	Color	Gravel	Bulk Density [b]	pH	C	N	C/N
	(cm)	Horizon	Clay %	Silt %	Sand %	Class		(moist)	(%)	(g/cm^3)		(%)		
BU1	1-0	Oi	-	-	-	-	-	-	-	-	-	42.0	1.2	33.7
	5-0	Oa	-	-	-	-	-	-	-	0.55	4.6	31.2	0.8	41.0
	0-5	BC	21.2	21.8	57.0	Sandy Clay Loam	1 vf,f gr	10 YR 4/6	75	1.53	5.4	0.4	*	**
	5-45	C	15.8	16.5	67.7	Sandy Loam	sg	10 YR 4/4	>75	1.56	4.7	0.7	*	**
BU2	1-0	Oi	-	-	-	-	-	-	-	-	-	33.6	1.2	27.7
	0-8	A	25.5	25.0	49.4	Sandy Clay Loam	1 vf,f gf	10 YR 3/3	<10	1.15	4.8	5.7	0.2	35.6
	8-35	E	23.0	31.4	45.6	Loam	1 vf,f gr	10 YR 6/4	25	1.49	4.7	0.4	0.0	441.5
	35-65	Bw	29.8	21.8	48.4	Sandy Clay Loam	1 vf,f abk	10 YR 4/6	25	1.53	4.8	0.3	0.0	**
	65-110	C	23.2	19.1	57.7	Sandy Clay Loam	sg	10 YR 3/4	50-75	1.56	5.0	0.1	0.0	**
BU3	1-0	Oi	-	-	-	-	-	-	-	-	-	37.6	1.3	28.0
	0-4	A	35.4	26.4	38.2	Clay Loam	1 vf,f gr	10 YR 3/3	10	1.00	4.6	8.7	0.3	34.8
	4-17	EB	28.5	27.5	44.0	Clay Loam	1 vf,f gr 1 vf,f abk	10 YR 4/6	15	1.44	5.1	1.1	0.0	30.6
	17-58	Bw	35.0	14.7	50.3	Sandy Clay	1 vf,f abk	10 YR 4/6	30	1.55	5.1	0.4	0.0	38.7
	58-85	C	36.6	14.2	49.2	Sandy Clay	sg	10 YR 4/4	50-75	1.57	5.4	0.2	*	**
BU4	2-0	Oi	-	-	-	-	-	-	-	-	-	23.0	0.9	25.7
	0-8	A	30.6	29.7	39.7	Clay Loam	1 vf,f gr	10 YR 3/4	<10	1.23	5.1	3.8	0.1	26.5
	8-70	Bw	14.4	16.1	69.5	Sandy Loam	1 vf,f gr 1 f abk	10 YR 4/6	25-50	1.59	5.0	0.2	*	**
	70-120	C1	21.0	20.5	58.5	Sandy Clay Loam	1 vf,f gr	10 YR 4/6	50-75	1.54	4.7	0.2	*	**
	120-200	C2	27.3	25.5	47.2	Sandy Clay Loam	sg	10 YR 3/4	75	1.58	5.2	0.2	*	**
BU5	0-10	Oe	-	-	-	-	-	-	-	0.51	4.0	34.3	2.0	17.2
	10-15	Oa	-	-	-	-	-	-	-	0.44	4.8	42.5	1.3	32.7
	15-37	Cg1	24.6	22.2	53.2	Sandy Clay Loam	sg	GLEY 1 5/5 GY	10	1.51	4.4	0.7	0.1	13.0
	37-58	Cg2	22.3	21.4	56.3	Sandy Clay Loam	sg	5-10% mottles 5 YR 5/6	10	1.53	4.2	0.6	0.1	11.0

Site	Interval (cm)	Genetic Horizon	PSD (%) Clay %	Silt %	Sand %	Textural Class	Structure [a]	Color (moist)	Gravel (%)	Bulk Density [b] (g/cm^3)	pH	C (%)	N (%)	C/N
EL1	0-5	A	28.4	21.3	50.3	Sandy Clay Loam	1 vf gr	10 YR 3/3	10	1.43	5.1	1.6	0.1	31.2
	5-18	Bw	20.0	21.8	58.2	Sandy Clay Loam	1 vf gr 1 vf abk	10 YR 4/4	25	1.53	5.0	0.7	0.0	54.7
	18-60	C	12.3	12.9	74.8	Sandy Loam	sg	10 YR 5/4	75	1.61	4.7	0.2	*	**
EL2	2-0	Oi	-	-	-	-	-	-	-		-	29.4	1.0	29.3
	0-5	A	27.9	28.9	43.1	Clay Loam	1 vf,f gr	10 YR 4/3	10	1.25	4.4	3.7	0.1	39.3
	5-40	Bw	23.0	17.2	59.8	Sandy Clay Loam	1 vf,f gr 1 vf,f abk	10 YR 4/6	25-50	1.55	4.4	0.6	0.0	38.4
	40-140	C	21.6	14.1	64.3	Sandy Clay Loam	sg	10 YR 5/6	50-75	1.6	5.5	0.3	*	**
EL3	3-0	Oi	-	-	-	-	-	-	-	-	-	39.6	1.5	26.8
	0-3	A	33.7	31.6	34.7	Clay Loam	1 f gr	10 YR 3/3	10	0.76	4.1	16.7	0.5	31.5
	3-38	EB	27.7	25.5	46.9	Sandy Clay Loam	1 f abk 1 f sbk	10 YR 5/3	50	1.45	4.3	1.2	0.0	44.4
	38-70	BC	18.9	22.4	58.7	Sandy Loam	1 f,m abk 1 f,m sbk	10 YR 4/4	25-50	1.54	5.3	0.4	0.0	314.4
	70-90	C	10.3	7.2	82.5	Loamy Sand	sg	10 YR 3/3	10-25	1.62	5.3	0.2	*	**
EL4	3-0	Oi	-	-	-	-	-	-	-	-	-	42.4	1.9	22.2
	0-10	AB	32.7	42.9	24.4	Clay Loam	1 f gr	10 YR 5/3	10	1.24	4.0	1.7	0.7	2.6
	10-35	Bt	40.4	31.9	27.6	Clay	1 f abk	10 YR 4/4	10-25	1.40	4.3	0.5	0.1	5.1
	35-85	BC	33.5	20.9	45.6	Sandy Clay Loam	1 f sbk 1 f abk	10 YR 4/6	25-50	1.53	4.7	0.4	*	**
	85-110	C	27.0	22.3	50.7	Sandy Clay Loam	sg	10 YR 3/4	50-75	1.54	4.9	0.2	*	**
EL5	0-20	Oe	-	-	-	-	-	-	-	0.58	4.3	20.9	0.8	26.6
	20-75	Cg	24.8	14.0	61.3	Sandy Clay Loam	sg	GLEY 1 4/5 GY	10	1.46	4.9	1.8	0.1	20.1

Site	Interval	Genetic	PSD (%)			Textural	Structure [a]	Color	Gravel	Bulk Density [b]	pH	C	N	C/N
	(cm)	Horizon	Clay %	Silt %	Sand %	Class		(moist)	(%)	(g/cm^3)		(%)		
EU1	3-0	Oi					-	-	-	-	-	29.6	1.8	16.4
	0-10	A	36.8	20.1	43.1	Clay Loam	1 vf,f gr	7.5 YR 3/2	10	1.11	4.4	6.7	0.5	14.4
	10-25	BC	20.2	18.5	61.3	Sandy Clay Loam	1 f gr	7.5 YR 4/4	25	1.44	4.8	1.9	0.2	12.3
	25-56	C	26.9	15.1	57.9	Clay Loam	sg	7.5 YR 4/6	25 (30)	1.5	5.5	1.3	0.1	13.2
EU2	1-0	Oi	-	-	-	-	-	-	-	-	-	12.8	1.0	12.3
	0-10	A	36.6	33.8	29.7	Clay Loam	1 vf,f gr	7.5 YR 3/2	<10	0.94	4.1	9.7	0.9	11.4
	10-18	Bw1	30.4	31.1	38.4	Clay Loam	1 f gr 1 f,m sbk	10 YR 4/4	10	1.04	4.0	7.6	0.2	37.8
	18-38	Bw2	28.2	25.4	46.4	Sandy Clay Loam	1 f gr 1 f,m sbk	10 YR 4/4	10	1.17	4.0	5.4	0.2	26.8
	38-51	BC	41.5	22.7	35.7	Clay	1 f,m gr	10 YR 4/4	10	1.34	4.2	1.9	0.2	11.2
	51-76	C	31.8	13.4	54.7	Sandy Clay Loam	sg	10 YR 4/6	25	1.54	4.4	0.8	0.1	12.8
EU3	2-0	Oi	-	-	-	-	-	-	-	-	-	26.3	0.8	31.2
	0-5	A	25.4	24.6	50.0	Sandy Clay Loam	1 f gr	10 YR 3/2	10	1.03	5.1	8.5	0.4	24.1
	5-20	E	16.2	20.9	62.9	Sandy Loam	1 f gr 1 f sbk	10 YR 6/4	25	1.53	4.4	0.5	0.0	102.2
	20-45	Bw	27.8	27.6	44.6	Clay Loam	1 f sbk	10 YR 4/6	25	1.39	4.1	0.4	*	**
	45-88	C1	21.7	29.0	49.3	Loam	sg	10 YR 4/6	75	1.50	4.8	0.4	*	**
	88-125	C2	15.6	4.0	80.4	Sandy Loam	sg	10 YR 3/4	75	1.66	5.3	0.4	*	**
EU4	5-0	Oi	-	-	-	-	-	-	-	-	-	42.4	1.5	28.7
	0-5	A	22.4	24.4	53.3	Sandy Clay Loam	1 vf gr	10 YR 3/2	10	0.85	5.1	13.9	0.5	27.7
	5-18	E	21.3	29.9	48.7	Loam	1 vf gr	10 YR 5/3	25	1.39	4.0	1.6	0.1	29.8
	18-38	Bw	27.4	16.8	55.8	Sandy Clay Loam	1 vf gr 1 vf sbk	10 YR 4/6	50-75	1.42	4.5	1.8	0.0	38.5
	38-65	C	14.8	16.9	68.2	Sandy Loam	sg	10 YR 4/6	>75	1.53	4.7	0.7	0.0	72.2
EU5	0-15	Oi	-	-	-	-	-	-	-	0.47	4.6	32.8	2.1	15.7
	15-25	Oe	-	-	-	-	-	-	-	0.59	5.2	27.3	1.5	18.2
	25-36	Oa	-	-	-	-	-	-	-	0.50	5.0	28.8	1.3	22.1
	36-46	Oe'	-	-	-	-	-	-	-	0.57	5.1	29.2	1.4	21.2
	46-66	Cg	19.8	13.9	66.3	Sandy Clay Loam	sg	GLEY 1 6/10 GY	10-25	1.54	4.5	0.9	0.1	17.6

Site	Interval (cm)	Genetic Horizon	PSD (%) Clay %	Silt %	Sand %	Textural Class	Structure [a]	Color (moist)	Gravel (%)	Bulk Density [b] (g/cm^3)	pH	C (%)	N	C/N
FL1	3-0	Oi	-	-	-	-	-	-	-	-	-	28.5	1.0	29.0
	0-4	A	24.4	27.1	48.6	Sandy Clay Loam	1 vf,f gr	10 YR 4/3	<10	1.46	4.4	1.0	0.0	28.0
	4-15	BC	17.0	38.0	45.0	Loam	1 vf,f gr 1 vf,f sbk	10 YR 4/6	75	1.38	4.5	1.0	0.0	19.8
	15-60	C	27.8	25.7	46.6	Sandy Clay Loam	sg	7.5 YR 5/4	>75	1.49	4.7	0.5	0.0	17.9
FL2	2-0	Oi	-	-	-	-	-	-	-	-	-	40.8	1.7	24.3
	0-5	A	30.4	34.5	35.1	Clay Loam	1 vf gr	10 YR 3/3	10	1.14	4.6	5.1	0.1	35.1
	5-22	E	23.5	20.3	56.2	Sandy Clay Loam	1 vf,f gr 1 vf,f abk	10 YR 5/3	25	1.48	4.3	1.1	0.0	63.4
	22-31	Bt	40.1	22.3	37.6	Clay	1 vf,f sbk	10 YR 3/4	25	1.44	4.8	0.7	0.0	15.3
	31-68	BC	33.0	25.8	41.3	Clay Loam	1 vf gr 1 vf abk	10 YR 5/6	50-75	1.47	4.9	0.6	*	**
	68-90	C	26.7	14.1	59.2	Sandy Clay Loam	sg	10 YR 4/6	>75	1.58	5.2	0.4	0.0	14.7
FL3	2-0	Oi					-	-	-	-	-	28.8	1.0	27.9
	0-8	A	27.8	33.3	38.8	Loam	1 vf,f gr	10 YR 3/3	<10	1.34	4.5	1.6	0.0	58.1
	8-18	E	29.9	31.2	38.9	Clay Loam	1 vf,f abk 1 vf,f sbk	10 YR 5/2	10	1.35	4.6	1.8	0.1	21.7
	18-46	Bt	34.1	25.9	40.0	Clay Loam	1 vf,f abk	10 YR 5/6	10-25	1.45	4.6	0.6	0.0	21.3
	46-74	BC	30.4	22.2	47.4	Sandy Clay Loam	m	10 YR 4/6	50-75	1.50	5.0	0.5	*	**
	74-100	C	23.1	16.0	60.9	Sandy Clay Loam	sg	10 YR 3/4	>75	1.59	5.3	0.3	0.0	14.4
FL4	5-0	Oi	-	-	-	-	-	-	-	-	-	31.9	1.5	21.3
	0-14	AE	33.0	30.2	36.8	Clay Loam	1 vf,f gr	10 YR 4/2	<10	1.34	4.5	1.6	0.0	35.9
	14-37	EB	22.6	38.0	39.4	Loam	2 vf,f gr 1 f,m sbk	10 YR 6/4	10	1.40	5.7	0.7	0.0	17.3
	37-76	Bw	25.0	27.3	47.7	Sandy Clay Loam	2 vf,f gr 1 f,m sbk	2.5 Y 5/4	10-25	1.51	5.3	0.2	*	**
	76-125	BC	30.0	31.0	39.2	Clay Loam	1 vf,f gr 1 f,m abk	2.5 Y 5/4	50	1.46	4.6	0.3	0.0	11.5
	125-175	C	27.0	30.0	42.9	Loam	sg	10 YR 4/4	50	1.49	5.3	0.2	*	**
FL5	0-5	Oe	-	-	-	-	-	-	-	0.47	4.2	33.1	2.3	14.3
	5-20	A	20.0	33.0	47.0	Loam	1 vf,f gr	10 YR 3/2	<10	0.72	4.7	19.0	1.9	9.9
	20-55	Cg1	27.2	23.8	49.0	Sandy Clay Loam	sg	GLEY 1 4/5 GY	50	1.45	4.7	1.0	1.4	0.7
	55-90	Cg2	32.5	21.6	45.9	Sandy Clay Loam	sg	mottles 5-20%		1.47	5.3	0.9	0.1	14.8
								5 YR 5/6						

Site	Interval (cm)	Genetic Horizon	PSD (%) Clay %	Silt %	Sand %	Textural Class	Structure [a]	Color (moist)	Gravel (%)	Bulk Density [b] (g/cm^3)	pH	C (%)	N (%)	C/N
FU1	2-0	Oi	-	-	-	-	-	-	-	-	-	44.8	1.5	29.5
	0-10	BA	33.1	33.4	33.5	Clay Loam	1 f gr	10 YR 4/4	<10	1.03	4.8	7.5	1.6	4.7
	10-61	Bw	20.5	9.8	69.7	Sandy Clay Loam	1 f gr 1 vf,f sbk	10 YR 4/6	10-25	1.56	4.5	1.1	0.4	3.1
	61-90	BC	18.0	17.2	64.8	Sandy Loam	1 vf,f gr	10 YR 4/6	>75	1.52	4.8	0.9	0.0	42.0
	90-100	C	14.9	27.0	58.1	Sandy Loam	sg	7.5 YR 4/4	25	1.50	4.9	0.5	0.1	9.3
FU2	6-0	Oi	-	-	-	-	-	-	-	-	-	10.6	0.5	23.6
	0-5	A	36.9	38.3	24.9	Clay Loam	1 vf gr	10 YR 3/2	<10	0.97	4.1	7.9	0.7	11.8
	5-16	Bw1	32.4	22.7	44.9	Clay Loam	1 vf,f gr	10 YR 4/4	10-25	1.39	5.6	8.1	0.3	32.0
	16-27	Bw2	28.9	26.3	44.8	Clay Loam	1 vf,f gr	10 YR 4/6	25	1.43	4.4	1.8	0.3	6.8
	27-46	BC	26.5	26.0	47.6	Sandy Clay Loam	1 vf,f gr 1 vf,f sbk	10 YR 4/6	10-25	1.42	4.9	1.2	0.1	17.3
	46-74	C1	24.7	25.0	50.3	Sandy Clay Loam	sg	10 YR 4/2	10	1.52	4.7	0.3	0.0	13.1
	74-80	C2	16.9	8.4	74.7	Sandy Loam	sg	10 YR 3/3	10	1.63	4.7	0.2	0.0	8.5
FU3	1-0	Oi	-	-	-	-	-	-	-	-	-	14.7	0.6	24.4
	0-5	A	36.6	35.6	27.8	Clay Loam	1 vf,f gr 1 vf,f abk	10 YR 2/2	<10	0.74	4.8	17.7	0.8	22.3
	5-13	EB	29.4	29.7	40.9	Clay Loam	1 vf,f gr 1 vf,f abk	10 YR 5/4	<10	1.25	4.4	2.7	0.9	2.8
	13-41	Bw	27.3	22.4	50.3	Sandy Clay Loam	1 vf gr	10 YR 5/6	50-75	1.48	4.6	0.8	0.2	3.2
	41-74	BC	10.6	6.4	83.0	Loamy Sand	sg	10 YR 4/6	50-75	1.61	4.9	0.4	0.0	16.8
	74-90	C	15.6	7.3	77.1	Sandy Loam	sg	10 YR 4/4	>75	1.62	4.9	0.3	0.0	54.7
FU4	5-0	Oi	-	-	-	-	-	-	-	-	-	40.1	1.5	26.0
	0-13	A	35.1	46.5	18.4	Silty Clay Loam	1 vf,f gr 1 vf,f abk	5 YR 3/3	<10	1.21	4.9	2.7	1.7	1.6
	13-33	E	24.6	31.0	44.4	Loam	1 vf,f gr 1 vf,f abk	5 YR 5/3	25-50	1.43	4.2	0.9	0.1	8.3
	33-61	Bw	19.0	24.0	57.0	Sandy Loam	2 f,m abk	7.5 YR 4/6	10-25	1.48	4.9	0.8	0.0	21.4
	61-94	BC	24.7	29.2	46.1	Loam	1 f abk 1 f sbk	10 YR 4/4	10-25	1.51	5.0	0.3	0.1	4.4
	94-120	C	24.9	37.3	37.8	Loam	sg	10 YR 4/3	10-25	1.36	4.9	0.2	*	**
FU5	0-23	Oe	-	-	-	-	-	-	-	0.53	-	25.6	1.0	25.1
	23-28	A	25.0	30.0	45.0	Loam	1 vf,f gr	10 YR 3/2	10	0.75	4.8	16.5	0.4	41.3
	28-56	2Cg	27.2	23.9	48.9	Sandy Clay Loam	1 vf,f abk	GLEY 1 5/5 GY	50	1.32	4.2	1.4	0.6	2.6

Site	*Interval (cm)*	*Genetic Horizon*	*PSD (%)*			*Textural Class*	*Structure* [a]	*Color (moist)*	*Gravel (%)*	*Bulk Density* [b] *(g/cm³)*	*pH*	*C*	*N*	*C/N*
			Clay %	*Silt %*	*Sand %*							*(%)*		
IL1	0-3	A	28.8	41.2	30.0	Clay Loam	1 vf,f gr	10 YR 4/3	25	1.10	4.8	5.1	0.2	22.1
	3-17	BC	24.1	36.2	39.7	Loam	sg	10 YR 4/4	50-75 (60)	1.28	4.8	1.6	0.2	9.0
	17-90	C	23.5	41.2	35.3	Loam	sg	10 YR 4/6	>75	1.30	4.9	0.8	0.1	11.9
IL2	0-14	A	31.1	19.2	49.7	Sandy Clay Loam	1 vf,f gr	10 YR 4/4	10-25	1.31	4.7	1.5	0.1	11.6
	14-40	BC	30.6	36.7	32.7	Clay Loam	1 vf gr	10 YR 4/6	75	1.40	5.1	0.7	0.0	17.8
	40-100	C	17.4	26.1	56.5	Sandy Loam	sg	10 YR 5/4	>75	1.50	5.8	0.4	0.0	21.0
IL3	2-0	Oi	-	-	-	-	-	-	-	-	-	35.8	1.5	24.7
	0-6	A	38.6	31.5	29.9	Clay Loam	1 vf gr	10 YR 3/3	<10	1.08	5.1	5.9	1.1	5.1
	6-25	Bw1	30.2	41.2	28.6	Clay Loam	1,2 vf,f,m abk	10 YR 4/4	10	1.32	4.9	1.1	0.2	5.2
	25-73	Bw2	23.4	46.6	30.0	Loam	1,2 vf,f,m abk	10 YR 4/6	20	1.33	5.0	0.6	0.1	10.3
	73-80	C1	19.5	21.9	58.6	Sandy Loam	sg	10 YR 4/6	10	1.51	5.0	0.7	0.0	24.3
	80-85	C2	17.4	17.4	65.2	Sandy Loam	sg	10 YR 4/6	11	1.46	4.6	1.6	0.1	27.0
IL4	0-18	AE	28.2	24.9	46.9	Sandy Clay Loam	1 vf,f gr 1-2 f,m sbk	10 YR 5/3	10	1.28	4.8	3.4	0.2	18.0
	18-100	C	26.0	43.0	30.9	Loam	sg	10 YR 4/4	>75	1.35	4.4	0.7	0.1	5.2
IL5	0-6	Oe	-	-	-	-	-	-	-	0.60	4.2	18.7	0.7	25.4
	6-13	A	15.0	30.0	55.0	Sandy Loam	1 vf gr	10 YR 3/2	<10	0.73	5.6	9.9	1.0	10.1
	13-30	Bg	24.6	29.6	45.8	Loam	1 vf,f gr	2.5 Y 6/2	10	1.15	5.2	5.6	0.4	14.0
	30-48	Oa	-	-	-	-	-	5 YR 5/6 mottles 10%	-	0.63	5.1	16.7	0.3	55.6

Site	Interval (cm)	Genetic Horizon	PSD (%) Clay %	Silt %	Sand %	Textural Class	Structure [a]	Color (moist)	Gravel (%)	Bulk Density [b] (g/cm^3)	pH	C (%)	N	C/N
IU1	2-0	Oi	-	-	-	-	-	-	-	-	-	19.1	0.8	23.8
	0-8	A	28.3	32.2	39.5	Clay Loam	1 vf gr	10 YR 3/2	10	0.95	4.5	10.2	1.4	7.4
	8-31	Bw	31.0	22.7	46.3	Sandy Clay Loam	1 vf,f gr 1 vf,f abk	10 YR 3/3	10	1.26	4.9	3.8	0.7	5.7
	31-37	BC	24.9	15.6	59.5	Sandy Clay Loam	1 vf,f abk	10 YR 4/6	10-25	1.44	4.5	1.9	0.1	15.6
	37-60	C1	29.7	22.2	48.1	Sandy Clay Loam	sg	10 YR 3/4	50	1.42	4.6	1.5	*	**
	60-100	C2	15.1	11.3	73.5	Sandy Loam	sg	10 YR 3/6	75	1.55	4.8	0.7	0.1	8.0
IU2	1-0	Oi	-	-	-	-	-	-	-	-		12.6	0.5	24.5
	0-8	A	33.2	24.8	42.1	Clay Loam	1 vf,f gr	10 YR 3/2	<10	1.08	4.4	7.1	0.7	10.0
	8-32	Bw	29.4	26.9	43.6	Clay Loam	1 vf,f gf 1 vf,f sbk	10 YR 3/4	10-25	1.35	4.6	2.1	0.5	4.2
	32-100	C	27.9	18.4	53.7	Sandy Clay Loam	sg	10 YR 3/4	>75	1.38	4.9	2.3	0.1	18.4
IU3	3-0	Oi	-	-	-	-	-	-	-	-	-	35.1	1.4	25.9
	0-8	A	38.9	2.3	58.8	Sandy Clay	1 vf,f gr	10 YR 2/2	<10	0.66	5.0	18.3	1.6	11.7
	8-38	Bw	26.6	22.5	50.9	Sandy Clay Loam	1 vf,f gf 1 f abk	10 YR 3/3	10-25	1.38	4.1	2.0	0.9	2.2
	38-68	BC	15.8	17.4	66.8	Sandy Loam	1 vf f gr	10 YR 4/4	10-25	1.47	5.0	1.0	0.1	14.1
	68-120	C	19.7	19.2	61.1	Sandy Clay Loam	sg	10 YR 4/6	50	1.51	5.0	0.9	0.0	31.7
IU4	3-0	Oi	-	-	-	-	-	-	-	-	-	1.1	0.1	14.5
	0-8	A	18.3	31.4	50.4	Loam	1 vf,f gr	10 YR 3/2	<10	0.83	4.9	4.5	0.0	150.5
	8-45	EB	24.5	31.9	43.6	Loam	1 vf gr 1 f abk	10 YR 5/3	25	1.43	4.9	4.3	1.6	2.7
	45-88	BC	24.5	11.2	64.2	Sandy Clay Loam	1 vf,f gr	10 YR 3/4	50-75	1.57	5.2	0.9	0.5	1.7
	88-120	C	15.5	11.3	73.2	Sandy Loam	sg	10 YR 3/4	75	1.59	5.6	0.5	0.1	8.0
IU5	0-20	Oe	-	-	-	-	-	-	-	0.52	4.41	20.8	0.9	24.4
	20-46	Btg	42.3	29.9	27.9	Clay	2 f,m abk	GLEY 2 5/10B	<10	1.16	5.1	4.0	*	**
	46-66	C	27.5	16.3	56.3	Sandy Clay Loam	sg	GLEY 2 5/10B	50	1.34	4.4	2.6	0.2	11.0

[a] 1 = weak, 2 = moderate; vf = very fine, f = fine, m = medium; gr = granular, sbk = subangular blocky, abk = angular blocky, sg = single grained. [b] Estimated by Rawls

- Sample not analyzed, * Below detection limits, **Not calculated

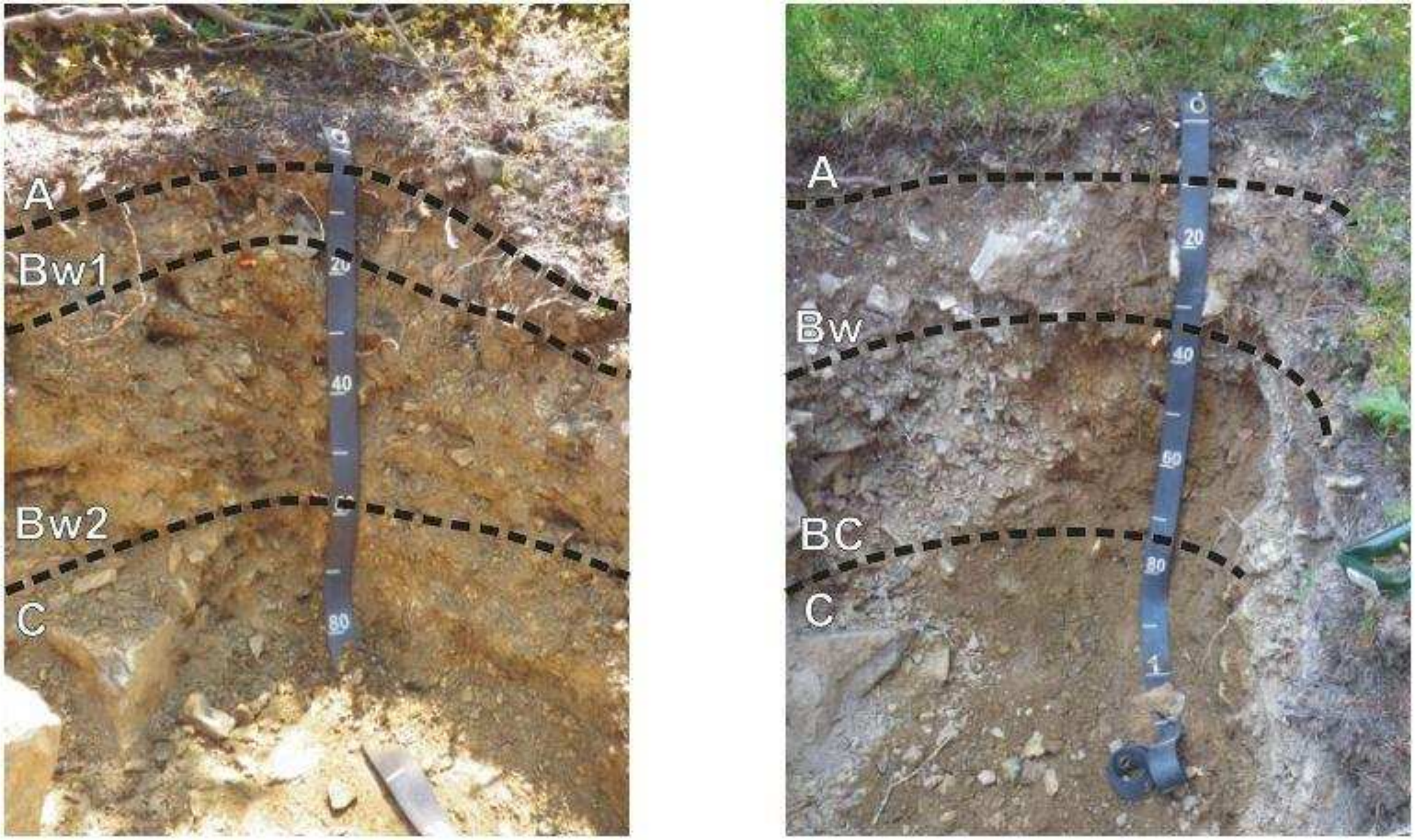

BL1 BL2

Figure 1-A-1. Pictures of soil pits at sites BL1 and BL2. The USDA taxonomic Subgroup classification of the two soils are Typic Haplocryept and Inceptic Haplocryalf, respectively.

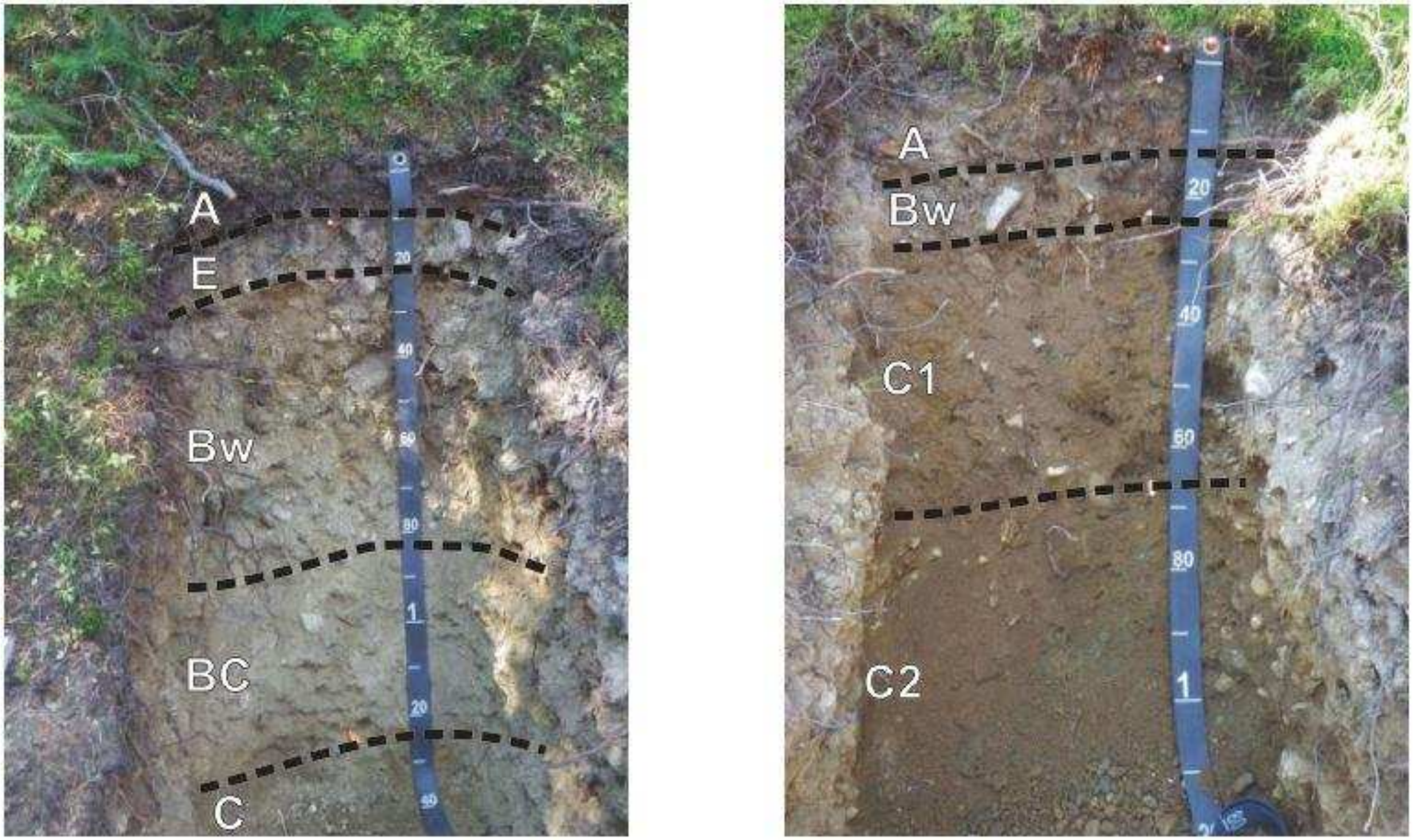

BL3 BL4

Figure 1-A-2. Pictures of soil pits at sites BL2 and BL3. The USDA taxonomic Subgroup classification of the two soils are Psammentic Hapludalf and Inceptic Hapludalf, respectively.

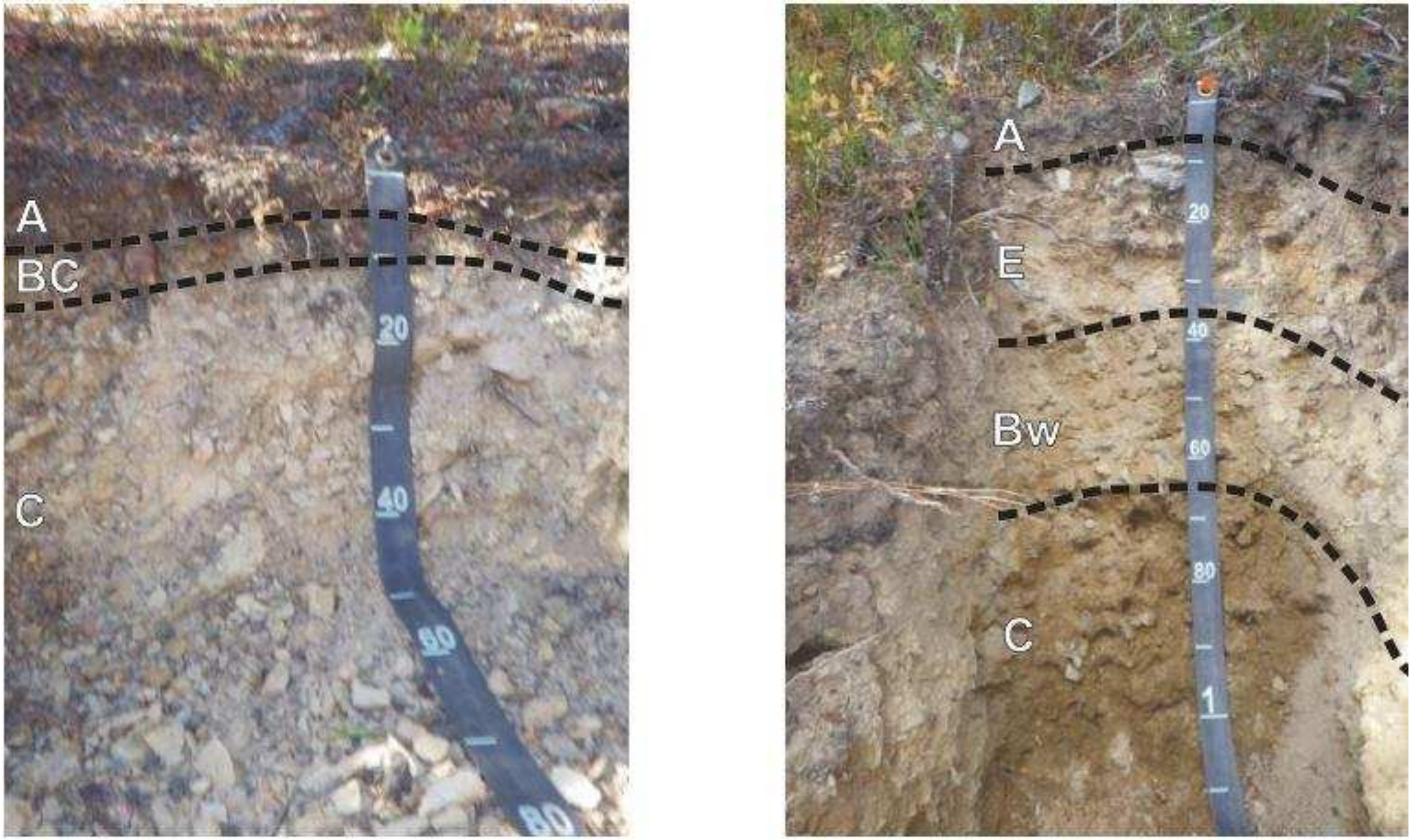

BU1 BU2

Figure 1-A-3. Pictures of soil pits at sites BU1 and BU2. The USDA taxonomic Subgroup classification of the two soils are Typic Cryorthent and Typic Haplocryept, respectively.

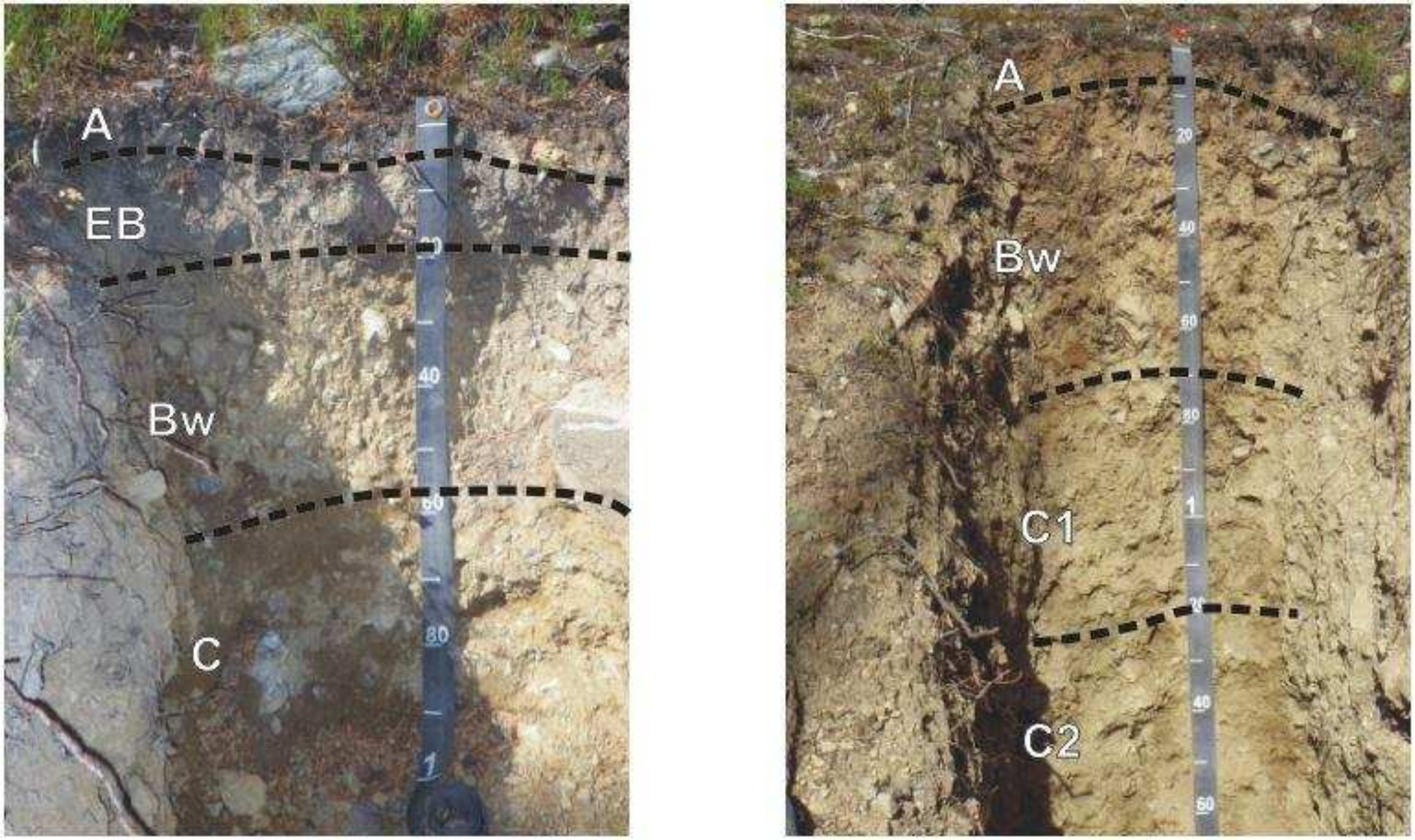

BU3 BU4

Figure 1-A-4. Pictures of soil pits at sites BU3 and BU3. The USDA taxonomic Subgroup classification of the two soils are Typic Haplocryept and Typic Haplocryept, respectively.

EL1 EL2

Figure 1-A-5. Pictures of soil pits at sites EL1 and EU2. The USDA taxonomic Subgroup classification of the two soils are Typic Haplocryept and Typic Haplocryept, respectively.

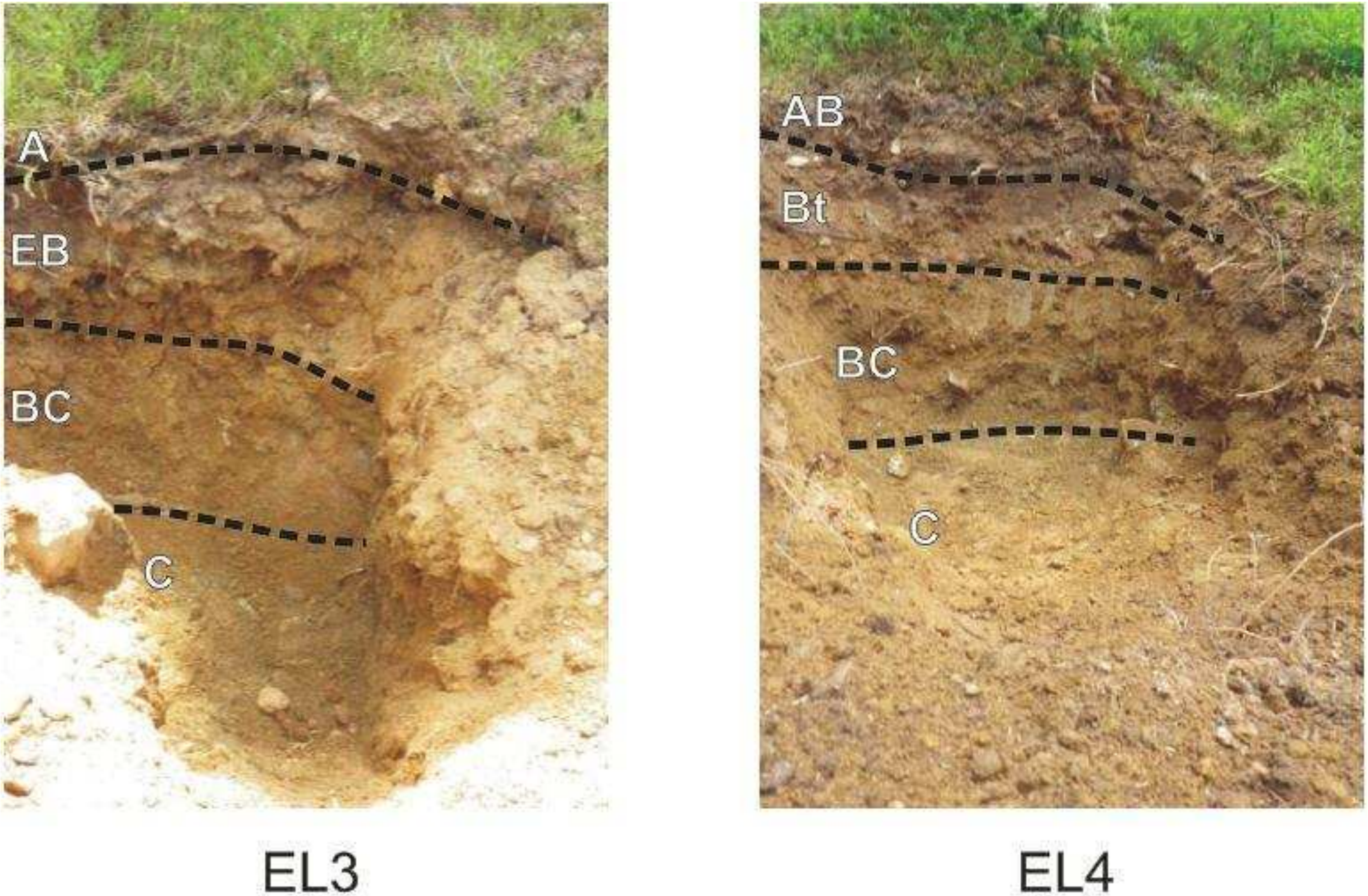

Figure 1-A-6. Pictures of soil pits at sites EL3 and EL4. The USDA taxonomic Subgroup classification of the two soils are Typic Cryorthent and Inceptic Haplocryalf, respectively.

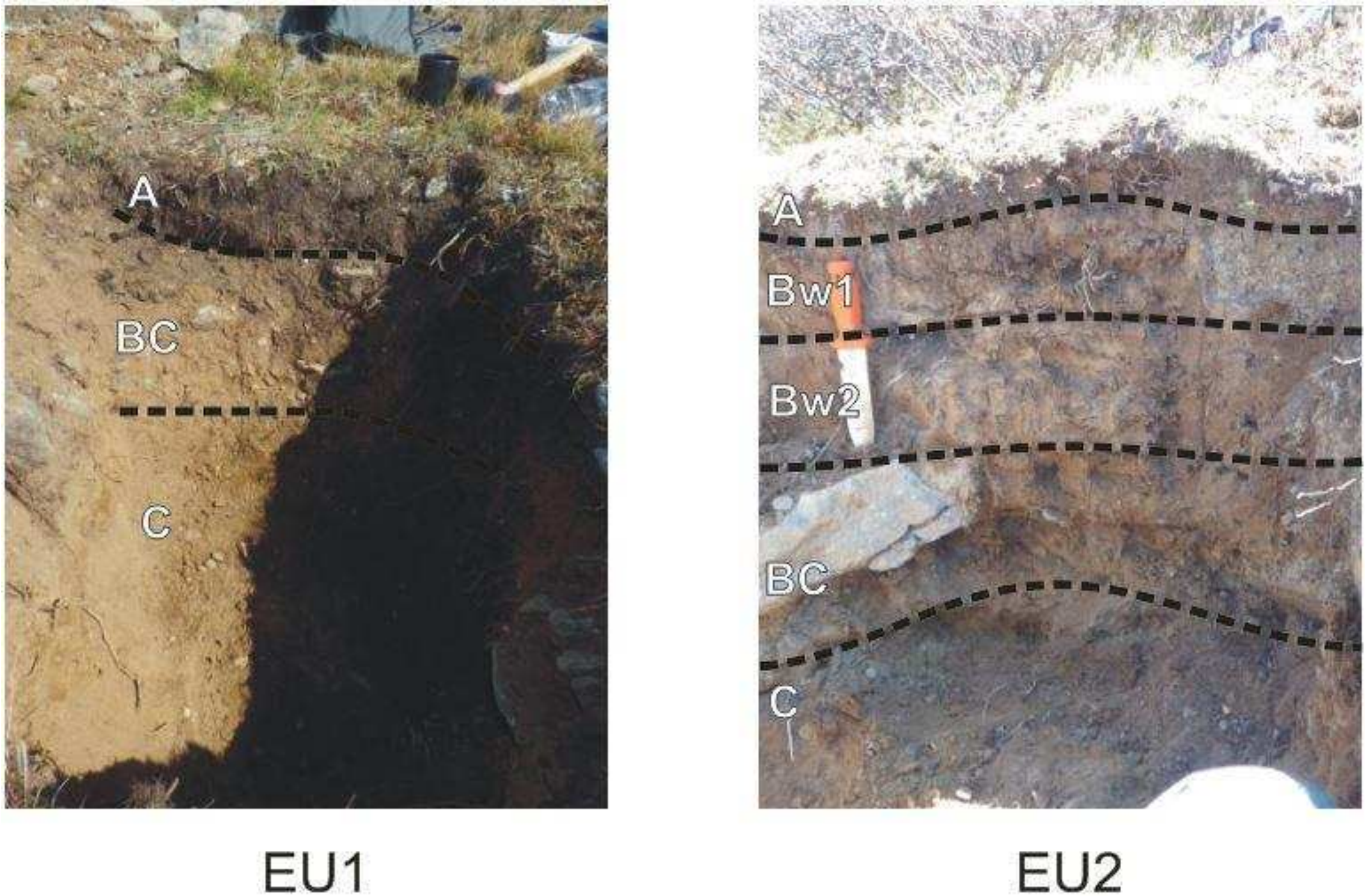

Figure 1-A-7. Pictures of soil pits at sites EU1 and EU2. The USDA taxonomic Subgroup classification of the two soils are Typic Ustorthent and Inceptic Haplocryalf, respectively.

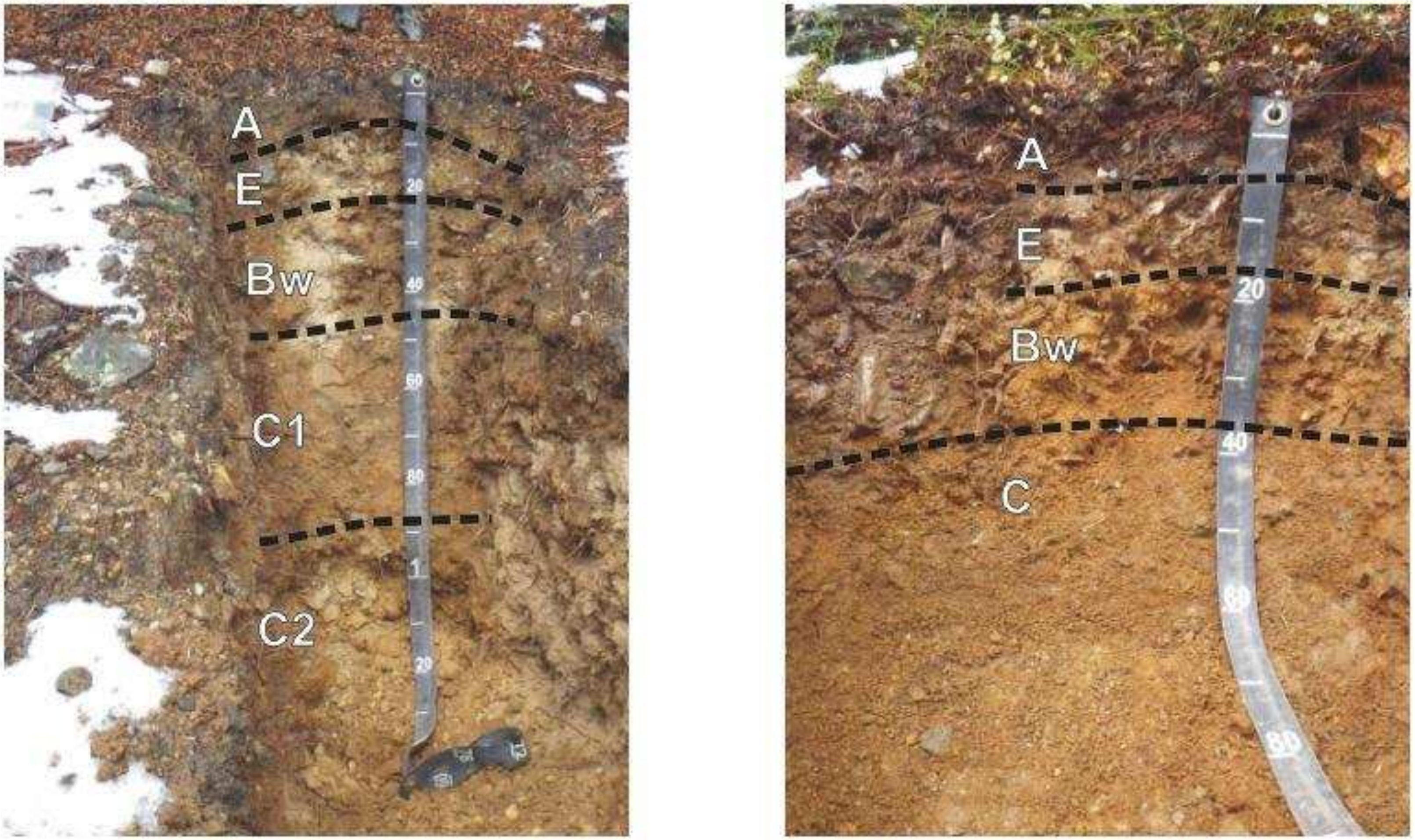

EU3 EU4

Figure 1-A-8. Pictures of soil pits at sites EU3 and EU4. The USDA taxonomic Subgroup classification of the two soils are Inceptic Haplocryalf and Psammentic Haplocryalf, respectively.

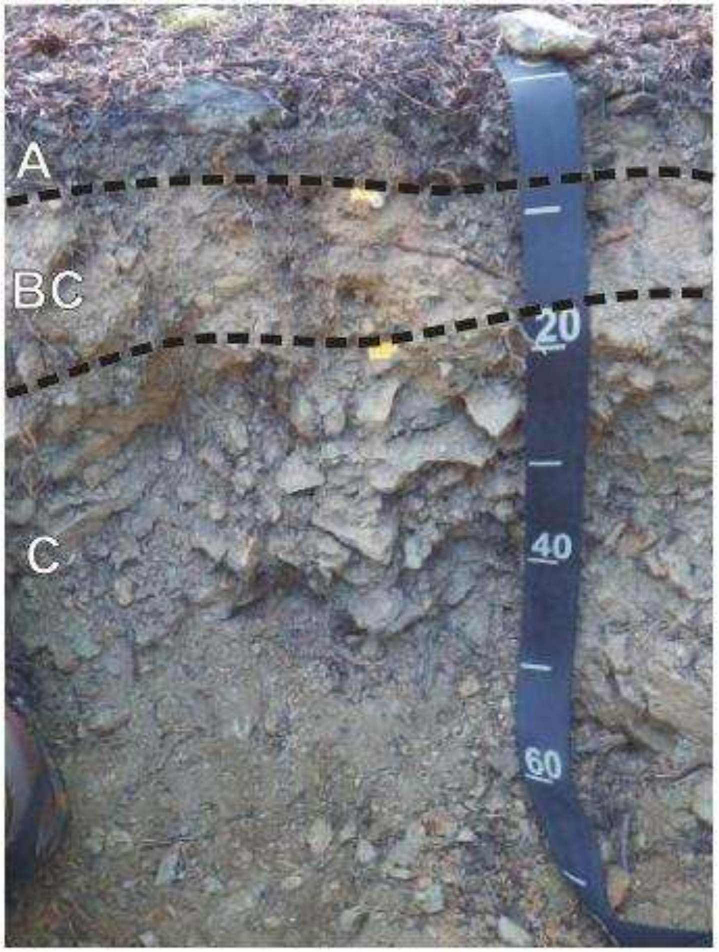

FL1

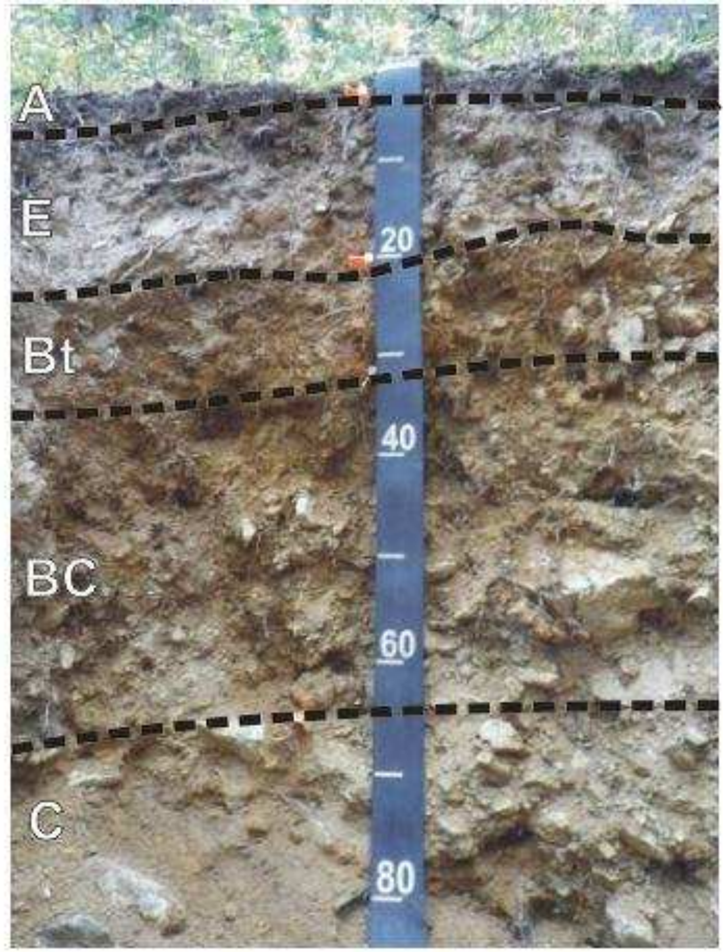

FL2

Figure 1-A-9. Pictures of soil pits at sites FL1 and FL2. The USDA taxonomic Subgroup classification of the two soils are Typic Cryorthent and Typic Haplocryalf, respectively.

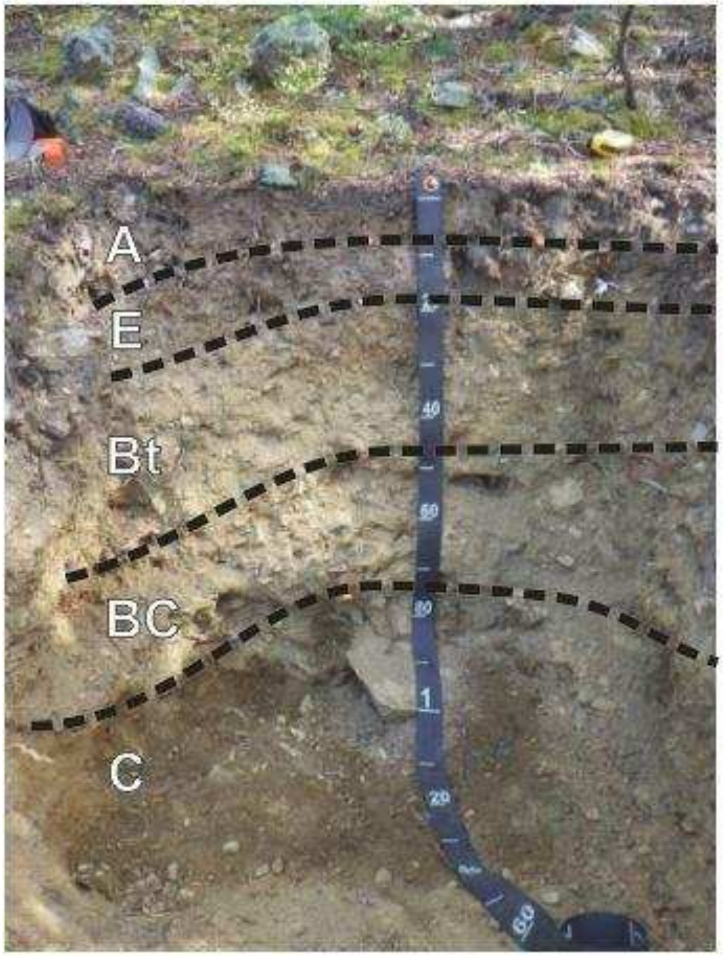

FL3

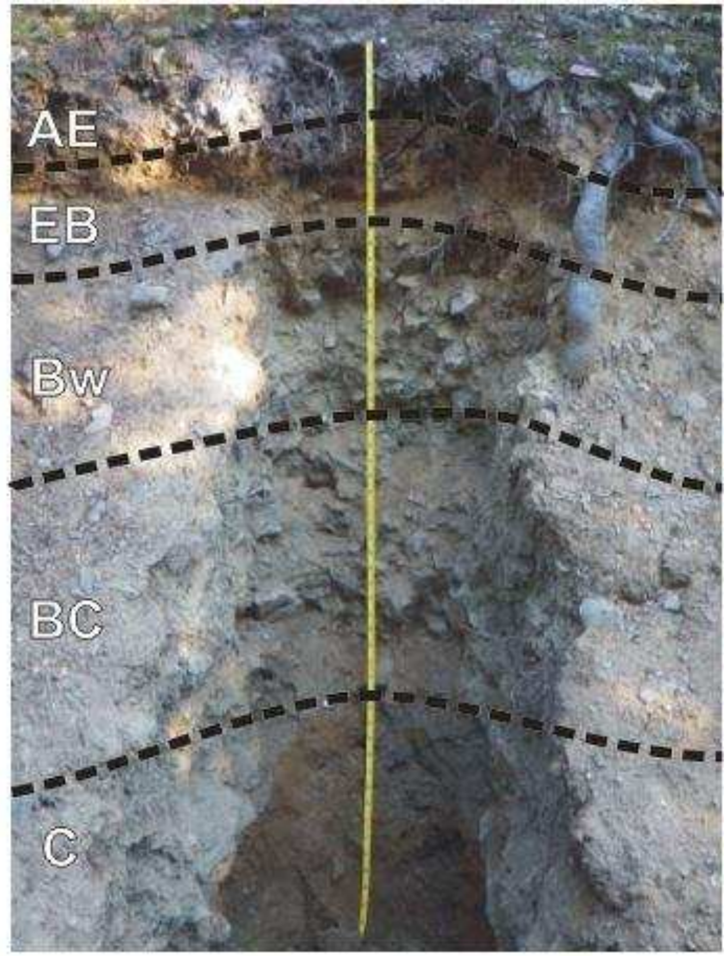

FL4

Figure 1-A-10. Pictures of soil pits at sites FL3 and FL4. The USDA taxonomic Subgroup classification of the two soils are Typic Haplocryalf and Typic Haplocryept, respectively.

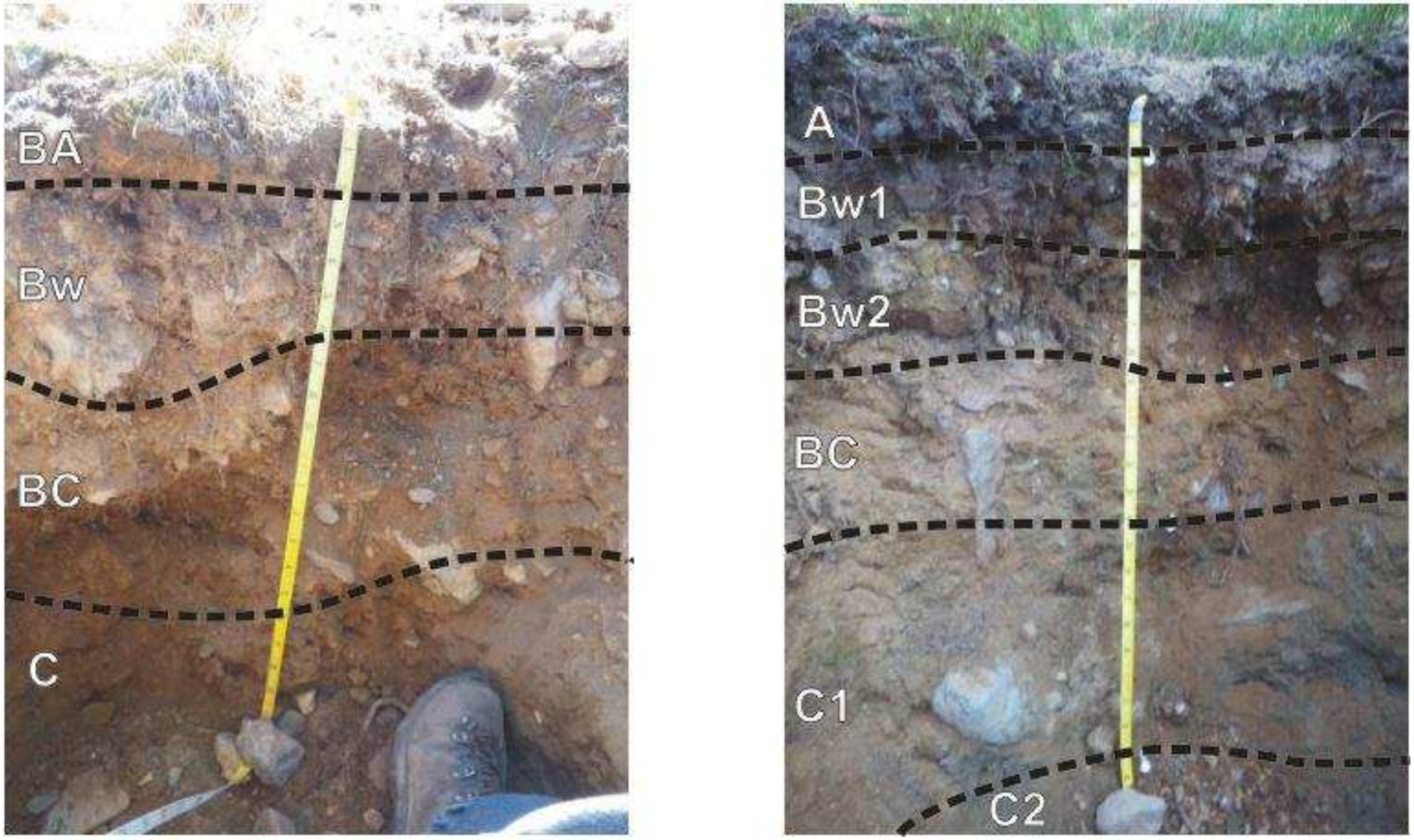

FU1 FU2

Figure 1-A-11. Pictures of soil pits at sites FU1 and FU2. The USDA taxonomic Subgroup classification of the two soils are Typic Haplocryept and Typic Haplocryept, respectively.

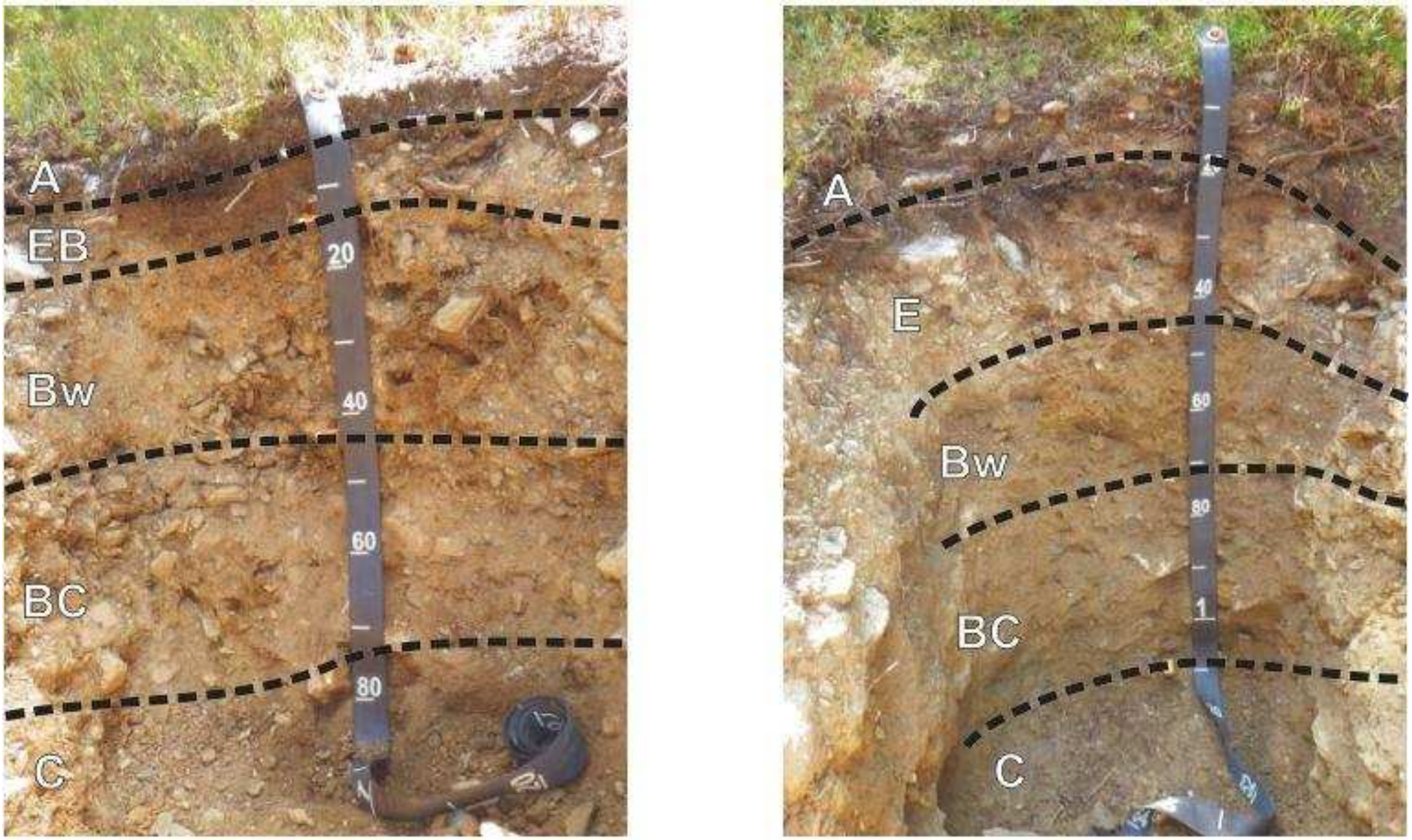

FU3 FU4

Figure 1-A-12. Pictures of soil pits at sites FU3 and FU4. The USDA taxonomic Subgroup classification of the two soils are Typic Haplocryept and Typic Haplocryept, respectively.

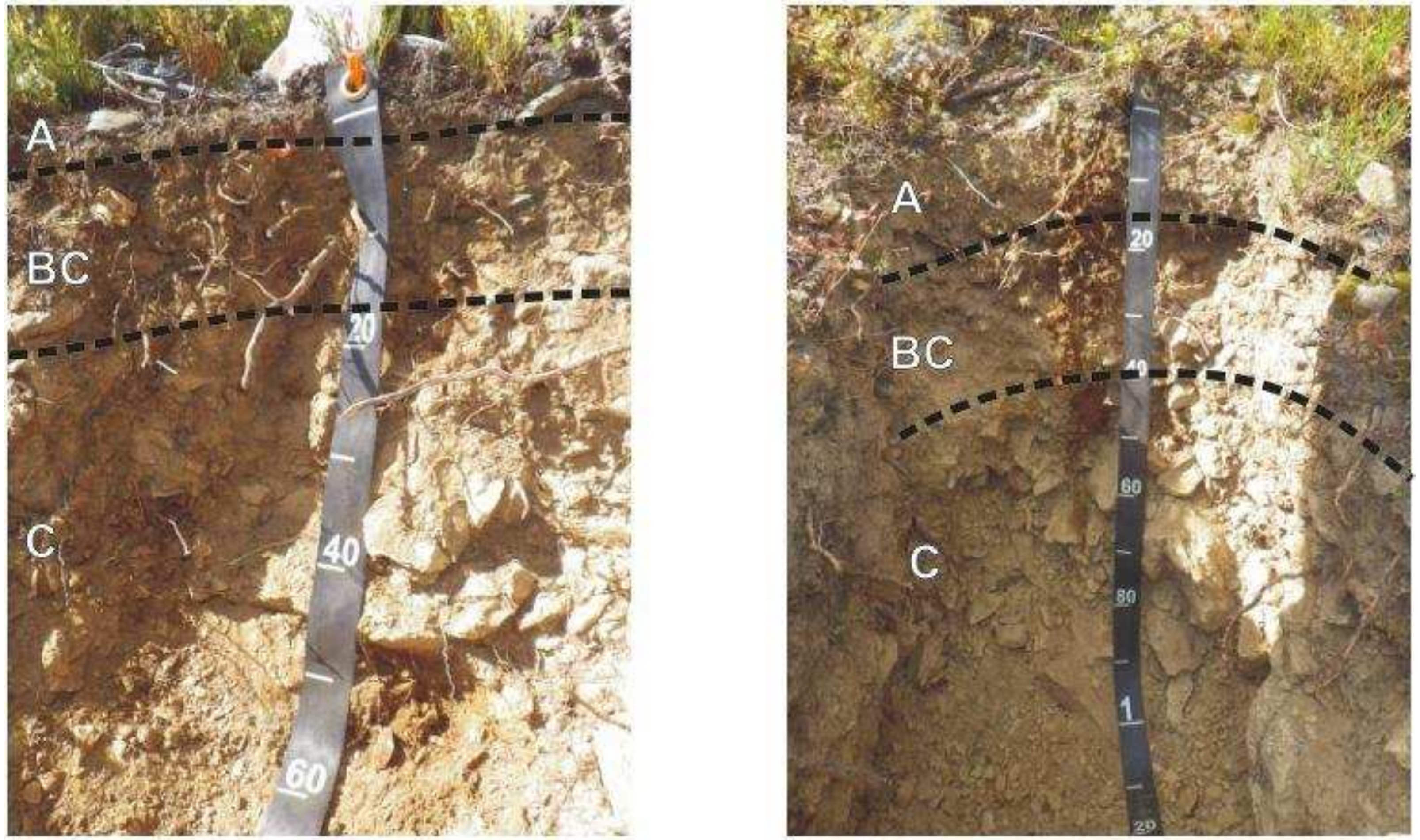

IL1 IL2

Figure 1-A-13. Pictures of soil pits at sites IL1 and IL2. The USDA taxonomic Subgroup classification of the two soils are Typic Cryorthent and Typic Cryorthent, respectively.

IL3 IL4

Figure 1-A-14. Pictures of soil pits at sites IL3 and IL4. The USDA taxonomic Subgroup classification of the two soils are Typic Haplocryept and Typic Cryorthent, respectively.

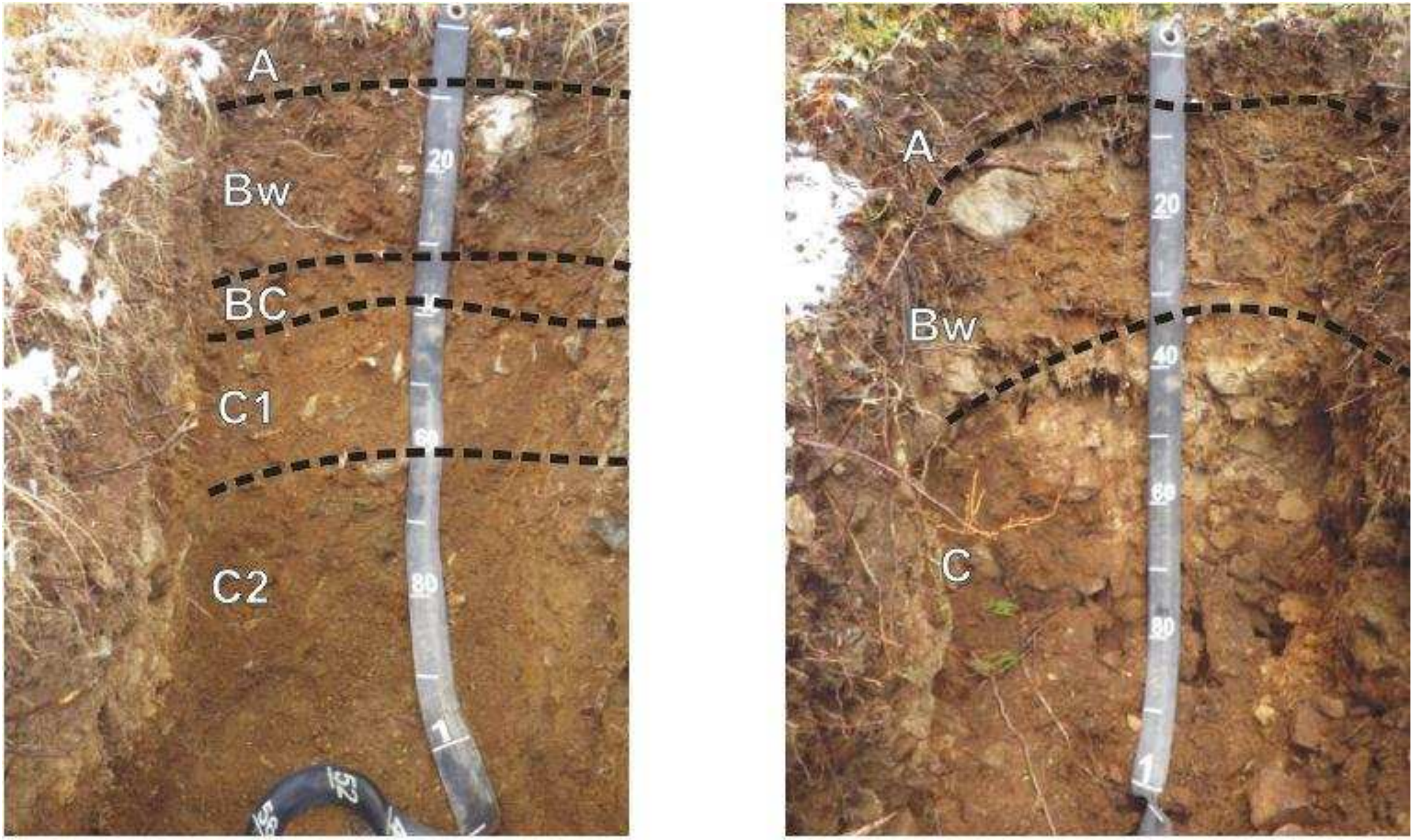

IU1 IU2

Figure 1-A-15. Pictures of soil pits at sites IU1 and IU2. The USDA taxonomic Subgroup classification of the two soils are Typic Haplocryept and Typic Haplocryept, respectively.

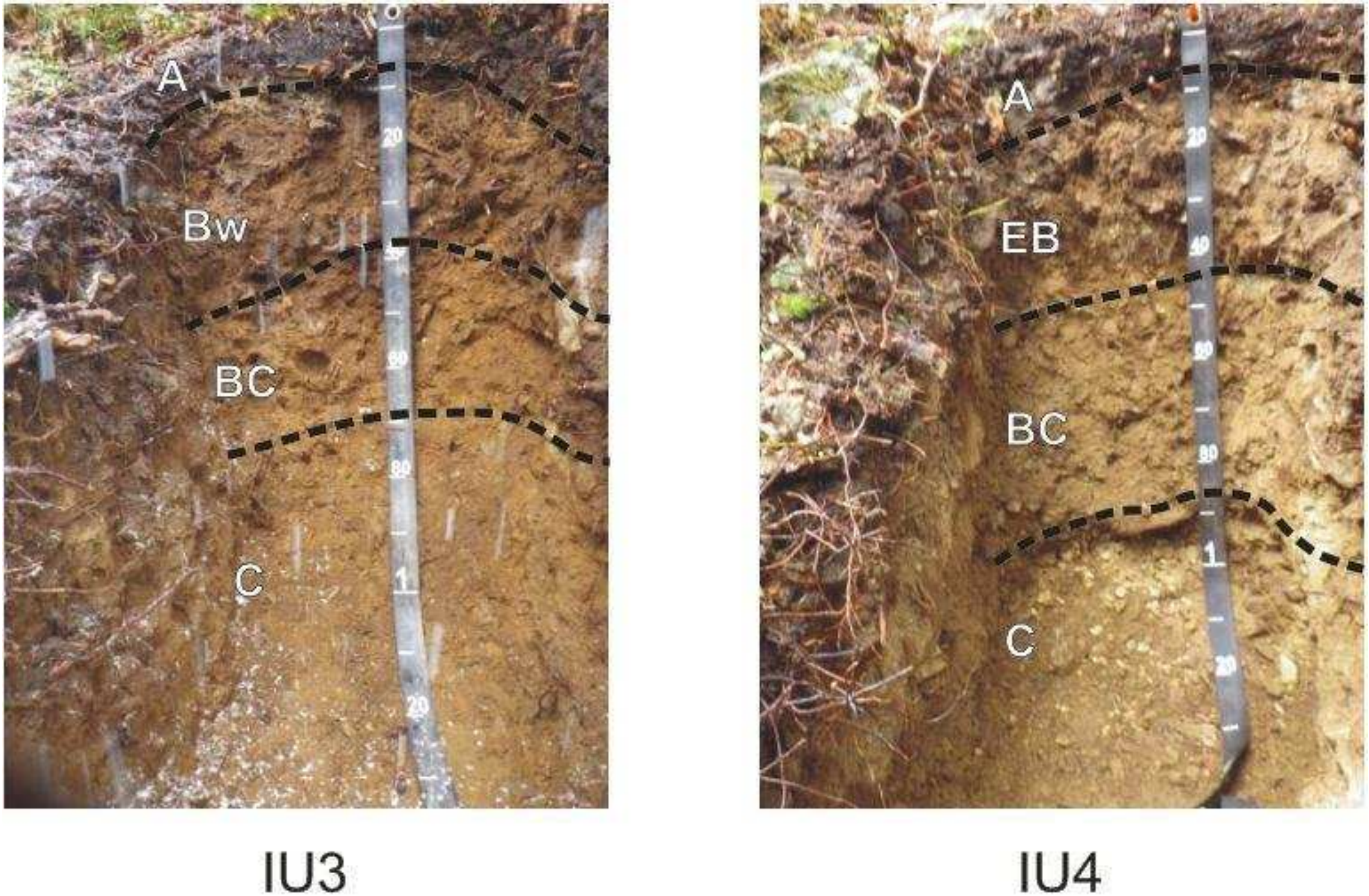

Figure 1-A-16. Pictures of soil pits at sites IU3 and IU4. The USDA taxonomic Subgroup classification of the two soils are Typic Haplocryept and Typic Cryorthent, respectively.

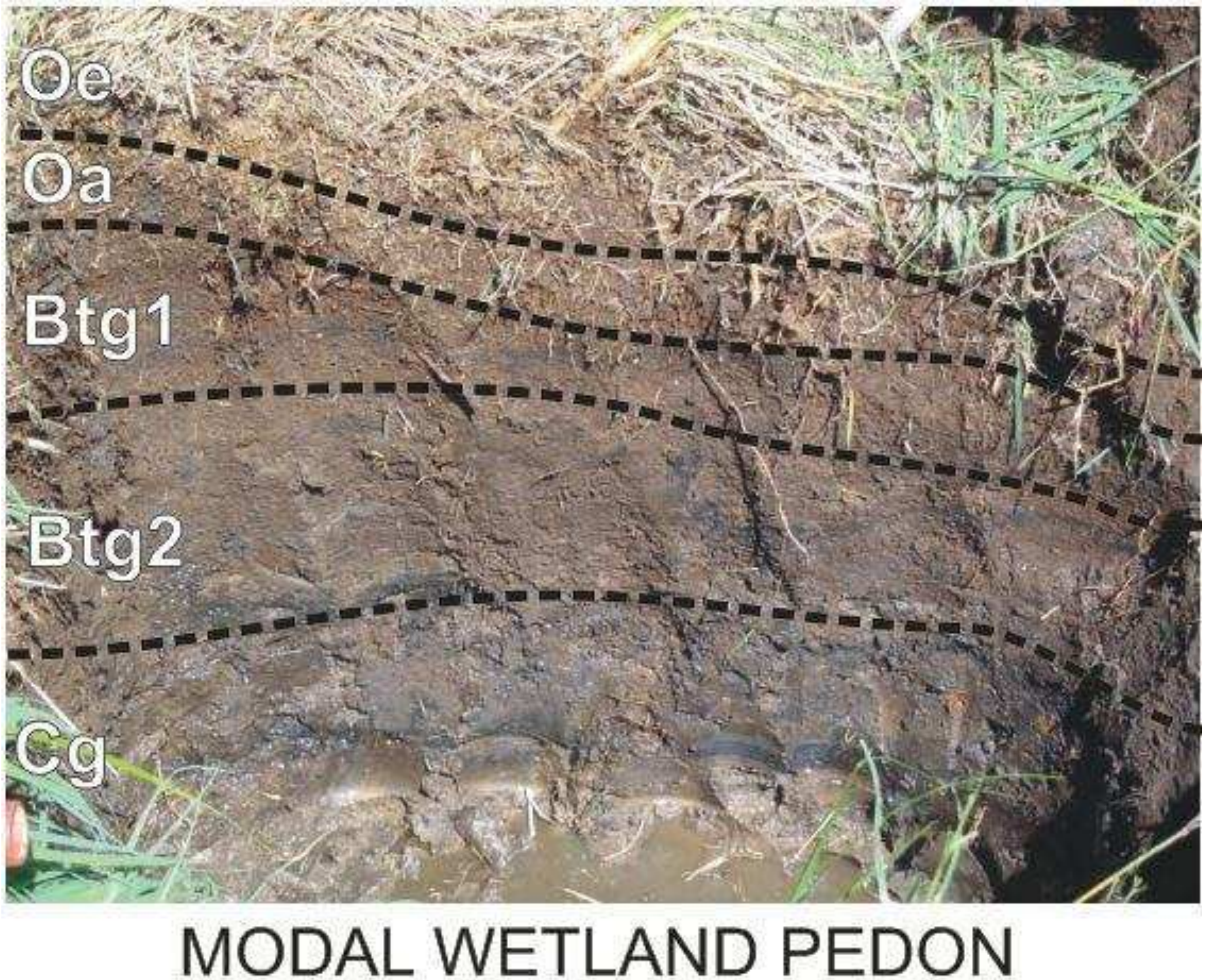

Figure 1-A-17. Picture of a typical wetland soil in the mountainbase landscapes. The USDA taxonomic Subgroup classification of soils in these landscapes is Typic Cryofibrist.

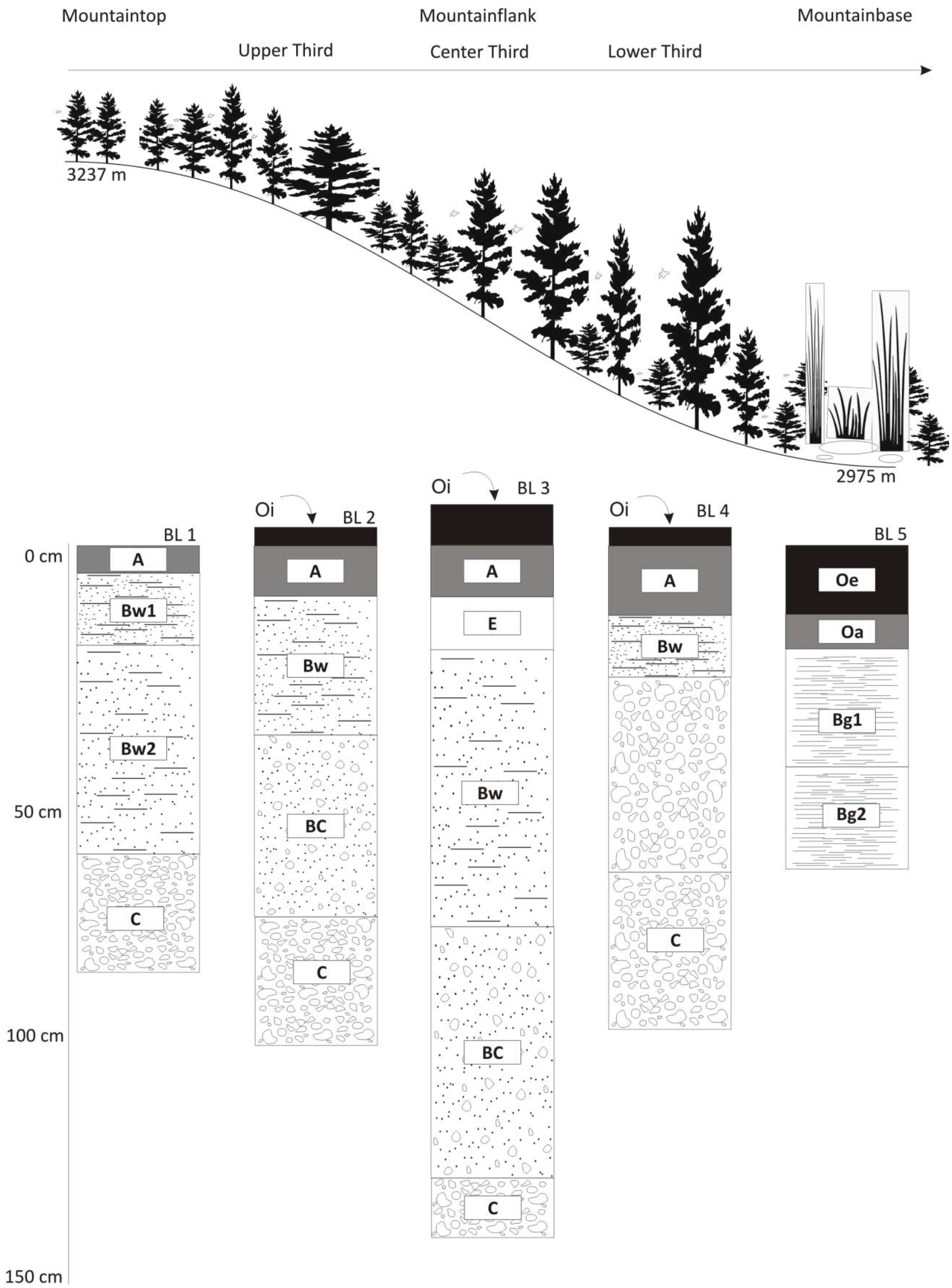

Figure 1-A-18. Representation of soil profiles along the Byers Creek lower catena. Noted in the figure is the starting and ending elevation of the catena and vegetation in the landscapes—trees represent forested landscape positions, the absence of trees represents alpine landscapes. All mountainbase landscapes contain a mixture of forest and wetland vegetation.

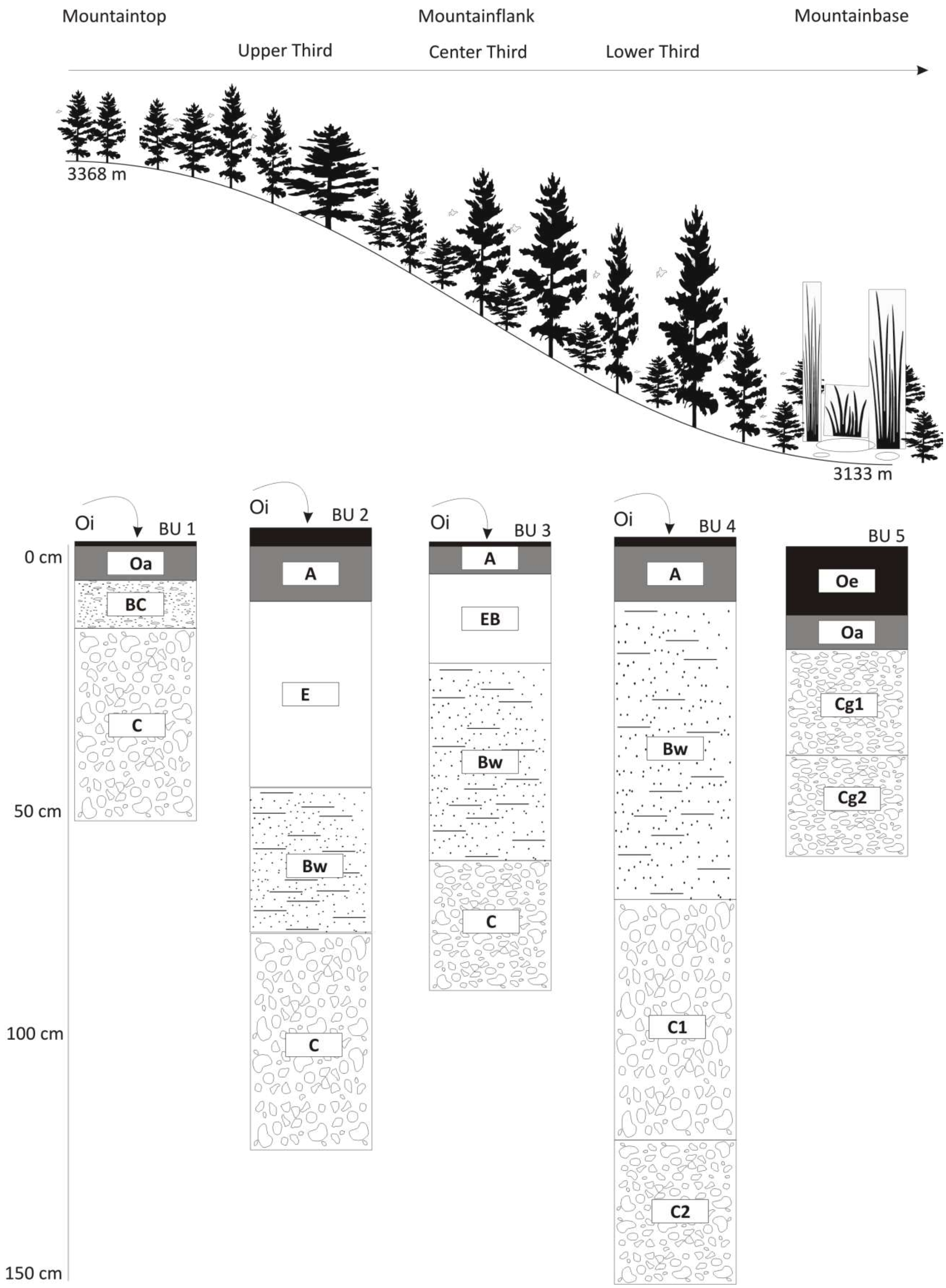

Figure 1-A-19. Representation of soil profiles along the Byers Creek upper catena. Noted in the figure is the starting and ending elevation of the catena and vegetation in the landscapes—trees represent forested landscape positions, the absence of trees represents alpine landscapes. All mountainbase landscapes contain a mixture of forest and wetland vegetation.

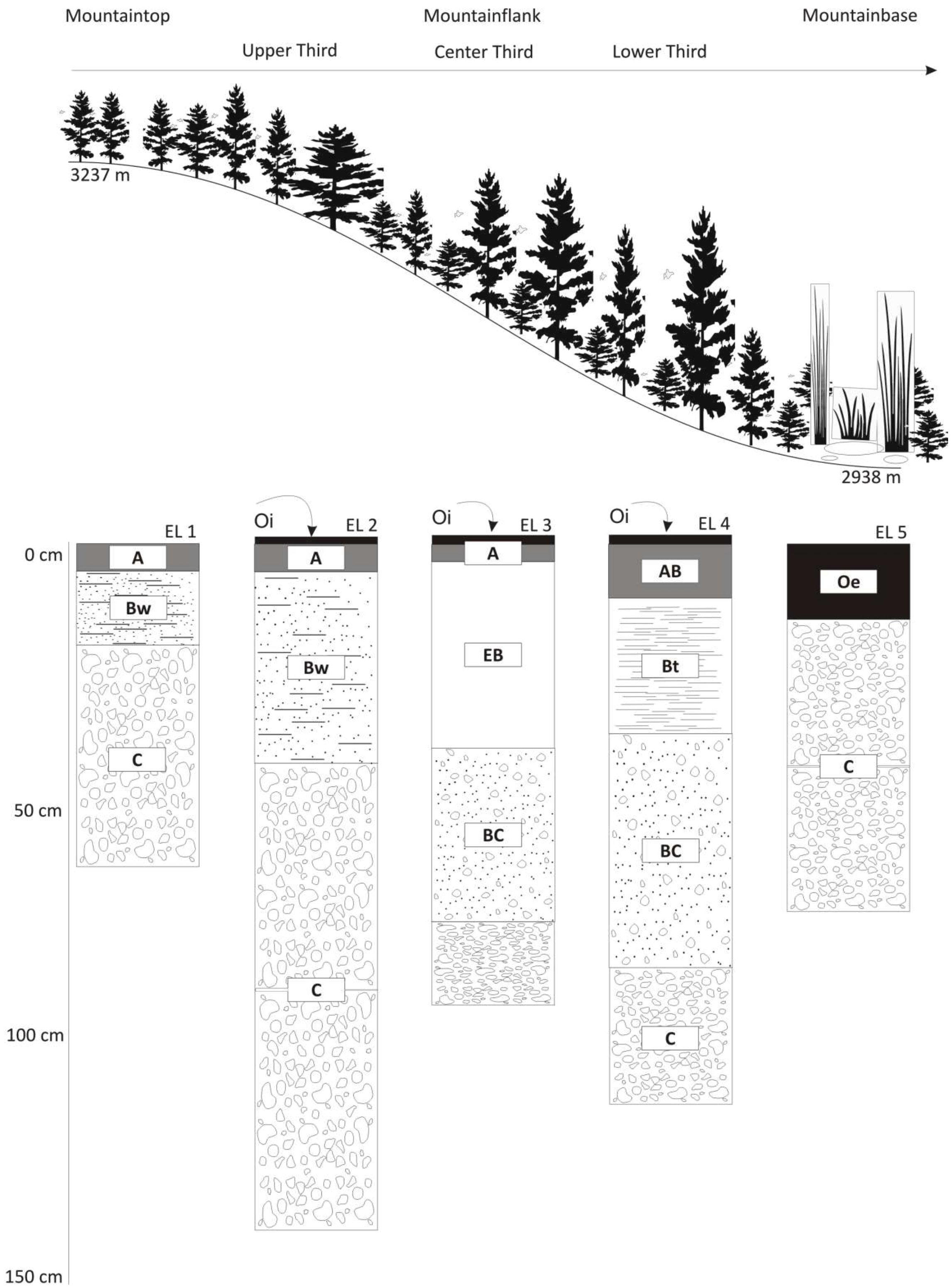

Figure 1-A-20. Representation of soil profiles along the East St. Louis Creek lower catena. Noted in the figure is the starting and ending elevation of the catena and vegetation in the landscapes—trees represent forested landscape positions, the absence of trees represents alpine landscapes. All mountainbase landscapes contain a mixture of forest and wetland vegetation.

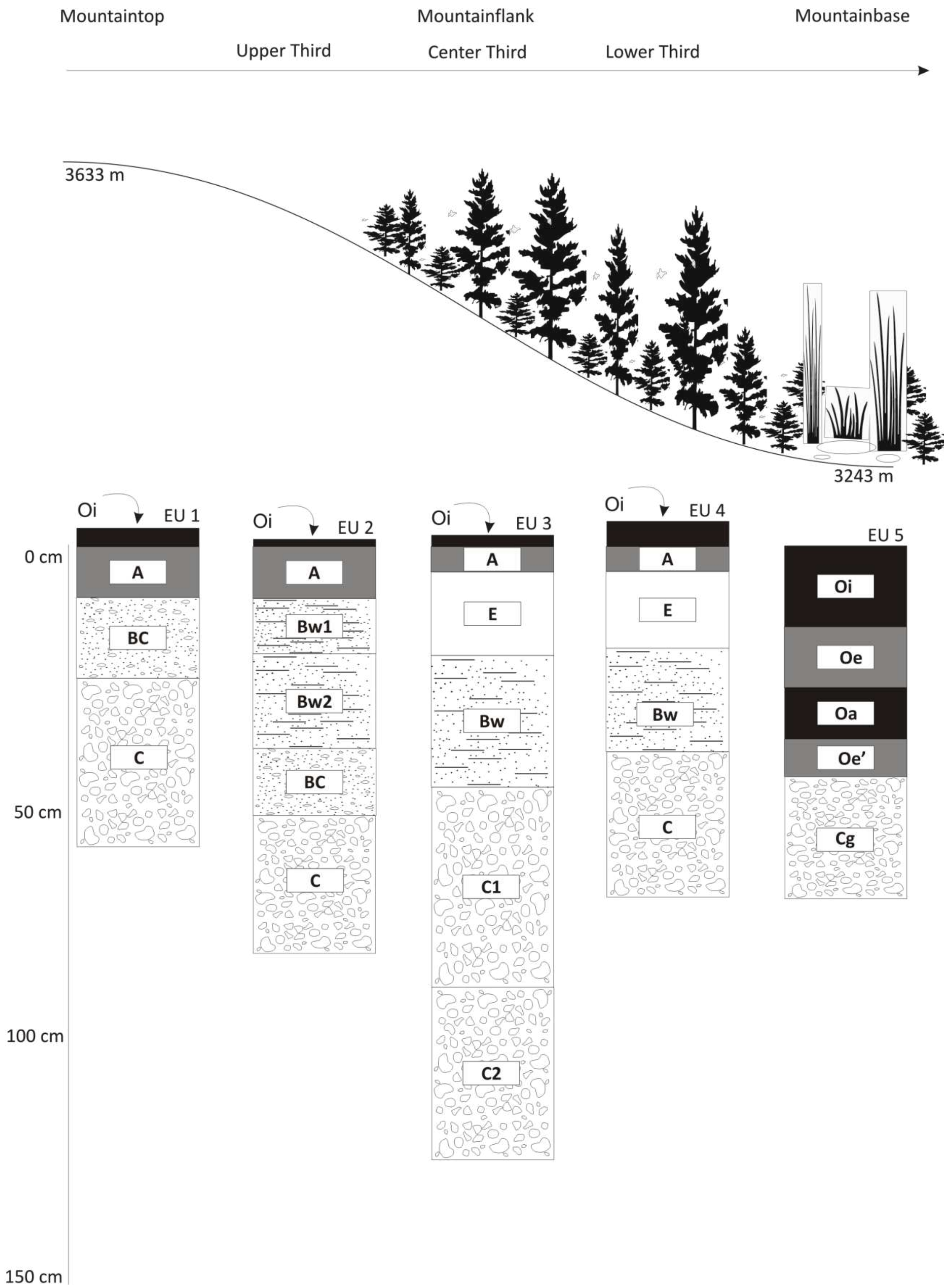

Figure 1-A-21. Representation of soil profiles along the East St. Louis Creek upper catena. Noted in the figure is the starting and ending elevation of the catena and vegetation in the landscapes—trees represent forested landscape positions, the absence of trees represents alpine landscapes. All mountainbase landscapes contain a mixture of forest and wetland vegetation.

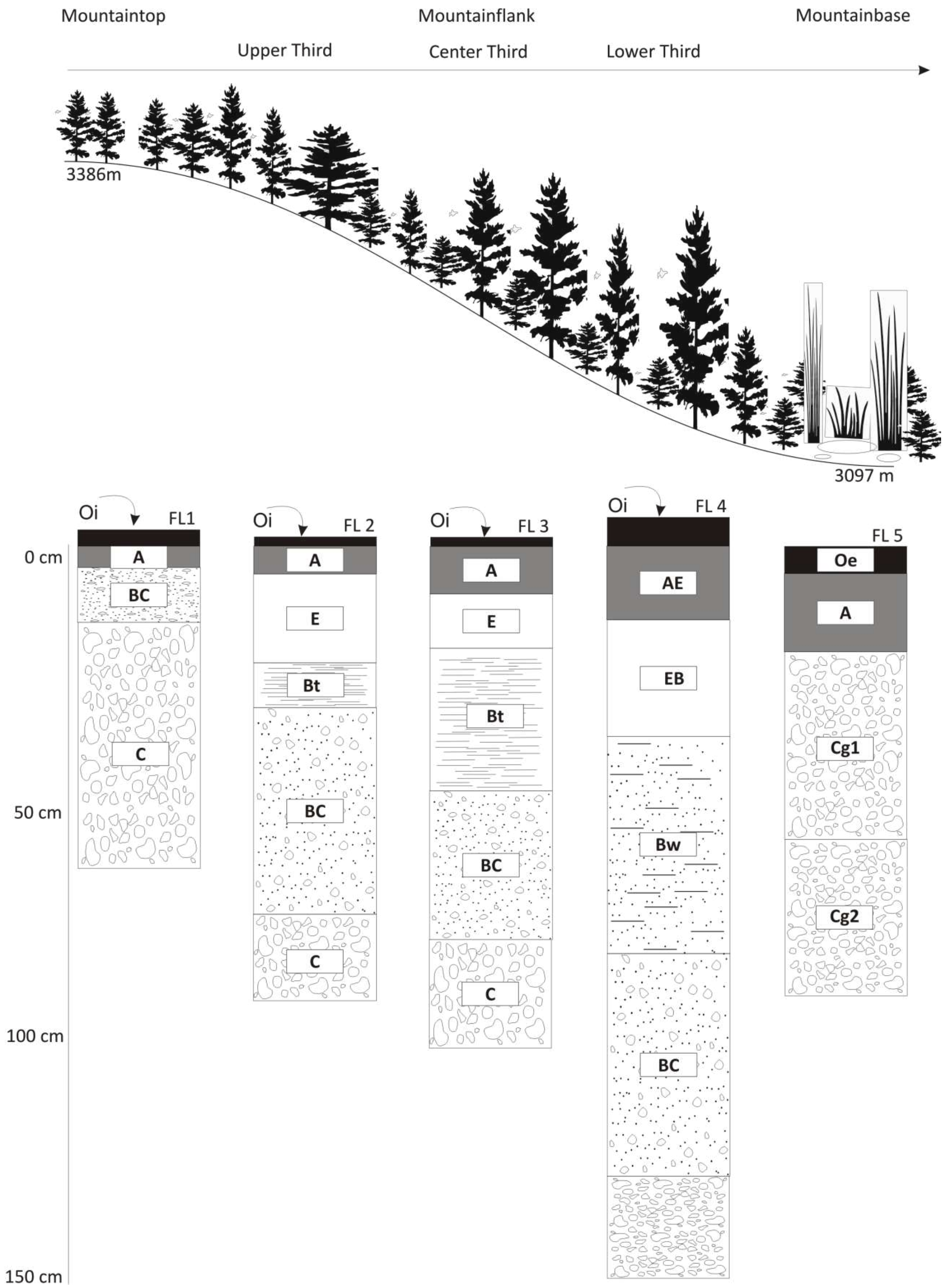

Figure 1-A-22. Representation of soil profiles along the Fool Creek lower catena. Noted in the figure is the starting and ending elevation of the catena and vegetation in the landscapes—trees represent forested landscape positions, the absence of trees represents alpine landscapes. All mountainbase landscapes contain a mixture of forest and wetland vegetation.

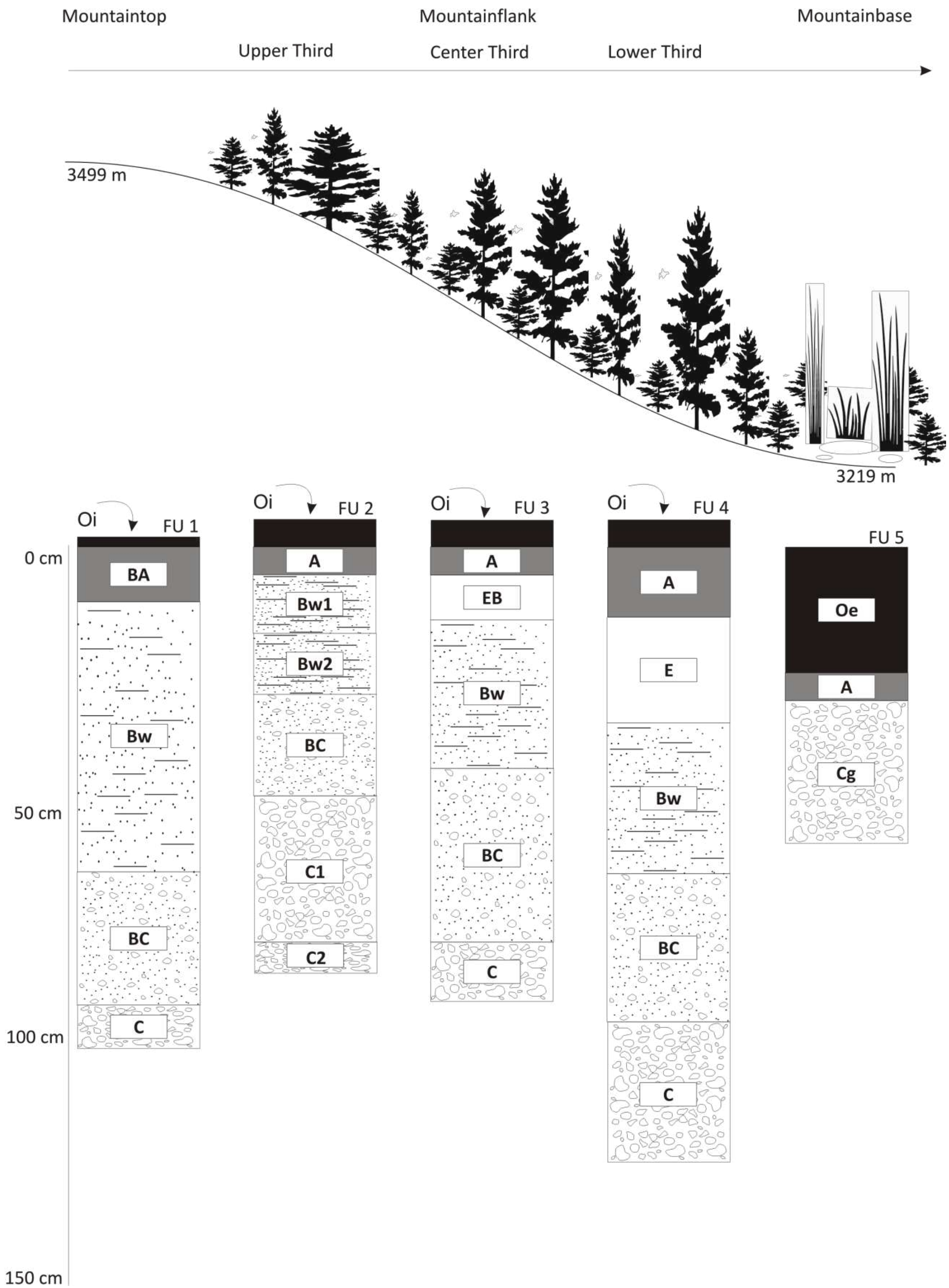

Figure 1-A-23. Representation of soil profiles along the Fool Creek upper catena. Noted in the figure is the starting and ending elevation of the catena and vegetation in the landscapes—trees represent forested landscape positions, the absence of trees represents alpine landscapes. All mountainbase landscapes contain a mixture of forest and wetland vegetation.

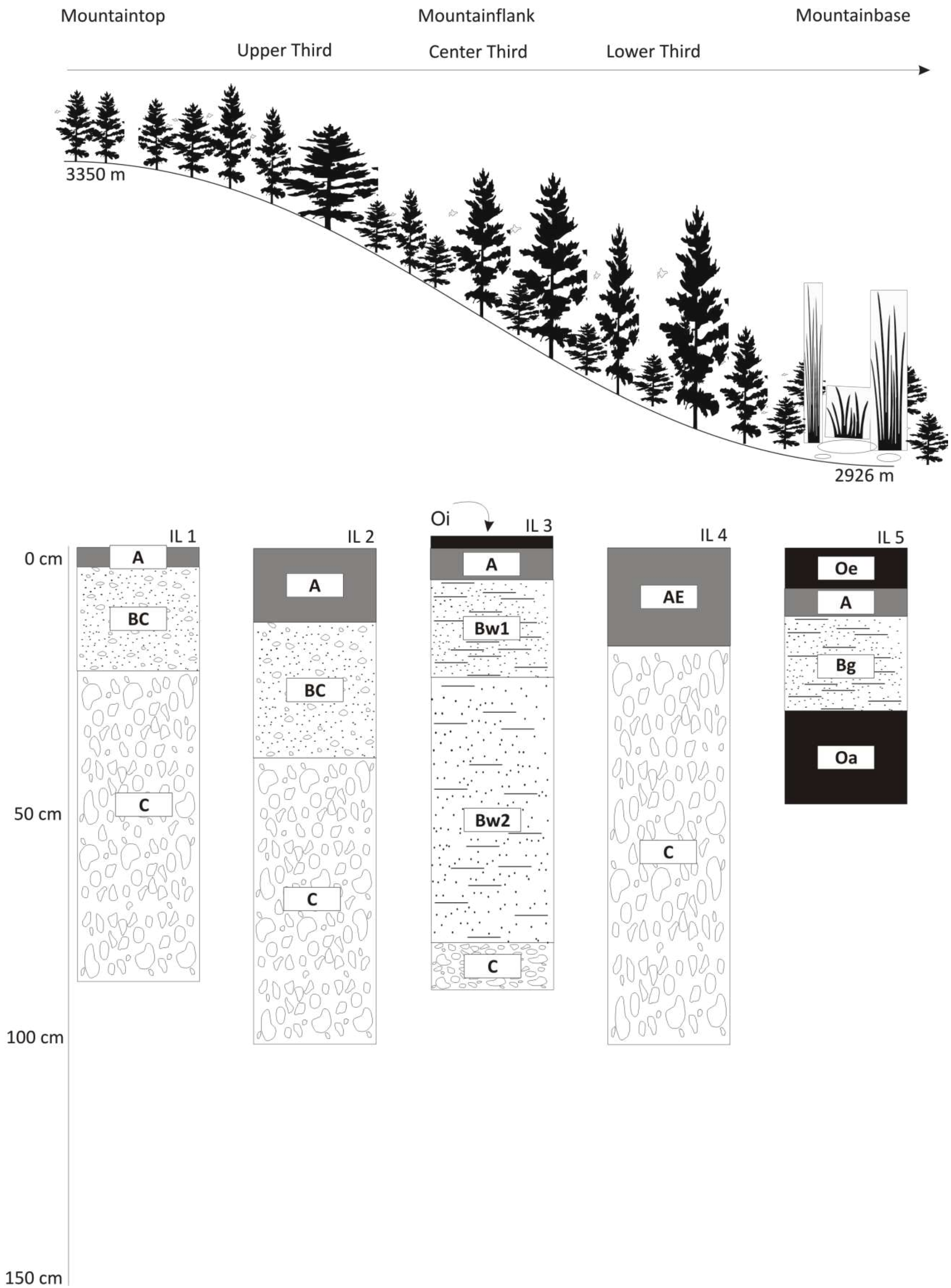

Figure 1-A-24. Representation of soil profiles along the Iron Creek lower catena. Noted in the figure is the starting and ending elevation of the catena and vegetation in the landscapes—trees represent forested landscape positions, the absence of trees represents alpine landscapes. All mountainbase landscapes contain a mixture of forest and wetland vegetation.

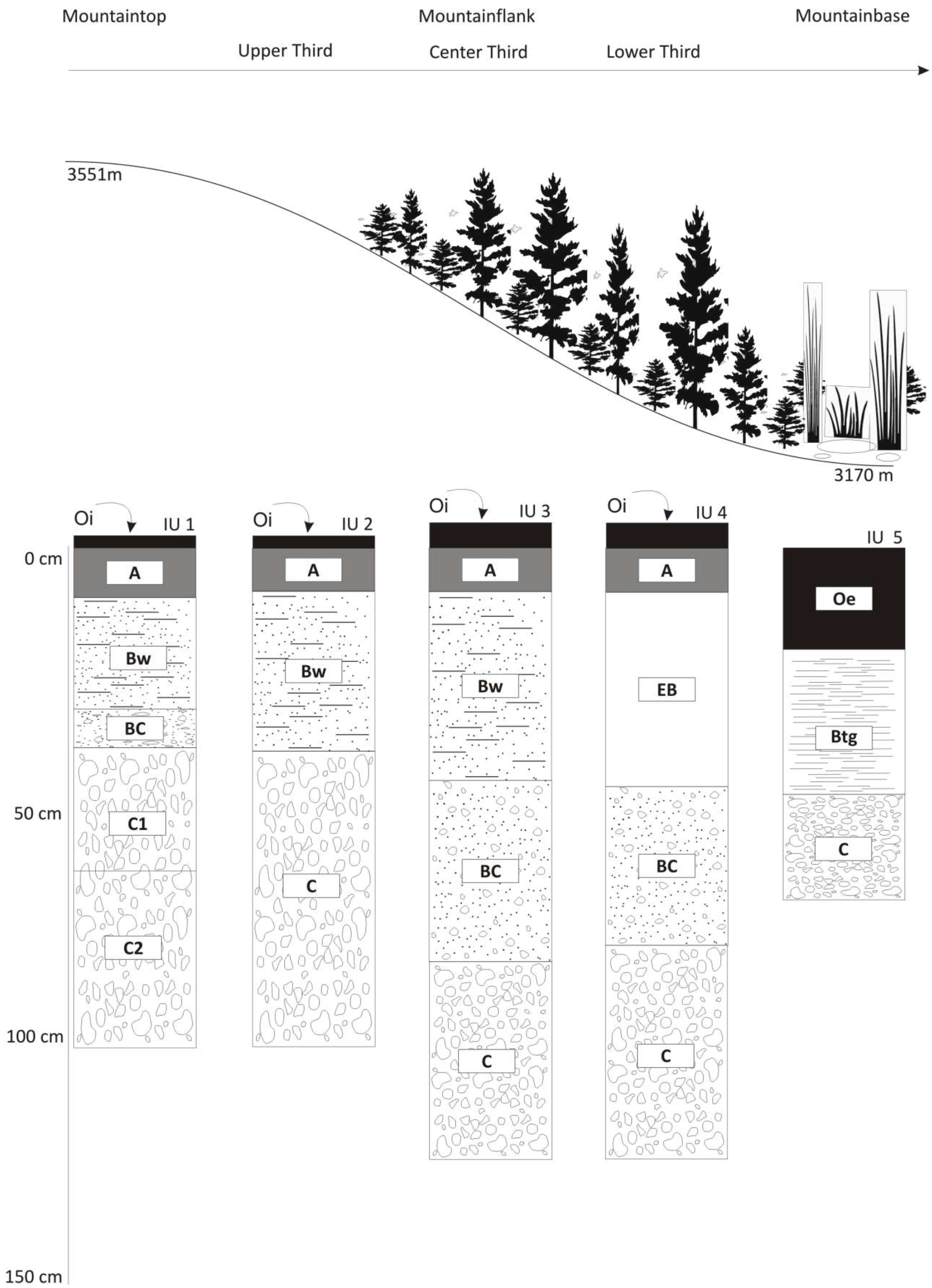

Figure 1-A-25. Representation of soil profiles along the Iron Creek upper catena. Noted in the figure is the starting and ending elevation of the catena and vegetation in the landscapes—trees represent forested landscape positions, the absence of trees represents alpine landscapes. All mountainbase landscapes contain a mixture of forest and wetland vegetation.

Appendix 2-A

2.A.1 Summary

Subsamples were taken from the < 2mm size fraction of each soil horizon, pulverized, prepared, and analyzed for a suite of major and trace elements by ICP-AES after acid digestion. This work was carried out at the Soil, Water, and Plant Testing Laboratory at Colorado State University under the direction of Dr. James Self. The major elements Ca, Na, Fe, Al, K, and Mg were reported on in this dissertation; Ti concentrations were utilized in the geochemical mass balance calculations. The raw elemental concentrations obtained from ICP-AES analysis are included in this appendix in table 2-A-1. Relatedly, samples from all the mountaintop soil horizons and from soils along the Byers Creek lower catena were analyzed for Sr^{86} and Sr^{87} concentrations by ICP-MS after acid digestion. The raw Sr^{86} and Sr^{87} data and Sr^{86}/Sr^{87} ratios are included in table 2-A-2.

Table 2-A-1. Elemental data for the soil horizons. Values are concentrations given in mg/kg of soil (ppm). Soil chemical analyses were carried out under the direction of and collaboratively with Dr. James Self, CSU Soil Testing Laboratory, Fort Collins, Colorado.

Horizon	Genetic	Al	Ca	Fe	K	Mg	Mn	Na	P	S	Si	Sr	Ti	Zn
Number	Horizon	(mg/kg)												
BL1_1	A	31460	12210	37130	5169	11980	2491	1148	475.8	245.3	18.18	17.37	4701	84.92
BL1_2	Bw1	36930	20210	51680	6340	14460	874.1	1701	844.1	175	17.12	15.11	6638	87.54
BL1_3	Bw2	47450	12020	63560	12280	15220	1037	949.7	656.4	134.8	45.37	14.26	8453	115.3
BL1_4	C	32990	3180	28240	5381	9892	390.8	412	314.2	126.2	45.46	15.72	4080	57.41
BL2_0	Oi	8610	7753	5878	2751	3896	4257	96.51	1082	838	<.0000	26.58	639.6	71.99
BL2_1	A	40220	3748	37010	6287	12260	448.3	416.9	420.5	89.59	80.63	13.24	5459	65.08
BL2_2	Bw	40300	3929	37390	6117	12290	465.4	423.9	409.6	80.23	30.77	13.02	5444	64.35
BL2_3	BC	50440	4384	43140	7691	12880	495.9	346.1	681.4	107.5	64.87	13.58	5042	68.45
BL2_4	C	54870	5196	44840	7921	13610	567.2	376.6	475.3	92.03	42.74	17.96	5120	67.62
BL3_0	Oi	8668	17550	5727	2884	4151	3592	108.5	1269	1301	15.97	62.74	736.5	96.41
BL3_1	A	39920	11120	37510	5104	11940	626.2	877.7	504.3	215.6	302	19.88	5312	63.74
BL3_2	E	44280	10810	39010	5557	12110	571.8	833.9	704.4	165.2	85.78	16.64	5066	61.22
BL3_3	Bw	41550	13080	39490	6355	12850	638.7	1026	573.5	132.3	28.23	14.77	5046	55.69
BL3_4	BC	50010	11920	45150	7067	13260	756.2	870.6	430.5	133.1	49.25	24.27	5520	69.45
BL3_5	C	45250	9320	40420	8647	12790	662.2	611.6	546.4	87.98	130.9	19.81	5325	55.89
BL4_0	Oi	7149	8200	4950	2962	3589	1835	86.94	1693	1322	43.71	31.64	654.5	57.66
BL4_1	A	32630	4665	32890	3910	9037	602.3	583	287.4	116.8	321.6	15.13	4100	56.01
BL4_2	Bw	36570	6438	38090	4199	10820	705.3	618.9	372.7	149.3	199.5	12.71	4040	58.68
BL4_3	C1	37830	7090	39250	4258	11090	733.5	679.2	421.3	135.9	219.1	12.94	4224	59.67
BL4_4	C2	30200	9782	38980	4441	10990	850.4	867	323.8	138.4	138.8	11.93	3656	50.13
BL5_1	Oe	9751	28690	6571	2613	6083	394.7	160.6	961.2	1592	<.0000	63.42	728.1	41.64
BL5_2	Oa	23860	28860	19270	3776	8075	1000	241.9	893.7	1528	14.37	47.77	1517	39.6
BL5_3a	Bg1	28410	7414	23840	4936	9564	495.6	393.9	208	137.6	62.6	17.27	3103	55.26
BL5_3b	Bg2	31450	8360	31120	4874	11590	865.6	372.4	436.4	129.8	170	15.6	3043	70.62

Horizon	Genetic	Al	Ca	Fe	K	Mg	Mn	Na	P	S	Si	Sr	Ti	Zn
Number	Horizon	(mg/kg)												
BU1_0	Oi	8499	14210	5623	2346	4396	3182	102.9	1013	1147	37.2	51.18	632.5	97.04
BU1_1	Oa	14590	6935	12720	2828	5892	1823	171.4	671.2	573.9	116.4	25.47	1388	47.83
BU1_2	BC	22650	878.1	18850	4308	6517	120.5	226.7	270.6	24.54	43.04	5.903	1290	28.36
BU1_3	C	20270	930.7	19690	6065	7285	411.9	259.4	268.2	26.97	30.01	6.385	2028	36.44
BU2_0	Oi	14340	9599	10850	3905	6160	3168	122.9	1123	834.7	5.958	37.2	1395	90.81
BU2_1	A	28880	4019	24130	5298	9664	2619	280.7	323.1	159.6	44.1	17.39	2890	76.87
BU2_2	E	27730	2093	26420	5305	10020	349.1	257.8	249.3	58.32	37.89	10.93	3312	70.2
BU2_3	Bw	34440	2194	30360	5488	11750	371.7	193.9	142.1	49.33	60.33	11.82	2424	60.51
BU2_4	C	48420	1707	44100	8002	13710	521.9	136.5	37.52	41.61	46.37	9.691	3084	84.32
BU3_0	Oi	15810	11880	11890	4483	6480	3805	147.3	944.7	883.4	5.958	45.91	1594	122.4
BU3_1	A	30510	6792	26880	5368	10180	2465	321.7	627.3	311.2	45.92	24.19	3309	85.54
BU3_2	EB	46490	4406	35300	5783	11740	382	292.8	971.2	84.3	87.46	19.47	3027	72.65
BU3_3	Bw	46160	4279	34440	5717	11900	358.2	291.9	646.1	89.99	181.6	18.9	2890	63.29
BU3_4	C	33690	3001	27970	5959	10640	392.4	204.5	292.7	36.32	7.579	11.11	2274	50.37
BU4_0	Oi	25160	7926	19390	5514	8211	2186	196.8	1033	694.5	27.51	32.25	2605	124.1
BU4_1	A	37650	3851	31880	5141	11130	1546	324.6	396.6	120.5	37.58	14.66	3679	105.8
BU4_2	Bw	44420	3257	37340	6708	12160	471.9	293.6	363.1	39.17	65.63	11.32	4052	92.77
BU4_3	C1	69570	3287	51300	12740	14890	450.7	402.2	412.7	63.16	72.74	14.86	4831	145.9
BU4_4	C2	53600	4171	42320	11980	13250	655.3	316	473.6	55.84	54.45	24.12	4175	108.2
BU5_1	Oe	19550	17850	21130	3347	6272	357.2	205.4	1620	2779	28.39	90.75	1305	34.39
BU5_2	Oa	34760	16880	28620	4800	10120	325.9	426.9	1018	1864	39.1	59.46	3024	47.16
BU5_3a	Cg1	32670	7354	31120	5500	11410	455.8	564.8	327	94.47	45.01	23.33	3819	53.79
BU5_3b	Cg2	36380	7767	38590	7078	12220	596.4	651.8	400.6	107.9	83.51	20.36	4278	62.4

Horizon	Genetic	Al	Ca	Fe	K	Mg	Mn	Na	P	S	Si	Sr	Ti	Zn
Number	Horizon	(mg/kg)												
EL1_1	A	29540	4231	25770	5154	11070	339.9	511.6	255.5	78.2	47.13	14.13	3859	58.58
EL1_2	Bw	40530	4557	33570	4902	12620	268	627.2	544.3	81.05	95.17	13.82	4410	67.42
EL1_3	C	29730	894.1	22980	6633	10910	252	355.6	195.6	28.19	54.25	7.407	3679	47.19
EL2_0	Oi	19840	7067	18940	4937	6868	1881	189.2	894.3	719.1	4.593	41.24	2041	84.56
EL2_1	A	35690	4364	42310	5612	10680	1367	423.3	354.3	148.6	35.92	22.16	4223	81.94
EL2_2	Bw	40470	4524	59420	6248	12080	1128	455.6	292.4	145.3	33.95	20.43	5089	95.25
EL2_3	C	42910	7710	43380	6027	11490	489.8	486.9	472.9	85.54	42.81	51.32	4829	122.2
EL3_0	Oi	9733	10880	7419	3024	4921	2048	145.7	1085	860.1	77.67	48.44	974.7	77.17
EL3_1	A	18930	6690	15360	4196	6259	1370	280.7	472.1	452.6	8.99	39.27	2144	64.34
EL3_2	EB	14480	3733	21380	5321	^<.0000	247.9	436.5	214.9	79.45	18.26	25.3	2412	50.21
EL3_3	BC	26840	5908	25040	5588	10300	340.7	445.8	436.1	95.35	57.82	27.11	3361	54.61
EL3_4	C	20480	25390	24620	6623	16750	434.6	1259	956.8	175.4	259.3	32.91	4741	50.23
EL4_0	Oi	8195	11480	5370	3458	3908	3161	97.43	1808	1536	33.4	39.75	693.3	64.09
EL4_1	AB	26520	4511	22060	8037	10890	267.2	560	481.6	90.23	270.9	22.74	3206	58.62
EL4_2	Bt	29800	4765	24710	10210	12950	296.4	414	393.3	53.46	9.839	21.57	1944	56.8
EL4_3	BC	32880	7001	26130	12410	13590	325.4	593.9	548.6	62.47	283.6	26.25	3119	62.36
EL4_4	C	30970	8439	26130	14630	13900	374.5	815.1	560.2	74.47	106.6	23.02	3046	61.74
EL5_1	Oe	34170	21290	17690	10540	11190	213.5	436.1	762.2	2966	199.4	64.6	2204	60.91
EL5_2	Cg	27070	6201	19660	11940	11780	270.3	478.3	386.9	415.9	56.9	22.16	2846	68.51

Horizon Number	Genetic Horizon	Al	Ca	Fe	K	Mg	Mn	Na	P	S	Si	Sr	Ti	Zn
		(mg/kg)												
EU1_0	Oi	19830	10030	13620	5679	6851	810.6	178.4	1457	1627	82.98	66.58	1647	90.14
EU1_1	A	21620	3455	17280	7806	8641	224	371.9	760.9	571.4	230.9	21.48	2549	47.05
EU1_2	BC	24270	2050	21510	10420	10270	233.1	397.7	419.4	270.3	229.6	12.66	2966	49.63
EU1_3	C	23300	785.7	22600	12470	10840	247.1	529.8	239	102.2	72.91	6.533	2807	50.08
EU2_0	Oi	34760	3213	23110	6527	7471	934.7	224.1	1931	1065	42.04	34.6	2888	67.82
EU2_1	A	27780	1507	20860	8317	9585	916	353.6	1522	925.5	240.6	15.91	2432	50.61
EU2_2	Bw1	36360	1295	24820	10720	10900	1023	472.4	1722	868.8	330.5	18.37	2925	61.72
EU2_3	Bw2	33870	1056	24140	9851	10420	805.2	381.5	1356	562.7	290.2	16.11	2735	53.3
EU2_4	BC	40430	957.8	26920	10900	11450	566.8	413.3	686.7	216.3	20.93	15.58	3040	67.5
EU2_5	C	27520	597.9	21270	12440	10840	455.5	389.1	254.4	82.73	212.8	7.358	2933	56.5
EU3_0	Oi	17140	12650	15060	5548	7512	2135	141.2	1309	722.3	56	79.04	2577	89.3
EU3_1	A	22910	12940	21500	12670	12750	1080	426.8	1456	273.7	237.5	56.32	3755	80.95
EU3_2	E	29400	9608	25040	13020	13740	312.9	474.9	1449	82.73	223.3	56.71	4876	75.44
EU3_3	Bw	27450	3094	23870	10860	12110	262.2	482.2	502.9	74.85	230.4	22.2	3600	68.02
EU3_4	C1	41080	3344	32390	17340	14500	349.3	498.1	603.1	66.96	121.4	25.17	4742	87.3
EU3_5	C2	22710	820.8	20070	13540	10750	235.7	414.2	166.6	33.95	163.8	5.967	2712	48.62
EU4_0	Oi	5784	17390	4075	2261	3393	4526	85	1138	1082	2.925	52.1	514.1	160
EU4_1	A	18510	11000	13980	7568	8177	2679	377	459.7	370.9	245.2	32.58	1833	94.47
EU4_2	E	28020	2202	21340	11050	10470	203.9	483.7	296.7	92.11	39.19	16.53	3202	64.79
EU4_3	Bw	34430	1813	31510	13860	13020	283.7	405.8	272.1	99.2	60.7	11.06	3305	83.58
EU4_4	C	33010	1315	27350	12080	12730	297	454.6	182.7	55.34	20.38	8.062	3013	83.85
EU5_1	Oi	15460	7238	12240	2686	4987	470.6	240.1	1607	2090	23.66	58.44	1088	49.57
EU5_2	Oe	25890	2895	19170	7911	10970	343	459.2	237.9	155.5	265	22.27	2652	68.83
EU5_3	Oa	31300	1755	35420	17240	13320	228.7	536.2	57.13	47.85	30.81	12.87	3494	109.2
EU5_4	Oe'	33840	2233	34560	16720	12510	197.7	800.5	93.45	79.01	35.68	17.3	3761	97.05
EU5_5	Cg	22200	2272	25590	9602	10550	163	527.4	92.57	64.74	23.18	15.18	2736	68.72

Horizon Number	Genetic Horizon	Al	Ca	Fe	K	Mg	Mn	Na	P	S	Si	Sr	Ti	Zn
		(mg/kg)												
FL1_0	Oi	16020	10520	17490	6642	6487	684	175.6	792.6	682.3	11.75	58.73	1681	59.47
FL1_1	A	26990	5404	22450	15600	12910	285.9	520.9	428.1	554.4	203.1	19.84	3366	77.78
FL1_2	BC	23400	20720	3900	5573	7786	52.59	328.1	527.7	3162	20.09	75.81	631.3	31.25
FL1_3	C	15490	25560	3414	3744	6179	29.38	248.4	553.1	10970	36.92	84.09	970.1	11.18
FL2_0	Oi	9405	9354	6523	3050	4628	2296	110.2	1278	1084	<.0000	47.6	735.7	71.58
FL2_1	A	22230	19390	4442	5584	7995	48.25	409	857.3	4015	16.16	73.16	1200	15.83
FL2_2	E	43720	18220	26660	9118	17270	309.3	1320	164.2	125.5	64.47	32.44	2852	57.85
FL2_3	Bt	44680	14280	33070	12130	16090	412.6	920.2	202.3	123	308.7	32.55	3735	89.38
FL2_4	BC	24460	9662	20740	8262	11830	252	825.8	155.8	92.1	240.6	23.14	2899	52.7
FL2_5	C	23270	10370	19530	8055	11530	336.3	763.5	181.5	115.7	42.06	24.79	2902	50.8
FL3_0	Oi	14600	10960	10820	3754	5995	1207	190.8	900	766.9	2.932	55.15	1467	67.34
FL3_1	A	31590	5823	26780	16970	13560	343.8	533.4	222.5	93.61	170.2	26.38	3313	70.14
FL3_2	E	26640	3800	24650	15300	13080	316.3	467.5	208.7	142.8	208.6	17.68	3179	60.75
FL3_3	Bt	30700	2887	27240	10780	13260	323.4	402.3	238.4	134.1	35.88	18.16	3220	69.69
FL3_4	BC	24530	2125	21240	9795	11350	245.4	435.5	150.1	89.86	224	16.24	3115	55.34
FL3_5	C	39360	20860	28270	9133	17440	362.6	1500	76.27	106.7	35.82	39.26	4025	62.25
FL4_0	Oi	18430	9103	13150	4687	6307	7465	222.2	1107	1046	11.26	45.85	1597	176.9
FL4_1	AE	27180	15280	23960	9093	12940	379.6	1081	301.2	113.1	13.32	28.16	3286	71.11
FL4_2	EB	36130	17030	29120	7576	14480	365.1	974.6	683.5	119.1	25.19	30.69	3215	69.53
FL4_3	Bw	33470	21220	29860	9243	15270	476.5	1314	236.7	121.3	34.42	33.98	3752	69.86
FL4_4	BC	30190	22650	28490	7997	14810	569.3	1180	167.3	130.8	14.94	45.19	3260	67.21
FL4_5	C	24890	19160	24280	7816	13480	434	1122	82.2	82.73	18.13	36.71	2937	51.12
FL5_1	Oe	11820	20030	29400	3342	5089	2467	177	1953	2546	0.3479	58.41	983.8	43.1
FL5_2	A	27030	23230	23740	6515	11220	222.9	560.2	644.4	1052	10.54	38.85	2190	65.31
FL5_3a	Cg1	27520	18070	26250	9115	13170	399.9	1044	312.7	141.6	16.72	30.91	3361	66.43
FL5_3b	Cg2	27450	17220	26600	8557	13080	401.1	1030	271	121.4	25.15	28.08	3188	62.94

Horizon Number	Genetic Horizon	Al	Ca	Fe	K	Mg	Mn	Na	P	S	Si	Sr	Ti	Zn
		(mg/kg)												
FU1_0	Oi	6811	20220	5145	1984	3666	3843	68.65	1105	1465	26.12	67.99	637.7	171
FU1_1	BA	27090	3871	20270	9064	10240	784.8	566.6	585.1	379.9	51.98	26.96	2884	75.32
FU1_2	Bw	28855	1000	22893	5053	6798	337.5	279.6	151	141.2	20.07	30.03	3000	80.84
FU1_3	BC	37940	751.1	30180	7252	9126	437.8	438.4	381.4	63.56	11.37	10.96	3592	47.21
FU1_4	C	43990	744.8	34950	7748	10200	477.6	426.7	232.2	55.43	7.577	9.522	4609	59
FU2_0	Oi	31540	3481	21980	7714	7999	985.6	263.7	1005	568.6	110.3	36.84	2934	133.4
FU2_1	A	34670	3297	22040	6636	8110	1091	418.2	544.6	281.5	16.82	27.14	3172	72.13
FU2_2	Bw1	30840	1402	25640	6447	8010	243.3	326.4	274.1	82.69	8.638	12.06	3781	40.93
FU2_3	Bw2	44170	873.4	35140	7059	10110	320.5	288.8	442.9	109.5	18.49	10.9	4168	58.01
FU2_4	BC	44970	1563	34070	7449	10930	402.6	286	386.8	92.44	4.245	11.79	3919	61.49
FU2_5	C1	43930	1753	36020	9110	11350	551	460.6	484.5	56.25	109.8	14.24	4316	66.25
FU2_6	C2	49650	2056	39910	7471	13270	587.6	449.8	530.6	65.57	27.89	17.23	4466	82.42
FU3_0	Oi	31630	6813	19770	7047	7840	2172	245.3	1251	568.6	13.25	52.98	2446	134.5
FU3_1	A	43760	4997	26010	5634	9316	3766	445.1	1361	467.3	31.67	38.16	2822	104.4
FU3_2	EB	53300	2359	35440	7031	10270	4833	459.2	1015	179.8	68.29	32.13	4186	99.16
FU3_3	Bw	26460	1208	22480	6491	8057	444.2	318.3	293.9	50.55	14.24	8.945	2612	43.88
FU3_4	BC	34280	1281	31190	6931	10060	320	242.2	277.7	42.83	80.6	9.892	3009	51.54
FU3_5	C	28190	1927	27330	7273	8732	449.6	388.1	297	41.2	73.2	13.06	2611	48.58
FU4_0	Oi	10040	9228	6934	3019	4688	3311	104.3	1245	1261	<.0000	64.81	918.7	98.9
FU4_1	A	41060	3444	26310	6885	9271	531.8	421	397.3	115.6	44.85	39.42	4027	56.95
FU4_2	E	42990	2651	35700	7330	10950	564.6	467.8	264.4	55.43	25.16	20.68	4408	64.26
FU4_3	Bw	58070	3069	43450	7405	12730	555.6	480.4	321.3	92.03	42.93	20.59	5239	88.69
FU4_4	BC	62940	12930	50800	6250	12950	850.1	825.6	276.6	104.6	35.46	42.57	4814	100.4
FU4_5	C	61490	15790	35460	7693	12310	1010	610.1	234.3	120.1	94.58	50.24	3456	155.3
FU5_1	Oe	31100	14700	13970	4630	7218	192.5	259	1048	2540	27.13	65.93	1816	39.68
FU5_2	A	55250	9138	29370	5328	10770	288.4	461.6	889.5	1316	46.37	51.42	4116	72.83
FU5_3	2Cg	47470	4766	52840	7330	12660	3257	373	487.4	202.2	83.35	21.76	5856	118.4

Horizon Number	Genetic Horizon	Al	Ca	Fe	K	Mg	Mn	Na	P	S	Si	Sr	Ti	Zn
		(mg/kg)												
IL1_1	A	53480	4979	59240	6762	12890	2924	398.1	403.5	166.9	53.95	25.12	6582	131.8
IL1_2	BC	49190	4407	56490	5952	12650	2910	361.8	342.4	159.9	25.16	22.48	6009	120.3
IL1_3	C	52910	3754	62450	6170	13190	2578	384.7	367.3	152.7	25	18.8	6510	143.1
IL2_1	A	42280	6749	47270	6356	12200	1183	527.7	486.2	105.9	39.56	17.94	4772	100.2
IL2_2	BC	43700	7343	45400	5362	12410	1020	586.8	459.4	114.8	33.95	21.56	5095	119.8
IL2_3	C	48170	7675	51190	6425	13140	1122	548.3	379.5	97.72	44.03	20.78	5179	106.9
IL3_0	Oi	18520	11960	11500	2967	6062	3949	145.8	1035	937.7	3.531	81.26	1275	61.33
IL3_1	A	38100	7555	31040	5566	10130	2758	487.2	496.2	225	59.17	38.31	3651	73.92
IL3_2	Bw1	41230	5836	33580	4992	10120	1736	508.4	527	132.7	206.6	30.17	4339	77.74
IL3_3	Bw2	40940	5542	37340	5210	11200	857.5	414	460.1	96.94	250.8	25.68	4806	84.91
IL3_4	C1	30980	5314	32010	4460	10220	631	389	328.5	101.8	21.37	19.47	3374	54.03
IL3_5	C2	32090	608.7	30140	6855	9171	328.4	338.6	314.3	138.8	13.64	6.919	3760	47.39
IL4_1	AE	40350	4965	44010	6781	11810	1513	345.7	472.2	133.6	4.395	17.64	4578	97.69
IL4_2	C	41390	6859	36510	6629	12090	636.6	468.2	666.2	107.9	18.79	18.87	4592	85.73
IL5_1	Oe	34010	17310	32160	6191	10220	778.4	340.9	983.4	1088	16.77	45.94	2998	96.25
IL5_2	A	39170	14670	38340	5537	11770	740.4	468.7	688	617.8	17.62	29.82	3917	80.31
IL5_3	Bw	39890	12560	40680	5498	11630	969.5	517.1	777.5	439.7	15.91	24.81	4077	69.53
IL5_4	Oa	38020	18490	35240	4948	10990	785.9	399.8	858.9	669	20.11	36.05	3550	64.48

Horizon Number	Genetic Horizon	Al	Ca	Fe	K	Mg	Mn	Na	P	S	Si	Sr	Ti	Zn
		(mg/kg)												
IU1_0	Oi	31920	4671	25690	6024	10120	1295	243.2	1243	1099	4.896	29.45	3207	99.07
IU1_1	A	35790	2871	32950	5546	11230	638.2	354.5	792.9	610.9	5.472	13.64	3593	68.77
IU1_2	Bw	41260	2789	36310	5714	12190	608.7	282.3	416.2	305.5	7.585	9.81	4353	73.85
IU1_3	BC	44190	3834	42250	6234	13920	566	320.4	191.6	163.6	3.485	8.182	5089	77.6
IU1_4	C1	45530	5485	42960	8283	14170	644.5	430.2	307.9	154.6	15.76	9.026	5373	81.28
IU1_5	C2	48020	5916	44840	9332	14460	719.4	392.2	306	107.5	3.486	10.38	5407	91.27
IU2_0	Oi	33140	8812	29850	7412	10120	1841	421.6	1091	621	851.5	33.8	3993	148.6
IU2_1	A	36280	6863	32570	5917	11230	1439	394.3	739.3	406.5	54.34	19.28	4153	107
IU2_2	Bw	45550	5046	39660	5025	12160	557.7	384.8	531.1	203.8	25.04	14.37	5042	107.4
IU2_3	C	50540	5101	42020	6036	12380	709.7	439.4	737.7	209.1	30.47	15.68	5270	114
IU3_0	Oi	14460	16190	11720	4010	6498	3205	160.5	1139	1223	57.64	47.49	1528	107.1
IU3_1	A	24820	13470	21280	5444	9365	3920	250.4	778	837.3	8.488	32.64	2572	71.28
IU3_2	Bw	47090	6177	43980	6759	13340	819.2	396.9	580.6	132.7	46.3	18.83	6401	92.14
IU3_3	BC	46850	6693	44060	7111	13800	542.6	419	635.7	129	12.71	16.62	5900	71.7
IU3_4	C	47300	6967	41500	7266	13950	554.6	478.5	521.3	118.1	22.92	19.04	5583	65.4
IU4_0	Oi	6761	21270	4711	2309	4007	3036	78.5	1094	1199	<.0000	49.46	554.3	124
IU4_1	A	29390	8485	23800	5421	9676	5928	303.4	649.9	423.8	17.88	28.17	2895	154.8
IU4_2	EB	38920	5666	35390	6052	11840	615	452.2	551.9	106.3	90.02	19.12	4847	121.8
IU4_3	BC	43660	7138	41330	6682	12640	488.4	385.9	744.9	104.2	15	16.81	4339	65.36
IU4_4	C	41330	7056	36600	7105	12690	466.1	396.8	588.7	83.9	23.49	16.58	4335	56.9
IU5_1	Oe	27300	17720	14440	4384	8523	172.8	308.1	1202	3311	230.2	51.1	2467	41.62
IU5_2	Btg	58740	8452	34110	6121	12820	515.3	411.7	681.2	454.3	280.2	28.67	5280	91.1
IU5_3	C	33260	6315	27030	5537	11300	382.6	464	292.9	600.3	8.639	15.81	3547	60.57

Table 2-A-2. Strontium isotope data for the soil horizons along the Byers Creek catena and of all the remaining mountaintop landscape soils. Values are concentrations given in mg/kg of soil (ppm). Soil chemical analyses were carried out under the direction of and collaboratively with Dr. James Self, CSU Soil Testing Laboratory, Fort Collins, Colorado.

Byers Creek Lower Catena					Mountaintop Landscape Soil Horizons				
Site Number	Genetic Horizon	Sr86 (mg/kg)	Sr87 (mg/kg)	Sr87/Sr86	Site Number	Genetic Horizon	Sr86 (mg/kg)	Sr87 (mg/kg)	Sr87/Sr86
BL1	A	12.95	9.24	0.7135	BU1	Oa	13.51	9.65	0.7143
	Bw1	11.58	8.29	0.7157		BC	12.85	9.22	0.7175
	Bw2	23.89	17.02	0.7123		C	10.88	7.78	0.7151
	C	12.85	9.18	0.7142	EL1	A	12.05	8.62	0.7151
BL2	A	7.79	5.58	0.7162		Bw	12.65	9.06	0.7160
	Bw	11.01	7.89	0.7165		C	10.45	7.46	0.7141
	BC	11.45	8.17	0.7134	EU1	A	9.96	7.15	0.7176
	C	15.05	10.72	0.7121		BC	13.12	9.37	0.7139
BL3	A	9.95	7.12	0.7155		C	9.14	6.52	0.7138
	E	10.04	7.20	0.7167	FL1	A	8.45	6.09	0.7210
	Bw	19.42	13.87	0.7144		BC	12.96	9.23	0.7124
	BC	6.75	4.83	0.7150		C	16.48	11.73	0.7119
	C	10.29	7.36	0.7156	FU1	BA	8.87	6.39	0.7206
BL4	A	6.85	4.93	0.7191		Bw	11.55	8.29	0.7176
	Bw	13.51	9.67	0.7161		BC	6.74	4.84	0.7180
	C1	7.15	5.13	0.7171		C	7.32	5.30	0.7239
	C2	8.85	6.40	0.7236	IL1	A	8.21	5.91	0.7200
BL5	Oe	18.11	12.94	0.7143		BC	15.85	11.33	0.7150
	A	6.82	4.97	0.7289		C	12.41	8.86	0.7141
	Bg1	12.21	8.72	0.7138	IU1	A	13.71	9.86	0.7189
	Bg2	7.12	5.11	0.7171		Bw	16.25	11.58	0.7125
						BC	7.51	5.43	0.7234
						C1	10.35	7.44	0.7189
						C2	9.45	6.75	0.7147